Application of Chemical Proteomics to Biomarker Discovery in Cardiac Research

Application of Chemical Proteomics to Biomarker Discovery in Cardiac Research

Toepassing van Chemical Proteomics voor Biomarker Identificatie in Hartonderzoek

(met een samenvatting in het Nederlands)

Proefschrift

ter verkrijging van de graad van doctor aan de Universiteit Utrecht op gezag van de rector magnificus, prof. dr. J.C. Stoof, ingevolge het besluit van het college voor promoties in het openbaar te verdedigen op woensdag 15 september 2010 des middags te 4.15 uur

door

Thin Thin Aye

geboren op 2 juni 1978, te Yangon, Myanmar

Promotor: **Prof. dr. A.J.R. Heck**
Co-promotor: **Dr. A. Scholten**

This thesis is dedicated to my beloved (late) father who supported me.

The cover picture was kindly provided by Dr. Arjen Scholten.

Table of Contents

Chapter 1

Introduction

Proteomics in cardiovascular research

Cardiovascular diseases (CVD) refer to the dysfunctional conditions of the heart, arteries, and veins that supply oxygen to vital, life-sustaining areas of the body. It is one of the main killers throughout the western world; claiming more than 17 million lives each year. According to the World Health Organization (WHO), an estimated 30% of mortalities result from various forms of CVDs; among which, a certain proportion can be partly attributed to genetic defects. For instance, hypertrophic cardiomyopathy originates from a variety of mutations in genes encoding sarcomere proteins, the structural proteins in heart muscle (myocardium) [1]. However, for CVDs such as myocardial infarction (MI) and congestive heart failure, it is unclear which genes are responsible for the onset of disease. It is well-known that apart from genetic predisposition, other environmental factors such as stress level, food intake and personal life-styles can contribute to phenotypes that can lead to CVDs. As such, proteins, the functional and dynamic entities of cells and tissues; rather than genes, are the most useful indicators for studying the onset, progression, as well as the therapeutic intervention of the various forms of CVDs. Proteomics, the study of protein expression, function and interaction in an organism at different states, is an invaluable technique for gaining insights into CVDs. This burgeoning area of research is aptly termed cardiovascular proteomics. This thesis will focus on the use of so-called shotgun and chemical proteomics technologies to study cardiac diseases at a global level, but also at the more targeted level of signal transduction.

1. Proteomics Methods and Applications in cardiac research

Cardiovascular proteomics can be arbitrarily divided into four sections for the convenience of discussion, namely (i) Protein Profiling - the identification of all the proteins present in a system, (ii) Quantitative Proteomics - the investigation of protein abundance in a relative or absolute manner in a specific system at different conditions or perturbations, (iii) Functional Proteomics - the study of protein functions via their interactions with DNA, metabolites or other proteins, (iv) Biomarker discovery - the search for protein candidates that can serve as specific and sensitive indicators of CVDs in which distinction between the onset of disease (diagnostic), disease progression (prognostic) and after therapeutic intervention (drug biomarkers) will be mentioned.

1.1. Protein profiling

Protein profiling is the large scale identification and classification of proteins in an organism. Recent advances in proteomic technologies permit large scale protein profiling by applying two main approaches; (i) gel-based protein profiling and (ii) gel-free protein profiling, also referred to as 2D-LC-MS/MS or MudPIT (Multi-dimensional Protein Identification). It is illustrated in Figure 1.

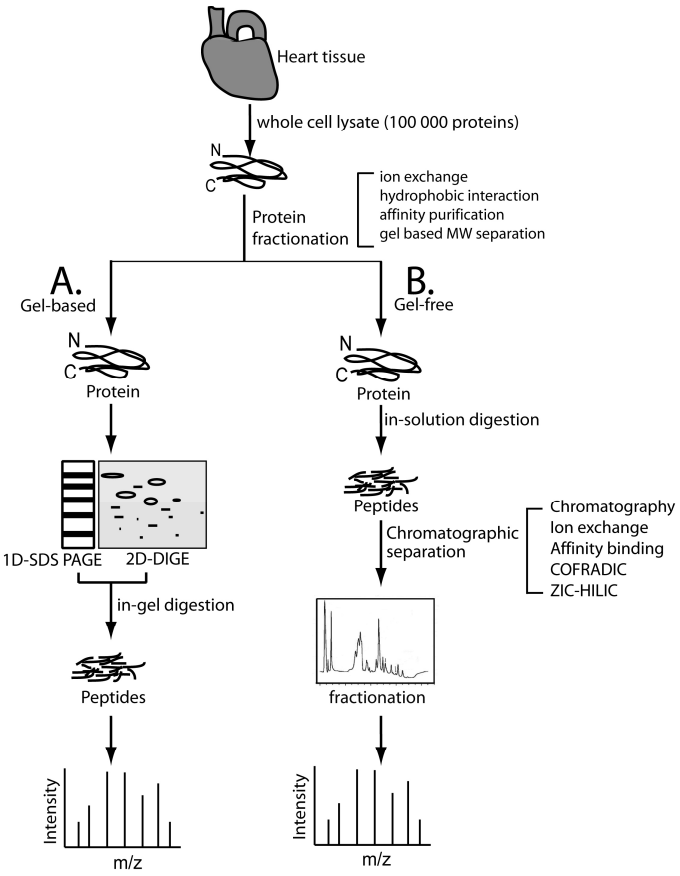

Figure 1. After protein extraction, for instance from heart tissue, samples are prepared for mass spectrometric analysis using gel based (A) and gel-free (B) workstreams. At each stage, separations can be varied to accomplish an optimal analytical depth. Mass spectrometric analysis can also be varied, using different instrumentation and different instrumental parameters.

1.1.1. Gel-based proteomics approaches

One of the most common approaches is the coupling of 1D SDS-PAGE (1-DE) with LC-MS/MS. The gel is cut into 10-70 pieces and subsequently digested and subjected to mass spectrometric analysis. Advantage of this approach is that it retains important protein molecular weight (MW) information in combination with the large scale identification of the proteins present, although the dynamic range and resolution obtained by using 1-DE is often too poor to analyze low abundant proteins and/or post-translational modifications (PTMs). Alternatively, 2-DE (two-dimensional gel electrophoresis) can be applied. In 2-DE, proteins are first separated by their respective isoelectric points (pI) with iso-electric focusing (IEF, 1st

dimension) followed by SDS-PAGE where proteins are again separated according to their MW (2^{nd} dimension). The combination of two orthogonal separation techniques results in the distribution of proteins as spots across two dimensional gel profiles with high resolution.

Therefore, 2-DE is somewhat suitable for the evaluation of PTMs. For instance, 2-DE was applied to uncover the differential phosphorylation states of troponins, which regulate Ca^{2+} sensitivity of the cytoskeleton to control contraction-relaxation cycles of the heart [2]. To date, 2DE gel protein-mapping public depositories of human cardiac proteins such as HSC-2DPAGE [3, 4], HEART-2DPAGE [5], and HP-2DPAGE [6] have been established. These can be used to compare profiles of tissues from healthy and diseased origin to uncover novel players in different pathological conditions of the heart. In addition, 2-DE heart protein databases for other animals, such as rat [7], dog [8], pig and cow are also under construction [9]. Nevertheless, 2-DE is typically biased against membrane proteins, low abundant proteins and proteins with extreme pIs and MWs. Typically, a 2-DE gel contains 1000-1500 spots, thereby limiting its application to the top 10 percent of the proteome. Also, after 2-DE, each spot has to be analyzed separately to uncover the identity of the protein, leading to a large amount of sample handlings. In order to circumvent this, profiling strategies based on chromatographic separation coupled with high resolution mass spectrometry were developed, now often termed MUDPIT or shot-gun, to allow large scale peptide sequencing of protein mixtures [10-13].

1.1.2. Gel-free proteomics approaches

MudPIT allows the identification of proteins which have variable pIs, molecular weights and chemical properties, making this method less biased. For instance, more than one thousand unique proteins from a human left ventricle tissue lysate could be identified in a single MudPIT analysis [14], indicative of the maturity of this technology. In another example, the large-scale investigation of sub-cellular localization and annotation of the cardiac proteome of mouse has been reported by using such shotgun proteomic methods [15]. Although it has been highly successful in determining the protein composition of biological samples, it still suffers from several drawbacks. First, the huge dynamic range of proteins expressed in complex biological mixtures, which easily exceeds six orders of magnitude in cells [16] and ten orders in body fluids [17] is currently not matched by the mass spectrometers that operate at maximally 4-5 orders of magnitude in dynamic range. This negates true comprehensive proteomics, as this prevents the detection of important low-abundance proteins like signaling proteins. Also, using two dimensional peptide separations, molecular weight information on proteins identified is lost.

1.2. Quantitative proteomics applied in cardiovascular research

The afore-mentioned profiling proteomics approaches may be fruitful to characterize the complex biological samples but it has less potential to study the dynamics of protein

expression, which plays a key role in many pathological effects. One important goal in cardiovascular proteomics is to assess protein concentration as a function of a distinct pathological perturbation. Nowadays, it is possible to obtain information on differential expression of many proteins by examining the intensities of protein spots/bands in a given gel or peak intensities within a MS spectrum. These and other so-called label-free quantitation methods have been developed. Another category of quantitative proteomics workflows makes use of stable isotope labels. Both classes of quantitative proteomics are discussed in more detail below and are summarized in Figure 2.

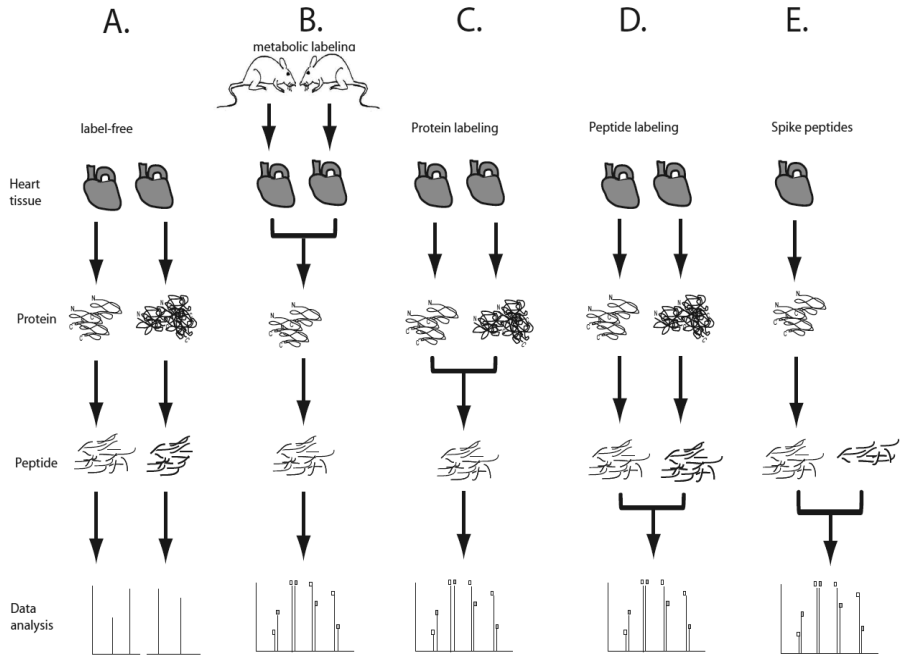

Figure 2. Schematic representation of several common quantitative mass spectrometry workflows. (A) Label-free quantitation, which compares two or more MS-analyses by peptide intensities, or spectral counts. Isotope Label-based quantitative proteomics can be sub-divided depending on incorporation of the stable isotope (B) at the metabolic stage, (C) after protein isolation, and (D) after digestion to peptides. In yet another approach, (E) synthetic stable isotope-labeled peptides are spiked into samples at given concentration as internal standard for isotope based absolute quantitation.

1.2.1. Label-free quantitative proteomics

In label-free quantitation**,** proteins are first digested to peptides before tandem MS (MS/MS) analysis and database searching for identification. This approach is schematically

depicted in Figure 2A. Relative protein abundance between two samples can be determined by i) chromatographic peak intensity measurements [18] or ii) the comparison of spectral counts [13, 19-21].

The use of peak intensity in LC-MS was first reported by Chelius *et al.* [22]. In this method, peptide peaks are first distinguished from background noise and from neighboring peaks (peak detection) and isotope patterns of detected peaks are assigned by deconvolution. LC-MS retention times are carefully adjusted in order to correctly match the corresponding mass peaks between multiple LC-MS runs (peak matching) to accommodate day-to-day variations of the chromatographic system. Chromatographic peak intensity (either peak area or peak height) is calculated and normalized to enable a more accurate matching and quantitation, making this method useful for the analysis of changes in protein abundances in complex biological samples. In the spectral counting approach, relative protein quantitation is achieved by comparing the number of identified MS/MS spectra from the same protein in each of the multiple LC-MS/MS datasets. The approach is rapid and sensitive within a protein dynamic range 3-4 order of magnitude. This method can also be automated and is amendable for large-scale proteome analysis.Gramolini *et al***.** performed a large scale proteomics survey of cardiac ventricle isolated from a mouse model of cardiomyopathy over-expressing a phospholamban mutant and demonstrated the impairment of Ca^{2+} handling at different time point. They used a rigorous comparative profiling strategy based on a relatively unbiased and sensitive method of protein detection and spectral counting to reveal the temporal patterns of differential protein expression [23].

Theoretically, an increase in protein abundance typically results in an increase in the number of its identified peptides, and *vice versa* [20, 24, 25]. Since larger proteins tend to contribute more peptides/spectra than smaller ones, simply because they can generate more peptides, spectral counting data needs to be adjusted to avoid abundance over-estimation of high MW proteins compared to low MW ones. A number of groups have proposed various types of normalized abundance factors based on transformed spectral counts. One of the simplest calculations is F_{abb}, in which the number of spectral counts in a protein is corrected by the protein's MW (spectral counts/MW) [26]. Another example of such an approach is the normalized spectral abundance factor (NASF) which is calculated as the number of spectral counts identifying a protein, divided by the protein's length (L) (spectral counts/L) for all proteins in the experiment [27].The Protein abundance index (PAI) is another example of a spectral count based quantitation method. It can be estimated by calculating the ratio between the number of observed peptides and the number of observable (i.e., theoretically predicted) peptides per protein [28] which shows a linear relationship with the logarithm of protein concentration. The index PAI value is later converted to an exponentially modified PAI (emPAI) which is proportional to protein content in a protein mixture [29].The values of emPAI can be calculated easily and do not require additional experimentation in protein

identification experiments. It can be routinely used for reporting approximate absolute protein abundances in a large-scale analysis.

Recently, a modified spectral counting strategy termed absolute protein expression (APEX) profiling was developed by the Marcotte group to measure the absolute protein concentration per cell from the proportionality between the protein abundance and the number of peptides observed [30, 31]. The key to APEX is the introduction of appropriate correction factors that make the fraction of expected number of peptides and the fraction of observed number of peptides proportional to one another. The protein's absolute abundance is indicated by an APEX score, which is calculated from the fraction of observed peptide mass spectra associated with one protein, corrected by the prior estimate of the number of unique peptides expected from a given protein during a MudPIT experiment. The critical correction factor for each protein (called O_i value) is calculated by using a machine learning classification algorithm to predict the observed peptides from a given protein based upon peptide length and amino acid composition. The APEX technique has recently been implemented in the APEX Quantitative Proteomics Tool [32], a free open source software for the absolute quantification of proteins. Very recently, the APEX-technique was shown to correlate well with real absolute quantitation experiments based on spiked internal standards analyzed by selected reaction monitoring mass spectrometry to determine protein concentrations [33].

Most recently, Griffin *et. al* developed a normalized label-free quantitative method called normalized spectral index (SI_N) which combines three MS abundance features: peptide count, spectral count and summed fragment-ion (MS/MS) intensity [34]. SI_N is calculated based on cumulative fragment ion intensity (MS/MS) for each significantly identified peptide (including all its spectra) of a particular protein. SI_N is highly reproducible by eliminating the variances between replicate MS measurements. It also accurately quantifies and predicts protein abundance of thousands of proteins in replicate MS measurements of the same and distinct samples.

1.2.2. Label-based quantitative proteomics

A common strategy to quantify proteins is to select a reference point or internal standard. This internal standard should have similar physiochemical properties to the analyte, so that it behaves identically during the chromatographic separation and subsequent MS analysis. Incorporation of stable isotopes is one of the best internal standards as it contains the above mentioned properties, while at the same time, it creates a mass difference that is easily detected in the mass spectrometer. A number of stable isotope labeling approaches have been developed for "shotgun" quantitative proteomics. These include SILAC (Stable Isotope Labeling by Amino acids in Cell culture) [35], ICAT (Isotope-Coded Affinity Tag) [19, 36], $^{18}O/^{16}O$ enzymatic labeling [37], ICPL (Isotope Coded Protein Labeling) [38], TMT (Tandem Mass Tags [39], iTRAQ (Isobaric Tags for Relative and Absolute Quantification) [40], and dimethyl labeling [41].

In metabolic labeling (Figure 2B), the incorporation of stable isotopes into proteins is performed by supplying these isotopes to the growth media consumed and metabolized by cells [35]. The isotope labels are then either incorporated as the single carbon or nitrogen source or incorporated via specific auxotrophic amino acids that contain heavy isotopes, called SILAC. The method of stable isotope metabolic labeling is also successfully used in variety of model organisms ranging from bacteria and yeast to drosophila and up to mammals [42]. Recently, a mouse bearing solely heavy isotope labeled lysine residues was developed by the Mann lab. This so-called SILAC-mouse is labeled through a diet containing only a $^{13}C_6$-substituted heavy version of lysine and to maintain this diet over several generations to achieve full labeling. No obvious effects on growth, behavior or fertility were observed in this mouse model [43]. It is a versatile tool for quantitative (tissue) proteomics. Initial MS analysis of different generations of these SILAC mice allowed following the incorporation rates of heavy lysine into newly synthesized proteins in various tissues under *in vivo* conditions.

Figure 2C and D represent chemical derivatization techniques to achieve isotope labeling of proteins and peptides respectively. This is particularly advantageous for human or animal tissue samples where metabolic-based incorporation cannot easily be achieved. A handful of different chemical derivatization platforms are available and they can be divided into two major classes, based on their specific readout by the mass spectrometer: i) quantitation based on the relative intensities of fragment ion peaks at fixed *m/z* values within an MS/MS spectrum (MS/MS-based quantation) such as iTRAQ and TMT and ii) quantitation based on the relative intensities of extracted ion chromatograms (XICs) for precursor ions within a single data set (MS-based quantitation). This method includes AQUA, ICAT and dimethyl labeling, but also SILAC uses this as the basis for quantitation. The detailed methodologies will be explained below.

The iTRAQ method uses amine-specific isobaric reagents to label the primary amines of the peptides. It can label up to eight different biological samples [44]. Labeled peptides from the different samples are mixed, analyzed and quantitated. The MS spectra of each peptide in the sample are simple and easy to interpret due to the isobaric nature of the tags. Upon fragmentation, the isobaric amine groups release reporter ions with distinct m/z (e.g. 114.1, 115.1, 116.1 and 117.1 for 4-plex iTRAQ). Measuring the relative intensities between reporter ions determines the relative abundance of the peptide in the respective samples. The relative abundance measurements at the protein level can be measured by combining the reporter ion intensities from multiple peptides. iTRAQ was successfully applied to determine the relative and absolute quantitation of drug-protein binding in which a mixed broad-specificity kinase inhibitor matrix is used in combination with free kinase inhibitors [45]. It was possible to identify new drug targets for clinically important kinase inhibitors. However, this labeling reagent is costly and less stable. Although current high accuracy instrumentation MS is able to identify MS/MS fragments at low m/z, ion statistics used in peak recognition

and quantitation is relatively poor compared to MS-based quantitation due to the overall lower amount of ions in MS/MS.

In the ICAT method, proteins from two or more different biological samples are labeled with a ^{13}C or ^{12}C-ethylene glycol linker with a biotin affinity tag and a thiol-specific reactive group that selectively couples to the side chain of reduced cysteine residues [19]. The labeled samples are mixed, digested, purified with an avidin column to allow enrichment of labeled peptides prior to MS-analysis [46]. The relative abundances of peptides are quantified according to their intensity ratios. A major advantage of this tagging system is that it facilitates the enrichment of the modified peptides via affinity purification of the biotin moiety, thereby enhancing the detection of low abundance proteins. However, a major bottleneck is that ICAT reagents selectively label the less frequent cysteine residues so that proteins without a cysteine will not be quantified using this method.

Dimethyl labeling through reductive amination was introduced into the proteomics field by Hsu *et. al.* [41]. Similar to iTRAQ and ICAT, labeling is performed after proteolysis. Formaldehyde reacts with the N-terminus or the amino group of the lysine side-chains to form an intermediate shiff base that is subsequently reduced to a methyl group by application of sodium cyanoborohydride ($NaBH_3CN$). The resulting secondary amine follows the same reaction to form a tertiary amine with two methyl groups. This results increase in a mass of 28 Da (2x $^{12}CH_3$) or 32 Da (2x $^{12}CHD_2$) per modified amino group. The method can be extended to a triplex strategy by introducing a third label using $^{13}CD_2O$ and $NaBD_3CN$. This strategy is applicable for the analysis of complex samples including cell lysate and affinity purified proteins [47, 48]. Fully-automated, online and on-column sequential triplex dimethyl labeling is the latest advance for this type of labeling [49]. Large advantage of this technique is that the cost of the reagents is minimal.

Probably the most direct approach for the introduction of stable isotope-labeled peptides is to chemically synthesize them and 'spike' known quantities into the sample as internal standards (Figure 2E). This approach applies well to the quantification of candidate biomarkers in body fluids [50]. To reduce interference from background ions, quantification can be performed on specific fragments of the peptide generated in a triple-quadrupole mass spectrometer using selected reaction monitoring (SRM), often also referred to as MRM. The MS is set to detect a preprogrammed precursor-fragment combination with very high sensitivity and specificity. The internal peptide standard is introduced during or after protein digestion. Because suitable internal standards need to be identified and synthesized, this approach is usually limited to a small number of preselected proteins for follow-up, rather than work as a discovery tool.

Although stable isotopic labeling technology for protein quantification has been applied successfully, it remains technically difficult to comprehensively characterize the global proteome due to the high costs of the labeling reagents, the nature of the methodology and especially by the dynamic range limitation of the mass spectrometers when analyzing

complex biological samples. Furthermore, simultaneous quantification of proteins from a large population of samples is also often problematic.

1.3. Functional proteomics approach

Differential changes in protein profile with the help of quantitative proteomics are heavily used to evaluate the involvement of critical pathways in a time- and disease-dependent manner. Although current sensitive MS analysis allows the identification of thousands of proteins in a single experiment, the biological role of these proteins are not revealed. And it is now evident that proteins do not act alone, but rather in a concerted way together with others in its vicinity. Hence, the functions of proteins and their molecular mechanisms can be implicated by their interacting protein partners, so called "guilt-by-association". This makes it important to investigate proteins in the context of their formed complexes, rather than on an individual basis [51, 52]. Illustrative examples of such protein complexes are signaling modules, which consist of multiple-signaling proteins which are responsible for the fast and efficient transmission of a specific stimulus. This can be achieved through physically tethering the signaling modules to a cellular compartment where its function is required. For instance, as described in this thesis, the protein kinase A anchoring proteins (AKAPs, see review [53]) tether a kinase called cAMP-dependent protein kinase (PKA) to distinct loci within the cells to accommodate specificity in space and time. This is much needed as PKA is implicated in a large amount of functions. For instance, in heart it plays a major role in contraction and relaxation through regulating the Ca^{2+} concentration in the cardiac myocytes. Furthermore, the importance of other heart signaling modules has been shown, including β-adrenergic receptor associating proteins [54], as well as many protein kinase C binding partners (see review [55]). However, many of these signaling molecules are relatively low abundant in the heart, when compared to the amount of cytoskeletal and other muscle proteins. Therefore, the earlier discussed protein profiling approach often does not permit the identification of these complexes, and if identified, only with a marginal amount of sequence coverage. Hence, methods to detect these low abundant proteins in a complex sample are required. Reduction of sample complexity can be achieved by proteome pre-fractionation techniques like immunodepletion of high-abundant proteins, subcellular fractionation and affinity purification methods. The latter has been applied in this thesis and will be the focus of the next paragraphs. The selective nature of the affinity purification methods allows a large enrichment of a specific subset of the proteome, allowing a more thorough investigation of these enriched proteins.

1.3.1. Key technologies in targeted proteomics

Targeted proteomics is a hypothesis-driven approach where proteome pre-fractionation is based on selective molecular interactions between 'bait', which can be a small molecule, ligand or a protein and its targets, i.e. (other) proteins. Up to date, there are several

methodologies applied to isolate protein complexes and identify their constituents. There are two main small molecule based approaches that are collectively called chemical proteomics (Figure 3, see review [56]).

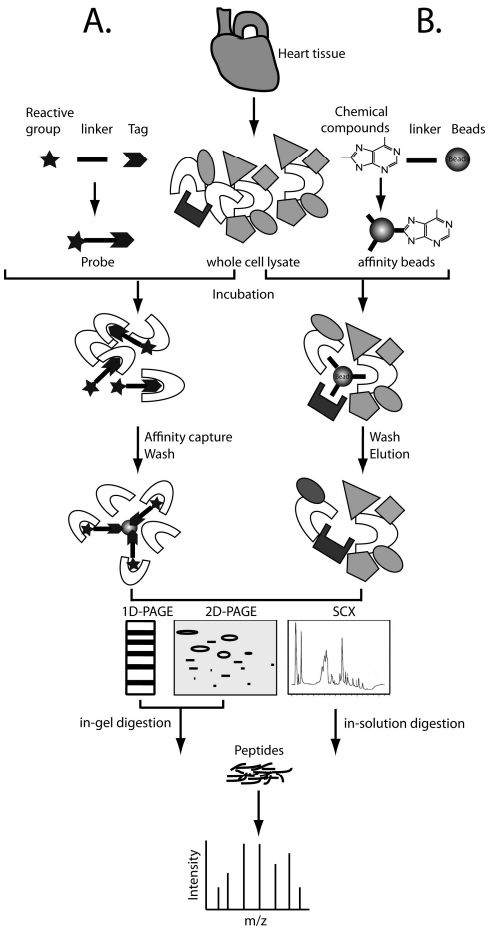

Figure 3. Targeted proteomics workflows strategies to enrich and characterize low abundant signaling complexes. (A) Cardiac tissue lysates are incubated with a soluble activity-based probe. After binding of the probe to its target(s), the reactive group is activated to form covalent interactions with the target proteins. Specific capture of the probe/protein complex can then be achieved; (B) Beads are directly coated with the affinity-based ligand and subsequently incubated with a protein lysate to isolate the ligand's targets. The enriched protein complexes are washed with mild buffer to remove non-specific binding. Subsequently common separation techniques can be applied, followed by digestion and LC-MS MS analysis.

As shown in Figure 3A, the first method, called ABPP, for activity based protein profiling, makes use of highly engineered small molecules (probes) that usually consist of four parts: an affinity region, a reactive moiety, a linker region and a coupling region. The affinity region is the actual 'bait' that interacts with the protein(s) of interest. Once bound, the reactive group can be activated. Usually these groups are photosensitive. Activation couples the probe covalently to its primary target. The linker connects the probe to affinity bait, called the coupling group, for which often biotin is used. This second bait allows the efficient purification of the targeted protein(s) from the complex lysate. The advantage of ABPP is the ability to monitor enzyme activity directly rather than being limited to proteins or mRNA abundance.

Recently, ABPP combined with MS analysis (ABPP-MudPIT) enabled the identification of hundreds of active enzymes from a single biological system [57]. It is especially useful for profiling inhibitor selectivity as the potency of an inhibitor can be tested against hundreds of targets simultaneously. The possible drawback of the ABPP approach is the bulky nature of the tag which affects the protein-binding affinity, probe uptake and cellular and tissue distribution thus hindering *in vivo* profiling experiments. It is also less suited for diluted large volume samples like body fluids, which would require large amounts of expensive probes. The alternative approach depicted in Figure 3B makes use of pre-immobilized small molecule 'baits'. This requires the generation of a linkable version of the compound of interest, for which many different chemistries can be used. The generated affinity-beads can be incubated with a complex protein lysate to isolate targets of the 'bait'. The affinity purification step is based on the highly specific reversible interaction of proteins with the immobilized compound. The captured sub-proteome can then be retrieved from the affinity beads by different elution steps. Typically this approach suffers from non-specific binding for which several approaches are reported to reduce it, such as by using competition binding assays [58] and varying the linker region between the beads and the compound [59].

There are also several protein-'bait' based methods, such as immunoprecipitation, and the use of tagged proteins, of which the tandem affinity purification (TAP-tag method) is an elegant example. The TAP-tag consists of two IgG binding domains of ProtA and a calmodulin binding peptide (CBP) separated by a TEV protease cleavage site [60]. In sequential affinity purification, interacting proteins of the tagged protein can be isolated and identified. A clear advantage of the small-molecule methods is that they can be applied to protein lysates of any origin, even to very rare human tissue. The protein based method requires ectopic expression of the tagged-version in a cell-line and negates the use of tissue samples.

Immunoprecipitation, which is feasible in primary tissue, requires the availability of a clean antibody, which is not arbitrary for most proteins. Also a proper control is often difficult to attain in such an approach. These disadvantages do not apply to chemical proteomics, although chemical proteomics also suffers from some drawbacks. For instance, it can only

target proteins that have affinity for small molecules and it requires upfront knowledge on chemical interaction characteristics of the target of interest, although the technique is also applied in the unbiased identification of drug targets. Both enrichment methods are highly suitable for coupling to MS for interaction analysis. In addition, due to the enrichment, more comprehensive analysis of PTMs becomes feasible. The affinity bead-based chemical proteomics setup is the method of choice in this thesis, where we apply it to the study of cardiac disease.

1.4. Proteomics and biomarker discovery

The discovery of novel biomarkers involves the profiling of biological samples in search for disease or drug related qualitative and quantitative changes in protein levels and/or modifications. This can be achieved by the comparative analysis of protein expression in normal and diseased tissues.

Therefore several requirements apply; (i) the ability to detect as many proteins as possible, (ii) a dynamic range that is wide enough to detect low abundant proteins, (iii) confident protein identification, (iv) high reproducibility and consistency of the platforms so that the biological differences can be sufficiently distinguished from technical ones, (v) the ability to quantify the significant differences over sample variability and (vi) the ability to profile and compare a large number of samples for validation. The initial mapping of healthy proteomes of plasma, urine, liver and heart have been reported [61, 62]. Currently, a protein database of cardiac proteins has been constructed [6, 63, 64], which also includes alterations of proteins observed in cardiomyopathic samples. An example of protein-based cardiac disease biomarkers derived exclusively from cardiac tissue are the cardiac troponins that are in clinical use for the diagnosis of acute myocardial infarction. Another CVD biomarkers are creatine kinase [65] and high-sensitivity C-reactive protein (CRP) [66].

The progress of biomarker discovery at the protein level is challenging due to the dynamic range of proteins present in the systems. Anderson *et al.* reported that the plasma proteome spans a linear dynamic range of 10-12 orders of magnitude [17] while current proteomic techniques only resolve protein abundance within 3-4 orders of magnitude. Although high abundant and tissue leakage proteins in the plasma can serve as a surrogate measure of cardiac disease progression, existing biomarkers provide less accurate value of predictive patient risk.

Hence, there is a noticeable shift in the approach to biomarker discovery away from the direct analysis of body fluids and towards comparing diseased and healthy primary tissues or proximal fluids. Major disadvantage of this approach is the necessity to measure the observed differential proteins back in a body fluid to avoid invasive test procedures. Recently, de Kleijn and group discovered that local ruptured plaques contain molecular information that is predictive for antherothrombotic events in all vascular territories and that the local antherosclerotic plaque acts as a potential source of prognostic biomarkers [67]. In their study,

they used longitudinal section of plaques and compared plaque proteins between two patient types; one with diagnostic cardiovascular event and one with follow-up treatment in order to investigate the prognostic effect using the complementary power of proteomics.

The future challenges for biomarker discovery will be the advancement of mass spectrometric instrumentation, developing novel and even better upfront sample separations, but also the further application of specific enrichment techniques to uncover lower abundant signature proteins that are indicative of protein changes in vivo. Thus proteomics will continue to be an indispensable approach to decipher cellular mechanisms and to link these mechanisms to cardiovascular disease and health.

1.5. Animal models of heart disease

Most of the technologies discussed above can identify a relatively large pool of proteins within a specific system or proteins which are able to interact with other proteins of interest. However, in order to further validate protein targets that affect or are affected by cellular functions in a living animal, in vivo experiments are required. Proteomics is also an emerging tool in this area of research. Thus far, a handful of animal models of human heart disease have been studied with proteomics. Recently, a gel-based kinase assay coupled to MS identification was used as an approach to map global kinase activity in the context of cardiomyopathy in the postnatal heart of transgenic mice expressing activated MKK6 (mitogen-activated protein kinase) [68]. A differential proteomic profiling study was performed on right ventricular hypertrophy using a rat model of pulmonary artery banding [69]. White *et. al* used proteomics to characterize global changes in cardiac protein expression in response to ischemia/reperfusion injury [70]. However, the gene expression pattern of small animals and larger mammals such as humans are different. Hence, investigation has to move into larger mammals such as dog [71] and bovine [72].

2. Scope and outline of this thesis

In cardiac research, the prognostic outcomes following diagnosis are still relatively poor. Although significant progress has been made in identifying genetic, physiological and environmental factors that predispose individuals to different cardiac diseases, the etiology of these has exhibited an unanticipated level of complexity. Heart muscle expresses several thousands of distinct proteins, several hundreds of which are likely tissue specific and critical for heart muscle function, performance and capacity [73]. Hence, the systematic identification of these proteins and the determination of their relative abundance in healthy and diseased cardiac tissue could provide better understanding of the molecular determinants of the disease. Finding the proteins that specifically change in response to certain pathologies is the ultimate goal of biomarker discovery.

Understanding the molecular mechanisms of signaling proteins is an important aspect of these goals as these often pose as promising therapeutic targets [74]. These signaling proteins are the orchestrators of tissue function. As a consequence, their function and behavior is very complex and dynamic with constant activation and deactivation through protein modification, allowing the system to quickly achieve equilibrium where cell function is optimal for the environmental conditions at hand. Under developing pathological circumstances, small but chronic alterations in this complex signaling network could result in the development of diseases such as cardiac hypertrophy, myopathy and ultimately heart failure. Hence, additional research into the molecular basis of signaling proteins is needed to better understand disease initiation and progression at the molecular level to ultimately help the further development of therapeutic strategies.

Protein kinases and phosphatases are one of the main signaling proteins that control cardiac contraction and rhythm. PKA (cAMP-dependent protein kinase) and PKG (cGMP-dependent protein kinase) are two important examples of kinases that are heavily involved in cardiac function. Chapter 2 reviews the various contributions of mass spectrometry to better characterize and understand PKA and PKG signaling. The in depth characterization of these kinases is reviewed with respect to their PTMs (especially phosphorylation), the similarities and differences between their various isozymes, the identification and specificity of their binding partners that have been studied by proteomics based methodologies. In addition, studies on structural properties by for instance native mass spectrometry, H/D exchange and ion mobility are also discussed. Combining mass spectrometry based data with other biophysical and biochemical data has been of great help to unravel the intricate regulation of kinase function in the cell in all its magnificent complexity.

PKA is the main target of the second messenger cAMP. PKA is a widely distributed and multifunctional kinase in many tissues and cell types, where it is involved in a multitude of different signaling pathways in many compartments of the cell. To prevent the simultaneous cross activation of parallel PKA pathways, its function is tightly regulated

through interaction of PKA with the highly diverse family of AKAPs (A-kinase anchoring proteins). These localize PKA activity in space and time. The genetically distinct different isoforms of PKA each bind to different AKAPs, however, for many AKAPs their specificity is largely unknown. Therefore, chapter 3 emphasizes on the development of a chemical proteomics method to screen the specificity of different PKA-isoforms towards their AKAPs directly in tissue and cell lysates. Based on the differential affinity chromatography characteristics of two cAMP-analogs coupled to mass spectrometry the specificity of many AKAPs are confirmed, but also new specificities are established by this method. The results described in this chapter also provide insight into the presence of cell or tissue specific AKAPs.

As mentioned above, we strongly consider signaling proteins as putative biomarkers for cardiac disease, as they are more likely to function at the onset of disease. In the heart, cAMP is a key regulator of excitation-contraction coupling (ECC) and mediates the sympathetic control over this mechanism through the activation of PKA [75]. It is also shown that in dilated cardiomyopthic hearts (DCM), where the ECC is severely hindered, there are alterations in cAMP signaling [76]. Therefore, in chapter 4, we investigated the potential of a cAMP based chemical proteomics method for its application in biomarker discovery. A large set of PKA-AKAP complexes were enriched from human left ventricle, thereby allowing their detailed study by mass spectrometry. Not only do the concentrations of certain cyclic nucleotide based proteins alter in DCM, also differential association of PKA to AKAPs was observed between the healthy and DCM stage. These data provide important clues on the specific dysregulation of specific PKA signaling nodes upon progression to DCM and pose as a promising new tool for biomarker discovery in cardiac diseases.

Chapter 5 describes the study of the healthy human left ventricle proteome in the finest detail, using a multifaceted analysis platform combining differential sample fractionations, enzymatic digestions and peptide fragmentation techniques (CAD and ETcaD) to enhance (i) protein coverage, (ii) sequence coverage, (iii) protein identification confidence and, (iv) accurate protein concentration determination. These absolute abundance data provide a valuable resource to identify putative novel biomarkers for cardiac disease, but also allow the specific evaluation of signaling pathways in the ventricle in the context of their abundance. Special emphasis is put on the expression levels of kinases and phosphatases in the healthy human left ventricle, in conjunction to endogenous phosphorylation sites identified.

With the recent advances in mass spectrometry, quantitative assessments of proteins hold immerse potential for biomarker discovery of cardiac disease. In addition, sub-proteomics analysis by means of depletion of abundant proteins, affinity purification and sub-cellular fractionation may facilitate the identification of vital molecules by reducing the complexity of the biological systems. With a panel of candidate diagnostic biomarkers, validation can be performed on larger sample sizes using various proteomics techniques. In

conclusion, chapter 6 summarizes and remarks on the various contributions of mass spectrometry-based proteomics which offers a promising platform to understand pathogenesis of cardiac disease and subsequently for discovery of biomarker for early detection.

References:

1 Maron, B. J. (2009) Hypertrophic cardiomyopathy centers. Am J Cardiol. **104**, 1158-1159

2 Stanley, B. A., Gundry, R. L., Cotter, R. J. and Van Eyk, J. E. (2004) Heart disease, clinical proteomics and mass spectrometry. Dis Markers. **20**, 167-178

3 Corbett, J. M., Wheeler, C. H., Baker, C. S., Yacoub, M. H. and Dunn, M. J. (1994) The human myocardial two-dimensional gel protein database: update 1994. Electrophoresis. **15**, 1459-1465

4 Corbett, J. M., Wheeler, C. H. and Dunn, M. J. (1995) Coelectrophoresis of cardiac tissue from human, dog, rat and mouse: towards the establishment of an integrated two-dimensional protein database. Electrophoresis. **16**, 1524-1529

5 Pleissner, K. P., Soding, P., Sander, S., Oswald, H., Neuss, M., Regitz-Zagrosek, V. and Fleck, E. (1997) Dilated cardiomyopathy-associated proteins and their presentation in a WWW-accessible two-dimensional gel protein database. Electrophoresis. **18**, 802-808

6 Muller, E. C., Thiede, B., Zimny-Arndt, U., Scheler, C., Prehm, J., Muller-Werdan, U., Wittmann-Liebold, B., Otto, A. and Jungblut, P. (1996) High-performance human myocardial two-dimensional electrophoresis database: edition 1996. Electrophoresis. **17**, 1700-1712

7 Li, X. P., Pleissner, K. P., Scheler, C., Regitz-Zagrosek, V., Salnikow, J. and Jungblut, P. R. (1999) A two-dimensional electrophoresis database of rat heart proteins. Electrophoresis. **20**, 891-897

8 Dunn, M. J., Corbett, J. M. and Wheeler, C. H. (1997) HSC-2DPAGE and the two-dimensional gel electrophoresis database of dog heart proteins. Electrophoresis. **18**, 2795-2802

9 McGregor, E. and Dunn, M. J. (2003) Proteomics of heart disease. Hum Mol Genet. **12 Spec No 2**, R135-144

10 Link, A. J., Eng, J., Schieltz, D. M., Carmack, E., Mize, G. J., Morris, D. R., Garvik, B. M. and Yates, J. R., 3rd. (1999) Direct analysis of protein complexes using mass spectrometry. Nat Biotechnol. **17**, 676-682

11 McCormack, A. L., Schieltz, D. M., Goode, B., Yang, S., Barnes, G., Drubin, D. and Yates, J. R., 3rd. (1997) Direct analysis and identification of proteins in mixtures by LC/MS/MS and database searching at the low-femtomole level. Anal Chem. **69**, 767-776

12 Peng, J. and Gygi, S. P. (2001) Proteomics: the move to mixtures. J Mass Spectrom. **36**, 1083-1091

13 Washburn, M. P., Wolters, D. and Yates, J. R., 3rd. (2001) Large-scale analysis of the yeast proteome by multidimensional protein identification technology. Nat Biotechnol. **19**, 242-247

14 Kline, K. G., Frewen, B., Bristow, M. R., Maccoss, M. J. and Wu, C. C. (2008) High quality catalog of proteotypic peptides from human heart. J Proteome Res. **7**, 5055-5061

15 Bousette, N., Kislinger, T., Fong, V., Isserlin, R., Hewel, J. A., Emil, A. and Gramolini, A. O. (2009) Large-scale characterization and analysis of the murine cardiac proteome. J Proteome Res. **8**, 1887-1901

16 Ghaemmaghami, S., Huh, W. K., Bower, K., Howson, R. W., Belle, A., Dephoure, N., O'Shea, E. K. and Weissman, J. S. (2003) Global analysis of protein expression in yeast. Nature. **425**, 737-741

17 Anderson, N. L. and Anderson, N. G. (2002) The human plasma proteome: history, character, and diagnostic prospects. Mol Cell Proteomics. **1**, 845-867

18 Wang, G., Wu, W. W., Zeng, W., Chou, C. L. and Shen, R. F. (2006) Label-free protein quantification using LC-coupled ion trap or FT mass spectrometry: Reproducibility, linearity, and application with complex proteomes. J Proteome Res. **5**, 1214-1223

19 Gygi, S. P., Rist, B., Gerber, S. A., Turecek, F., Gelb, M. H. and Aebersold, R. (1999) Quantitative analysis of complex protein mixtures using isotope-coded affinity tags. Nat Biotechnol. **17**, 994-999

20 Liu, H., Sadygov, R. G. and Yates, J. R., 3rd. (2004) A model for random sampling and estimation of relative protein abundance in shotgun proteomics. Anal Chem. **76**, 4193-4201

21 Gilchrist, A., Au, C. E., Hiding, J., Bell, A. W., Fernandez-Rodriguez, J., Lesimple, S., Nagaya, H., Roy, L., Gosline, S. J., Hallett, M., Paiement, J., Kearney, R. E., Nilsson, T. and Bergeron, J. J. (2006) Quantitative proteomics analysis of the secretory pathway. Cell. **127**, 1265-1281

22 Chelius, D. and Bondarenko, P. V. (2002) Quantitative profiling of proteins in complex mixtures using liquid chromatography and mass spectrometry. J Proteome Res. **1**, 317-323

23 Gramolini, A. O., Kislinger, T., Alikhani-Koopaei, R., Fong, V., Thompson, N. J., Isserlin, R., Sharma, P., Oudit, G. Y., Trivieri, M. G., Fagan, A., Kannan, A., Higgins, D. G., Huedig, H., Hess, G., Arab, S., Seidman, J. G., Seidman, C. E., Frey, B., Perry, M., Backx, P. H., Liu, P. P., MacLennan, D. H. and Emili, A. (2008) Comparative proteomics profiling of a phospholamban mutant mouse model of dilated cardiomyopathy reveals progressive intracellular stress responses. Mol Cell Proteomics. **7**, 519-533

24 Gao, J., Friedrichs, M. S., Dongre, A. R. and Opiteck, G. J. (2005) Guidelines for the routine application of the peptide hits technique. J Am Soc Mass Spectrom. **16**, 1231-1238

25 Zybailov, B., Coleman, M. K., Florens, L. and Washburn, M. P. (2005) Correlation of relative abundance ratios derived from peptide ion chromatograms and spectrum counting for quantitative proteomic analysis using stable isotope labeling. Anal Chem. **77**, 6218-6224

26 Scholten, A., Poh, M. K., van Veen, T. A., van Breukelen, B., Vos, M. A. and Heck, A. J. (2006) Analysis of the cGMP/cAMP interactome using a chemical proteomics approach in mammalian heart tissue validates sphingosine kinase type 1-interacting protein as a genuine and highly abundant AKAP. J Proteome Res. **5**, 1435-1447

27 Florens, L., Carozza, M. J., Swanson, S. K., Fournier, M., Coleman, M. K., Workman, J. L. and Washburn, M. P. (2006) Analyzing chromatin remodeling complexes using shotgun proteomics and normalized spectral abundance factors. Methods. **40**, 303-311

28 Rappsilber, J., Ryder, U., Lamond, A. I. and Mann, M. (2002) Large-scale proteomic analysis of the human spliceosome. Genome Res. **12**, 1231-1245

29 Ishihama, Y., Oda, Y., Tabata, T., Sato, T., Nagasu, T., Rappsilber, J. and Mann, M. (2005) Exponentially modified protein abundance index (emPAI) for estimation of absolute protein amount in proteomics by the number of sequenced peptides per protein. Mol Cell Proteomics. **4**, 1265-1272

30 Lu, P., Vogel, C., Wang, R., Yao, X. and Marcotte, E. M. (2007) Absolute protein expression profiling estimates the relative contributions of transcriptional and translational regulation. Nat Biotechnol. **25**, 117-124

31 Vogel, C. and Marcotte, E. M. (2009) Absolute abundance for the masses. Nat Biotechnol. **27**, 825-826

32 Braisted, J. C., Kuntumalla, S., Vogel, C., Marcotte, E. M., Rodrigues, A. R., Wang, R., Huang, S. T., Ferlanti, E. S., Saeed, A. I., Fleischmann, R. D., Peterson, S. N. and Pieper, R. (2008) The APEX Quantitative Proteomics Tool: generating protein quantitation estimates from LC-MS/MS proteomics results. BMC Bioinformatics. **9**, 529

33 Malmstrom, J., Beck, M., Schmidt, A., Lange, V., Deutsch, E. W. and Aebersold, R. (2009) Proteome-wide cellular protein concentrations of the human pathogen Leptospira interrogans. Nature. **460**, 762-765

34 Griffin, N. M., Yu, J., Long, F., Oh, P., Shore, S., Li, Y., Koziol, J. A. and Schnitzer, J. E. Label-free, normalized quantification of complex mass spectrometry data for proteomic analysis. Nat Biotechnol. **28**, 83-89

35 Ong, S. E., Blagoev, B., Kratchmarova, I., Kristensen, D. B., Steen, H., Pandey, A. and Mann, M. (2002) Stable isotope labeling by amino acids in cell culture, SILAC, as a simple and accurate approach to expression proteomics. Mol Cell Proteomics. **1**, 376-386

36 Han, D. K., Eng, J., Zhou, H. and Aebersold, R. (2001) Quantitative profiling of differentiation-induced microsomal proteins using isotope-coded affinity tags and mass spectrometry. Nat Biotechnol. **19**, 946-951

37 Mirgorodskaya, O. A., Kozmin, Y. P., Titov, M. I., Korner, R., Sonksen, C. P. and Roepstorff, P. (2000) Quantitation of peptides and proteins by matrix-assisted laser desorption/ionization mass spectrometry using (18)O-labeled internal standards. Rapid Commun Mass Spectrom. **14**, 1226-1232

38 Kellermann, J. (2008) ICPL--isotope-coded protein label. Methods Mol Biol. **424**, 113-123

39 Dayon, L., Hainard, A., Licker, V., Turck, N., Kuhn, K., Hochstrasser, D. F., Burkhard, P. R. and Sanchez, J. C. (2008) Relative quantification of proteins in human cerebrospinal fluids by MS/MS using 6-plex isobaric tags. Anal Chem. **80**, 2921-2931

40 Ross, P. L., Huang, Y. N., Marchese, J. N., Williamson, B., Parker, K., Hattan, S., Khainovski, N., Pillai, S., Dey, S., Daniels, S., Purkayastha, S., Juhasz, P., Martin, S., Bartlet-Jones, M., He, F., Jacobson, A. and Pappin, D. J. (2004) Multiplexed protein quantitation in Saccharomyces cerevisiae using amine-reactive isobaric tagging reagents. Mol Cell Proteomics. **3**, 1154-1169

41 Hsu, J. L., Huang, S. Y., Chow, N. H. and Chen, S. H. (2003) Stable-isotope dimethyl labeling for quantitative proteomics. Anal Chem. **75**, 6843-6852

42 Gouw, J. W., Krijgsveld, J. and Heck, A. J. Quantitative proteomics by metabolic labeling of model organisms. Mol Cell Proteomics. **9**, 11-24

43 Kruger, M., Moser, M., Ussar, S., Thievessen, I., Luber, C. A., Forner, F., Schmidt, S., Zanivan, S., Fassler, R. and Mann, M. (2008) SILAC mouse for quantitative proteomics uncovers kindlin-3 as an essential factor for red blood cell function. Cell. **134**, 353-364

44 Bantscheff, M., Boesche, M., Eberhard, D., Matthieson, T., Sweetman, G. and Kuster, B. (2008) Robust and sensitive iTRAQ quantification on an LTQ Orbitrap mass spectrometer. Mol Cell Proteomics. **7**, 1702-1713

45 Bantscheff, M., Eberhard, D., Abraham, Y., Bastuck, S., Boesche, M., Hobson, S., Mathieson, T., Perrin, J., Raida, M., Rau, C., Reader, V., Sweetman, G., Bauer, A., Bouwmeester, T., Hopf, C., Kruse, U., Neubauer, G., Ramsden, N., Rick, J., Kuster, B. and Drewes, G. (2007) Quantitative chemical proteomics reveals mechanisms of action of clinical ABL kinase inhibitors. Nat Biotechnol. **25**, 1035-1044

46 Smolka, M. B., Zhou, H., Purkayastha, S. and Aebersold, R. (2001) Optimization of the isotope-coded affinity tag-labeling procedure for quantitative proteome analysis. Anal Biochem. **297**, 25-31

47 Boersema, P. J., Aye, T. T., van Veen, T. A., Heck, A. J. and Mohammed, S. (2008) Triplex protein quantification based on stable isotope labeling by peptide dimethylation applied to cell and tissue lysates. Proteomics. **8**, 4624-4632

48 Boersema, P. J., Raijmakers, R., Lemeer, S., Mohammed, S. and Heck, A. J. (2009) Multiplex peptide stable isotope dimethyl labeling for quantitative proteomics. Nat Protoc. **4**, 484-494

49 Raijmakers, R., Berkers, C. R., de Jong, A., Ovaa, H., Heck, A. J. and Mohammed, S. (2008) Automated online sequential isotope labeling for protein quantitation applied to proteasome tissue-specific diversity. Mol Cell Proteomics. **7**, 1755-1762

50 Anderson, L. and Hunter, C. L. (2006) Quantitative mass spectrometric multiple reaction monitoring assays for major plasma proteins. Mol Cell Proteomics. **5**, 573-588

51 Gavin, A. C., Bosche, M., Krause, R., Grandi, P., Marzioch, M., Bauer, A., Schultz, J., Rick, J. M., Michon, A. M., Cruciat, C. M., Remor, M., Hofert, C., Schelder, M., Brajenovic, M., Ruffner, H., Merino, A., Klein, K., Hudak, M., Dickson, D., Rudi, T., Gnau, V., Bauch, A., Bastuck, S., Huhse, B., Leutwein, C., Heurtier, M. A., Copley, R. R., Edelmann, A., Querfurth, E., Rybin, V., Drewes, G., Raida, M., Bouwmeester, T., Bork, P., Seraphin, B.,

Kuster, B., Neubauer, G. and Superti-Furga, G. (2002) Functional organization of the yeast proteome by systematic analysis of protein complexes. Nature. **415**, 141-147

52 Ho, Y., Gruhler, A., Heilbut, A., Bader, G. D., Moore, L., Adams, S. L., Millar, A., Taylor, P., Bennett, K., Boutilier, K., Yang, L., Wolting, C., Donaldson, I., Schandorff, S., Shewnarane, J., Vo, M., Taggart, J., Goudreault, M., Muskat, B., Alfarano, C., Dewar, D., Lin, Z., Michalickova, K., Willems, A. R., Sassi, H., Nielsen, P. A., Rasmussen, K. J., Andersen, J. R., Johansen, L. E., Hansen, L. H., Jespersen, H., Podtelejnikov, A., Nielsen, E., Crawford, J., Poulsen, V., Sorensen, B. D., Matthiesen, J., Hendrickson, R. C., Gleeson, F., Pawson, T., Moran, M. F., Durocher, D., Mann, M., Hogue, C. W., Figeys, D. and Tyers, M. (2002) Systematic identification of protein complexes in Saccharomyces cerevisiae by mass spectrometry. Nature. **415**, 180-183

53 Ruehr, M. L., Russell, M. A. and Bond, M. (2004) A-kinase anchoring protein targeting of protein kinase A in the heart. J Mol Cell Cardiol. **37**, 653-665

54 Pouyssegur, J. (2000) Signal transduction. An arresting start for MAPK. Science. **290**, 1515-1518

55 Vondriska, T. M., Pass, J. M. and Ping, P. (2004) Scaffold proteins and assembly of multiprotein signaling complexes. J Mol Cell Cardiol. **37**, 391-397

56 Bantscheff, M., Scholten, A. and Heck, A. J. (2009) Revealing promiscuous drug-target interactions by chemical proteomics. Drug Discov Today. **14**, 1021-1029

57 Barglow, K. T. and Cravatt, B. F. (2007) Activity-based protein profiling for the functional annotation of enzymes. Nat Methods. **4**, 822-827

58 Scholten, A., van Veen, T. A., Vos, M. A. and Heck, A. J. (2007) Diversity of cAMP-dependent protein kinase isoforms and their anchoring proteins in mouse ventricular tissue. J Proteome Res. **6**, 1705-1717

59 Shiyama, T., Furuya, M., Yamazaki, A., Terada, T. and Tanaka, A. (2004) Design and synthesis of novel hydrophilic spacers for the reduction of nonspecific binding proteins on affinity resins. Bioorg Med Chem. **12**, 2831-2841

60 Puig, O., Caspary, F., Rigaut, G., Rutz, B., Bouveret, E., Bragado-Nilsson, E., Wilm, M. and Seraphin, B. (2001) The tandem affinity purification (TAP) method: a general procedure of protein complex purification. Methods. **24**, 218-229

61 Hanash, S. (2004) HUPO initiatives relevant to clinical proteomics. Mol Cell Proteomics. **3**, 298-301

62 Omenn, G. S. (2004) Advancement of biomarker discovery and validation through the HUPO plasma proteome project. Dis Markers. **20**, 131-134

63 Evans, G., Wheeler, C. H., Corbett, J. M. and Dunn, M. J. (1997) Construction of HSC-2DPAGE: a two-dimensional gel electrophoresis database of heart proteins. Electrophoresis. **18**, 471-479

64 Pleissner, K. P., Sander, S., Oswald, H., Regitz-Zagrosek, V. and Fleck, E. (1996) The construction of the World Wide Web-accessible myocardial two-dimensional gel

electrophoresis protein database "HEART-2DPAGE": a practical approach. Electrophoresis. **17**, 1386-1392

65 Watanabe, M., Okamura, T., Kokubo, Y., Higashiyama, A. and Okayama, A. (2009) Elevated serum creatine kinase predicts first-ever myocardial infarction: a 12-year population-based cohort study in Japan, the Suita study. Int J Epidemiol. **38**, 1571-1579

66 Ji, S. R., Ma, L., Bai, C. J., Shi, J. M., Li, H. Y., Potempa, L. A., Filep, J. G., Zhao, J. and Wu, Y. (2009) Monomeric C-reactive protein activates endothelial cells via interaction with lipid raft microdomains. Faseb J. **23**, 1806-1816

67 de Kleijn, D. P., Moll, F. L., Hellings, W. E., Ozsarlak-Sozer, G., de Bruin, P., Doevendans, P. A., Vink, A., Catanzariti, L. M., Schoneveld, A. H., Algra, A., Daemen, M. J., Biessen, E. A., de Jager, W., Zhang, H., de Vries, J. P., Falk, E., Lim, S. K., van der Spek, P. J., Sze, S. K. and Pasterkamp, G. (2009) Local Atherosclerotic Plaques Are a Source of Prognostic Biomarkers for Adverse Cardiovascular Events. Arterioscler Thromb Vasc Biol

68 Fernando, P., Deng, W., Pekalska, B., DeRepentigny, Y., Kothary, R., Kelly, J. F. and Megeney, L. A. (2005) Active kinase proteome screening reveals novel signal complexity in cardiomyopathy. Mol Cell Proteomics. **4**, 673-682

69 Faber, M. J., Dalinghaus, M., Lankhuizen, I. M., Bezstarosti, K., Dekkers, D. H., Duncker, D. J., Helbing, W. A. and Lamers, J. M. (2005) Proteomic changes in the pressure overloaded right ventricle after 6 weeks in young rats: correlations with the degree of hypertrophy. Proteomics. **5**, 2519-2530

70 White, M. Y., Cordwell, S. J., McCarron, H. C., Prasan, A. M., Craft, G., Hambly, B. D. and Jeremy, R. W. (2005) Proteomics of ischemia/reperfusion injury in rabbit myocardium reveals alterations to proteins of essential functional systems. Proteomics. **5**, 1395-1410

71 Heinke, M. Y., Wheeler, C. H., Chang, D., Einstein, R., Drake-Holland, A., Dunn, M. J. and dos Remedios, C. G. (1998) Protein changes observed in pacing-induced heart failure using two-dimensional electrophoresis. Electrophoresis. **19**, 2021-2030

72 Weekes, J., Wheeler, C. H., Yan, J. X., Weil, J., Eschenhagen, T., Scholtysik, G. and Dunn, M. J. (1999) Bovine dilated cardiomyopathy: proteomic analysis of an animal model of human dilated cardiomyopathy. Electrophoresis. **20**, 898-906

73 Gramolini, A. O., Kislinger, T., Liu, P., MacLennan, D. H. and Emili, A. (2007) Analyzing the cardiac muscle proteome by liquid chromatography-mass spectrometry-based expression proteomics. Methods Mol Biol. **357**, 15-31

74 Sridhar, R., Hanson-Painton, O. and Cooper, D. R. (2000) Protein kinases as therapeutic targets. Pharm Res. **17**, 1345-1353

75 Lissandron, V. and Zaccolo, M. (2006) Compartmentalized cAMP/PKA signalling regulates cardiac excitation-contraction coupling. J Muscle Res Cell Motil. **27**, 399-403

76 Movsesian, M. A. and Bristow, M. R. (2005) Alterations in cAMP-mediated signaling and their role in the pathophysiology of dilated cardiomyopathy. Curr Top Dev Biol. **68**, 25-48

Chapter 2

A Multi-Angular Mass Spectrometric View at Cyclic Nucleotide Dependent Protein Kinases:

In Vivo Characterization and Structure/Function Relationships

Arjen Scholten[1,2]
Thin Thin Aye[1,2]
Albert J.R. Heck[1,2]

[1]Department of Biomolecular Mass Spectrometry, Bijvoet Center for Biomolecular Research and Utrecht Institute for Pharmaceutical Sciences, Utrecht University, Sorbonnelaan 16, 3584 CA Utrecht, the Netherlands
[2] Netherlands Proteomics Centre, Utrecht University, The Netherlands

Mass Spectrom Rev. 2008 Jul-Aug;27(4):331-53. Review.

Abstract

Mass spectrometry has evolved in recent years to a well-accepted and increasingly important complementary technique in molecular and structural biology. Here we review the many contributions mass spectrometry based studies have made in recent years in our understanding of the important cyclic nucleotide activated protein kinase A (PKA) and protein kinase G (PKG). We both describe the characterization of kinase isozymes, substrate phosphorylation, binding partners and post-translational modifications by proteomics based methodologies as well as their structural and functional properties as revealed by native mass spectrometry, H/D exchange MS and ion mobility. Combining all these mass spectrometry based data with other biophysical and biochemical data has been of great help to unravel the intricate regulation of kinase function in the cell in all its magnificent complexity.

Contents

2.1. Introduction

2.1.1. Kinases, signaling and second messengers

Protein kinases represent a large and diverse class of proteins that play essential roles in intracellular signal transduction. All kinases catalyze the same chemical reaction; phosphorylation by transferring the γ-phosphate of ATP to the hydroxyl moiety of the substrate. Modulation of kinase activity is vitally important and their malfunction is linked to many diseases. In eukaryotic systems a plethora of possibly more than 500 genes encode for kinases, as a whole often referred to as the "kinome"(*1*), illustrating their importance and specificity of function. Organisms coordinate activities at every level of their organization often through complex multiprotein signaling complexes. In multicellular organisms, intercellular signaling events can act over great distances to induce physiological responses. In many cases, detection of a primary signal by cognate receptors affects the level of a second messenger that in turn controls the activity of kinases or phosphotases. Classic examples of such second messenger molecules are the cyclic nucleotides cyclic adenosine monophosphate (cAMP) and cyclic guanosine monophosphate (cGMP). A rise in cAMP concentration is induced by binding of, among others, catecholamines to a G-coupled β-adrenergic receptor, that is directly associated to adenylate cyclase that converts ATP into cAMP(*2*). cGMP can be induced by nitric oxide (NO) that originates from nearby different cell types. NO directly activates the intracellular soluble guanylate cyclase (sGC) that produces cGMP from GTP(*3, 4*). The formation of cGMP can also be initiated by a membrane bound guanylate cyclase (pGC) that responds to extracellular binding of natriuretic peptides(*5*). The second messenger molecules may activate a range of proteins, including both kinases and phosphotases. The major target of the second messenger molecules cAMP and cGMP are the protein kinases PKA (cAMP-dependent protein kinase) and PKG (cGMP-dependent protein kinase), respectively, the main subjects of this review. Through the years PKA, and to a lesser extent PKG, have been the subject of extensive investigation and much of the knowledge we currently have on kinase activity and regulation originates from these studies. In recent years mass spectrometry has taken an important role in these studies, for instance in the characterization of isozymes of the kinases, their post-translational modifications and interaction partners in the multi-protein signaling scaffolds, but also in the more in-depth structural analysis of conformational adaptation of the kinases upon activation, co-factor binding or binding to a scaffold. Here we review many of these recent studies, highlighting specifically the role of mass spectrometry, in all its flavors ranging from state-of-the art proteomics analysis using nanoLC MS/MS to more structural biology oriented studies using H/D exchange monitored by mass spectrometry to monitor protein folding and conformations.

Figure 1 displays an overview of the areas of research wherein mass spectrometry has contributed to enhance our understanding of the important kinases PKA and PKG. Before we review these mass spectrometry based studies we provide an introduction on the current knowledge about the protein kinases PKA and PKG.

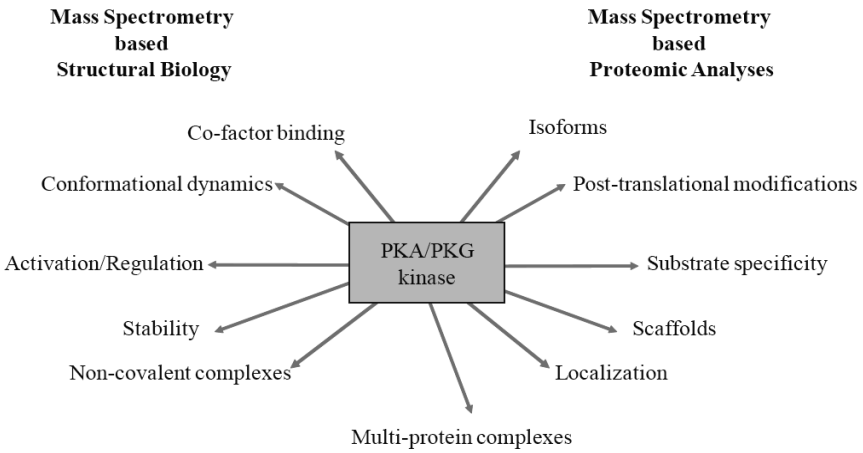

Figure 1. Schematic outline of this review, depicting the areas of research wherein mass spectrometry has contributed to our improved understanding of the kinases PKA and PKG.

2.1.2. The cyclic nucleotide dependent protein kinases PKA and PKG

2.1.2.1. Genes, isozymes, distribution and localization

The major target of cGMP is cGMP-dependent protein kinase (PKG). Mammals have two PKG genes, prkg1(*6, 7*) and prkg2(*8*), that encode, PKG type I and type II, respectively. PKG I has two splice variants, Iα and Iß that yield PKG forms with distinct differences in their first 80-100 amino acids.(*9, 10*) All PKG isozymes form dimeric protein structures with similar domain architectures, as depicted in Figure 2. At the very N-terminus reside the dimerization domain, followed by the autoinhibitory sequence, two cGMP binding domains and a catalytic domain. Binding of cGMP to both cGMP binding domains fully activates the protein to phosphorylate intracellular targets. Different types of PKG have different tissue distributions: the Iα-isozyme is mainly found in lung, heart, dorsal root ganglia and cerebellum. The Iß isozyme is highly expressed in platelets, hippocampal neurons and olfactory bulb neurons. The main effecter of cAMP is PKA. Although PKA has a similar domain architecture to PKG, it is composed of two genetically distinct subunits, the regulatory subunit (PKA-R) and the catalytic subunit (PKA-C), which form a hetero-tetrameric holoenzyme [$(PKA\text{-}R)_2$-$(PKA\text{-}C)_2$]. Upon stimulation by cAMP, the holoenzyme dissociates into [$R_2(cAMP)_4$] and two free, and active, PKA-C subunits that can phosphorylate intracellular targets (Figure 2). As cAMP levels drop, it dissociates from the PKA-R dimer, thereby preparing it to bind, and inactivate, PKA-C again (*14, 15*). The mammalian PKA family is quite diverse and includes four types of PKA-R and three of PKA-C, each encoded by a unique gene; PKA-RIα, -RIIα, -RIß, RIIß and PKA-Cα and –Cß and -Cγ.(*16, 17*).

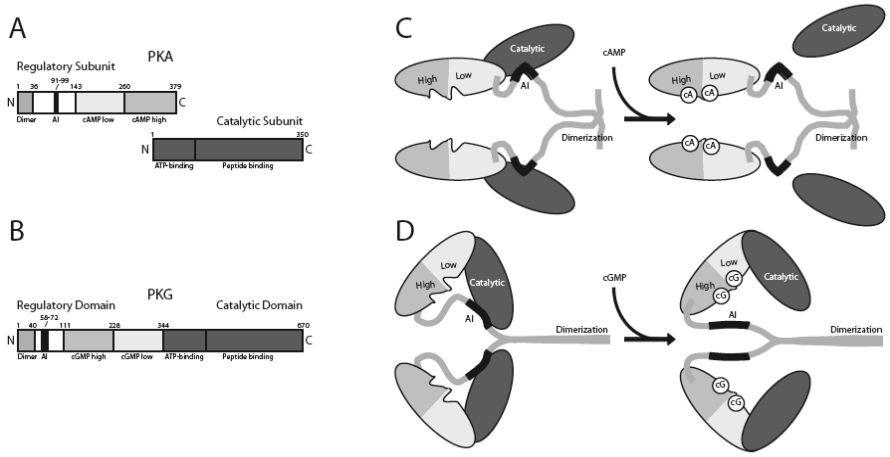

Figure 2. Domain organization and structural models of PKA and PKG, in their inactivated and activated form. A) Domain organization of PKA. B) Domain organization of PKG. Domains with high sequence homology between PKA and PKG are depicted in similar colors. AI=auto-inhibitory domain. C) Structural model of PKA activation. PKA is a holo-enzyme consisting of a regulatory subunit dimer and two catalytic subunits. Activation of PKA occurs when four molecules of cAMP bind to the R subunit dimer, two to each subunit. When both cAMP binding sites are occupied the R subunit adopts a confirmation with low affinity for the C subunit and the holo-enzyme dissociates. D) Structural model of PKG activation. Activation of PKG occurs when four molecules of cGMP bind. They induce a significant conformational change in the protein whereby the auto-inhibitory (AI) domain which obstructs activity is discharged. Smooth muscle, including uterus, vessels, intestine and trachea contain both Iα and Iß isozymes(11). Myristoylation anchors PKG type II at the plasma membrane(12). This type is only present in kidney, cerebellum and mucosa.(13) [Color Figure can be viewed in the online issue, which is available at www.interscience.wiley.com]

The current available evidence suggests that each PKA-R isozyme can generate homo-dimers, which can associate with either PKA-C isozyme.(*18, 19*). To make things even more complex, also the existence of a PKA-RIα/RIß heterodimer was reported.(*20*) A further diversification of PKA family members in mammals is attained by the presence of multiple splice variants of the C-subunits.(*21*) This eventually leads to a large variety of different PKA holoenzymes. Concerning tissue distributions, it was demonstrated that RIα is expressed in the heart and central nervous system, whereas RIß expression is more restricted to nervous tissues such as the spinal cord and the brain.(*22*) Furthermore, RIIα and RIIß are both expressed in the brain, and show distinct patterns of expression with RIIα predominantly expressed in the heart and RIIß expressed mainly in the liver and fat tissue(*23*). The differential expression pattern hints towards different functional assignments of the different

PKA subtypes, thereby suggesting they are not redundant proteins. This is further reiterated by studies using different PKA-R knock-out mice models as reviewed earlier (*24*).

Where and when enzymes become active has profound implications on the cellular processes that they control. For PKA, strong spatial resolution is attained through the interaction of the regulatory subunit dimer with the diverse family of A-kinase anchoring proteins (AKAPs), which localizes cAMP signaling complexes, often including phosphatases and phosphodiesterases, to discrete intracellular compartments(*25*). Since the discovery of the first AKAP, MAP2 (*26*), the family of PKA anchoring proteins has grown to (including splice variants) more than 50 very diverse members. An overview of the in the literature described AKAPs, including the nomenclature synonyms and splice variants, the tissues they have been primarily detected in, and the concomitant proteins observed in the scaffolding complexes, is given in Table 1.

Table 1. Summary of AKAP nomenclature, described binding partners and tissue distribution. For AKAP7 and AKAP9, specific splice isoforms, depicted between brackets, form different complexes or show different tissue distributions.

Gene symbol	Synonyms Splice variants	Proteins in complex	Tissue(s)	Refs
AKAP1	D-AKAP1 sAKAP84 AKAP121 AKAP149	PKA, PP1, PDE4A, PTPD1, AMY-1	Testis, sperm	(*27-32*)
AKAP2	AKAP-KL PALM2-AKAP2	PKA	Kidney, lung, cerebellum, heart	(*33, 34*)
AKAP3	AKAP110 FSP95 SOB1	PKA, AKAP4, PDE4A, Sp17, Ropporin1, ASP, $G_{\alpha}13$, Fibrous sheath protein 1 and 2	Testis, sperm	(*35-40*)
AKAP4	p82 AKAP82 Fsc1	PKA, AKAP3, Fibrous sheath protein 1 and 2	Testis, sperm	(*38, 41*)
AKAP5	AKAP150 AKAP75 AKAP79	PKA, AMPA-R, PP2B, PKC, β_2-AR, Kir2.1, SAP97, PSD-95, NMDA-R,L-type Ca^{2+}-channels, GABA-A-R, IQGAP1, Adenylate Cyclase V and VI, ASIC1a and ASIC2a	Brain, neurons	(*42-53*)
AKAP6	mAKAP AKAP100	PKA, PDE4D3, RyR, PP1, NCX1, PKC, PP2A, nesprin-1α, Epac1, ERK5-kinase, PDK1	Skeletal muscle, heart, brain	(*54-61*)
AKAP7	AKAP15 AKAP18	PKA, Ca_v - and Na_v-channels, AQP2 channels	Pancreas, brain (α and ß), placenta (γ), kidney and heart (δ)	(*62-66*)
AKAP8	AKAP95	PKA, p68 RNA helicase, D-type Cyclins, PDE4A, AMY-1, ACAP-D2/Eg7, Caspase-3, G_1-S Cylcins, Fidgetin, HDAC3	Brain, thyroid, T-lymphocytes	(*30, 32, 67-75*)
AKAP9	AKAP350 AKAP450	PKA, NMDA-R, PP1, PKCε, KCNQ1 channel, TACC1, Casein kinase 1,	Brain, skeletal muscle, heart,	(*76-87*)

	CG-NAP Yotiao	Intracellular Cl^- channel (CLIC), γ-tubulin complex 2 and 3 (GCP2/3), Ran, PDE4D3, IP_3-receptor	testis, pancreas (Yotiao) Brain, colon, liver (AKAP350) Kidney (AKAP450)	
AKAP10	D-AKAP2	PKA, PDZK1	Testis, kidney, lung	(*88, 89*)
AKAP11	AKAP220	PKA, PP1c, GSK3ß		(*90-92*)
AKAP12	Gravin AKAP250 SSeCKS	PKA, PKC, $ß_2$-AR, CaM, Cyclin-D, GalT, Src	Brain, testis	(*93-99*)
AKAP13	AKAP-Lbc Ht31	PKA, Rho, 14-3-3, CTNNAL1, tTG	Heart, placenta, lung	(*100-104*)
AKAP14	T-AKAP80 AKAP28	-	Testis	(*105*)
VIL2	Ezrin Villin 2	PKA, CFTR, NHERF, E3KARP, NHE3	Spleen, intestine, uturus, kidney, heart	(*106-108*)
WAVE1	SCAR	PKA, Abl (Abelson tyrosine kinase), Arp2/3, NAP125, PIR121, HSPC300, Abi, WRP, Rac, profilin	Brain	(*109-111*)
Rab32	-	PKA	Liver, Kidney	(*112*)
SKIP	-	PKA, Sphingosine kinase type 1	Heart	(*113, 114*)
BIG2	Brefeldin A inhibited GEP2	PKA, exocyst protein 70, AMY1	Heart, brain, placenta, kidney, pancreas	(*115*) (*116-118*)
MTG16b	Myeloid Translocation Gene 16b	PKA, PDE4A, PDE7A	T-lymphocytes	(*30, 119*)
Myosin VIIA		PKA, Vezatin	Eyes, ears	(*120, 121*)
MyRIP	Slac2-c	PKA, Rab27, Myosin-Va/VIIA	brain, kidney, heart, liver, lung, muscle, testis and pancreas	(*122, 123*)
Pericentrin	-	PKA, PKC	Kidney, thymus, liver	(*124, 125*)
MAP2	Microtubule associated protein 2	PKA, Tubulin, ERK3	Brain, testis	(*126-128*)
Myosprin	CMYA5	PKA, dysbindin, desmin	Heart, Skeletal muscle	(*129-131*)
Merlin	Schwannomin	PKA, Ezrin	Neurons, hippocampus	(*132, 133*)
Synemin	-	PKA, many cytoskeletal proteins	Heart, brain	(*134*)
$α_4$-integrin		PKA, paxillin	Ubiquitous	(*135, 136*)

The most important similarity between AKAPs is their ability to anchor PKA-R. Much effort has been put in the characterization of the PKA-AKAP interaction. Early on, deletion mapping studies identified a region of MAP2 that mediates association with PKA-RII (*137, 138*). Later work by Carr *et al.* identified the interaction domain to be an amphipathic helix of approximately 14-17 amino acid residues long (*139*). An amphipathic helix is defined as an alpha helix with opposing polar and non-polar faces, i.e. a hydrophilic and a hydrophobic side. Although no strong consensus sequence has emerged, helical wheel alignments of over

20 AKAPs have shown the presence of the amphipathic helix to be essential for PKA anchoring. Further evidence for this was provided by the introduction of presumed helix disrupting residues in the amphipathic helix domain that revealed an abolished PKA-R interaction both *in vitro* and *in vivo* (*139, 140*). Most AKAPs known to date have high affinity specifically for the RII regulatory subunit of PKA, whereas a few bind also or even more specifically to RI. For instance, the dual specificity AKAP mAKAP (AKAP6) binds to both RI and RII, in a similar fashion via the amphipathic helix.

Recently, it was shown that α4 integrins bind specifically to the RI sub-unit of PKA (*135*). However this interaction requires the intact holo-enzyme and seems to bind through a different kind of interaction as observed for the other AKAPs, i.e. not via the dimerization motif of the RI dimer, extending the repertoire of PKA scaffolding proteins in cAMP-signaling even further.

2.1.2.2. Structural Features

PKG and PKA belong to the family of serine/threonine kinases. Both are activated by cyclic nucleotides and share many common structural features. Both kinases contain three functional domains: An amino-terminal domain that mediates dimerization, intracellular localization and auto-inhibition; a regulatory domain that has two in-tandem cyclic nucleotide binding pockets; and a catalytic domain consisting of an ATP/Mg^{2+} and a substrate binding site. In Figure 2 schematic representations are given of the domain structure of PKA and PKG. Besides the strong similarities, the striking difference between the two is that PKA forms the earlier mentioned [$(PKA\text{-}R)_2$-$(PKA\text{-}C)_2$]- hetero tetramer, whereas PKG is a homodimer, whereby the regulatory and catalytic domain are present on a single polypeptide. In recent years, crystallographic structures of PKA-R, PKA-C and the hole-enzyme, have greatly contributed to our understanding of protein kinase function and regulation. (For review, Taylor *et al.* (*14, 15*)). To date, there is no crystal structure of PKG available. Below, the three different functional domains of PKA and PKG will be discussed in more detail.

2.1.2.2.1. The N-terminal domain: dimerization, intracellular localization and autoinhibition

For both cyclic nucleotide kinases, the N-terminus regulates the same three functions, dimerization, intracellular localization and auto-inhibition. For PKA, detailed NMR in solution structure determination by Newlon *et al.* (*141*) allowed a comprehensive view on the interaction between the two PKA-R monomers. In addition, they describe the interaction of the PKA-R dimer with a representative AKAP-anchoring domain peptide, which allowed the first view at the molecular mechanism underlying PKA-R's intracellular localization through interaction with AKAPs (*141-143*). The $(PKA\text{-}R)_2$ molecule forms a so-called X-type four helix bundle dimerization motif with an extended hydrophobic face. This hydrophobic face is essential for the interaction with the non-polar side of the AKAP's amphipathic helix motif.

The structure of the dimerization domains of all PKG isozymes (Iα, Iß and II) are very different from PKA. They dimerize through an α-helix with a hydrophobic leucine/isoleucine zipper motif. This helix contains either a leucine, or isoleucine, at every first out of seven amino acids, also referred to as a heptad repeat.(*144-146*) The presence of this motif, makes all the PKG isozymes homodimeric proteins.(*147-150*) Deletion studies within the N-terminal domain revealed several of its functions. It was established early on that proteolytic cleavage of PKG Iα yielded a fragment, later designated as PKG Δ1-77 that is monomeric(*151*), binds two cGMP molecules and is constitutively active.(*152*) These data indicate that the N-terminus keeps PKG in the inactive state, or auto-inhibited and assures dimerization. The autoinhibitory region of PKG contains a pseudo-substrate sequence (K/R-K/R-X-G/A-I/V-S-A-E-P/S) that efficiently inhibits it in absence of bound cGMP.(*153*) Later, the autoinhibitory domain was pinpointed to be located around Ile63 and Ser64 in PKG Iα.(*154, 155*) Besides regulation of PKG by cGMP, a more complex regulating mechanism of PKG was proposed when it was found that both PKG isozymes can autophosphorylate several residues in their N-termini.(*149, 156-158*) Although the exact physiological role of the autophosphorylation events is unclear, it was found that recombinant autophosphorylated PKG showed an increased affinity for cAMP *in vitro*.(*158-160*)

Although PKG Iα and Iß do not differ in sequence beyond the N-terminus, the activation constant (K_a) is shifted 15-fold up for PKG Iß.(*148*) Therefore it was hypothesized that the N-terminus also mediates PKG's affinity for cGMP. PKG Iα was observed to have a high and a low affinity site, that bind cGMP with 10 and 150 nM K_d values respectively, while PKG Iß has two low affinity sites. (*148, 161*) High affinity binding of cGMP to PKG Iα is based on positive cooperativity between the two binding sites, i.e. binding of one molecule cGMP facilitates the binding of another. Clearly this was mediated by the N-terminus as PKG Δ1-77 had lost cooperativity.(*162*).

Although much less well defined as PKA-AKAP interactions, for PKG it was found that the N-terminus is essential for interaction with so-called G-kinase anchoring proteins (GKAPs).(*163-165*) Interestingly, PKG type II is myrisotylated at the amino terminus, localizing the enzyme to the plasma membrane and enabling it to phosphorylate the intestinal chloride channel CFTR.(*12, 166*)

2.1.2.2.2. Cyclic nucleotide binding domains

Throughout cyclic nucleotide binding proteins, the motifs present in these pockets is well conserved across species, even as far as *E. Coli* and *Drosophila*.(*167, 168*). All cAMP and cGMP binding sites show high structural and sequence conservation. Crystallographic structures of PKA-R showed that each cAMP-binding domain is composed of a helical subdomain and an eight-stranded β-barrels where cAMP binds. The essential feature of the β-barrel is a conserved phosphate binding cassette (PBC) that anchors the cAMP. The cAMP binding domains are joined to the dimerization domain by a flexible linker, which also

includes the autoinhibitory sequence that docks to PKA-C in the absence of cAMP. There is also strong conservation between cAMP and cGMP binding domains. Interestingly, a single residue seems to determine cAMP/cGMP specificity. In PKG (and cGMP specific phosphodiesterases (PDE) and cyclic nucleotide gated ion channels (CNG), the cGMP specificity (>100 fold over cAMP) is largely determined by the presence of a single threonine (e.g. T177 and T301 in human PKG Iα) that specifically interacts with the guanine base of cGMP.(*169*) In PKA, this residue is replaced by an alanine (e.g. A211 and A335 in human PKA-RIα), thereby providing an almost entirely hydrophobic environment for the more hydrophobic adenine moiety. When the threonine of PKG's cGMP binding domain is substituted by an alanine, the cGMP specificity over cAMP is annulled. Likewise, the implementation of a threonine on the invariant alanine in PKA increases its affinity for cGMP.(*170, 171*) Another important site in these pockets is the glutamate within the conserved sequence F-G-E (about 10 amino acids upstream of the earlier mentioned T or A residues), which forms a hydrogen bond with the riboside 2'-hydroxyl group of either cGMP or cAMP. An arginine next to the threonine (or alanine) is essential and conserved to chelate the cyclic phosphate diester.(*172-174*)

2.1.2.2.3. Catalytic domain

Not only PKA and PKG, but all eukaryotic protein kinases, show high structural similarity in their catalytic domains; the two-lobed catalytic core consists of a small lobe with the ATP-binding domain and a large lobe that harbors the peptide (substrate) binding and catalytic site.(*175, 176*) From extensive crystallographic analyses of PKA-R and PKA-C in the presence and absence of cAMP, ATP and peptide substrates and inhibitors, major aspects of the structure function relationships could be studied. Some of the results obtained with PKA could be extrapolated to PKG, for which a crystal structure is still lacking. The study by Dostmann *et al*. in which the catalytic domain of PKG is modeled to PKA-C is most useful in this respect.(*177*)

Extensive studies utilizing peptide libraries revealed very similar substrate specificity for PKA and PKG: KRAERKA<u>S</u>IY and TQAKRKK<u>S</u>NA, or more generally R(R/K)X(S/T), and (R/K2-3)(X/K)(S/T), respectively. (*177, 178*) Therefore it is believed that subtle differences in the substrate interaction sites on the large catalytic lobe of PKG and PKA determine substrate specificity. Many substrates of PKA and PKG can be phosphorylated by both kinases *in vitro*, once again reiterating the importance of compartmentalization for them *in vivo*. The crystallographic structure of the PKA-C subunit in complex with the inhibitor peptide PKI 5-24 and Mg^{2+}/ATP revealed many of the kinase/substrate interactions involved in catalysis.(*179, 180*) Extrapolation of these results to PKG shows many similarities.(*181*) First there is the GXGXXGXV motif that starts at Gly366 that is postulated to function as a hydrophobic pocket to bind the adenine ring of ATP. Further towards the C-terminus resides the linker region (Lys431-Ser454) that links the two lobes. Conserved Glu443 of this linker is

believed to function as the electronegative interactor with one of the basic residues in the substrate consensus sequence (possibly Lys6 in TQAKRKKSNA). The region between Tyr481 and Asn488 is candidate to function as the catalytic loop with Asp483 as the possible proton acceptor of the serine or threonine hydroxyl group. Lys485, also in the catalytic loop is implicated to facilitate phosphotransfer by neutralizing the negative charge of the γ-phosphate. The very C-terminus of PKG is likely to contribute to substrate recognition, as it does in PKA.(*182*)

In the cleft between the two lobes, the actual phosphotransferase reaction takes place. The most important structural feature within the catalytic domain of PKG is the permanent phosphorylation of Thr516 (in PKG Iα).(*183*) This phosphorylation is essential for catalytic activity. In many other kinases a similar phosphorylation at a threonine or tyrosine residue in the catalytic domain is essential for activity and in several cases this event is actually working as the on/off switch of the protein. Therefore the region that contains this phosphorylation is also designated as the activation loop (*184*). It is believed that hydrogen bonds of the phosphate oxygens permit proper orientation of the substrate.

2.2. Mass Spectrometry based Proteomic Analyses

2.2.1. Characterization of isozymes

The identification of specific isozymes of PKA and PKG occurring *in vivo* is not straightforward. For instance, initially, two different isozymes of PKA, type I and type II, were identified based on their pattern of elution from cellulose columns (*185*), but this method requires significant band shifts, and is typically unable to resolve more homologue isozymes. Moreover, also for the PKA catalytic subunit several isoforms have been observed. The specific isozymes of PKA (and PKG) have high sequence similarity (for PKA see Figure 3), but often only a single isozyme is recruited for specific tasks (*186, 187*). Illustrative is the identification of PKA-isozyme specific interactions with different AKAPs (*188*). This makes the proper analysis of specific isozymes in the study of cyclic nucleotide signaling function imperative. Hitherto, the identification of specific isozymes of PKA and PKG *in vivo* in a complex sample, such as a protein lysate, relies heavily on the use of enrichment techniques based on specific antibodies, which however turned out to be quite cumbersome as all PKA (and PKG) isozymes have high sequence and structural homology.

In recent years, mass spectrometry, and specifically nanoLC MS/MS, has developed towards becoming the standard on high-throughput protein identification. One of the major challenges in the mass spectrometric identification of proteins in highly complex mixtures is the limited dynamic range. This makes the identification of somewhat lower abundant proteins (signaling proteins like PKA and PKG) in the presence of high abundant housekeeping proteins (like actin, GAPDH, myosin etc.) intrinsically difficult. Therefore, the characterization and identification of e.g. cAMP/cGMP signaling proteins by mass spectrometry requires a pre-fractionation. For instance, by the use of abovementioned

PKA/PKG targeted antibodies or alternatively by using affinity resins using immobilized cAMP or cGMP. The latter approach is nowadays often referred to as chemical proteomics (*75, 189, 190*). For isozyme characterization, identification by a few peptides, which is still the standard in most proteomics experiments, is not sufficient. Isozyme characterization requires high sequence coverage of the proteins of interest, which can be best obtained by a combination of protein enrichment, in-solution digestion by a variety of proteases and state-of-the-art nanoLC-MS/MS analysis. A specific enrichment with immobilized cAMP proved very valuable in the identification of all *in vivo* occurring PKA-R isozymes in mammalian tissue within a single experiment (*34*).

To illustrate this in Figure 3 the sequences of all four known PKA R subunits in human (RIα, RIβ, RIIα and RIIβ) are aligned, whereby the obtained sequence coverage in chemical proteomics experiments in human heart tissue is indicated (unpublished data). Peptides that are potentially shared by different isozymes are gray-colored, whereas for isozymes specific/unique peptides are in boxes. These unique peptides are true indicators of the presence of the isozyme in the sample. In principle these unique detected peptides provide means for differential and absolute quantification of the isozyme, using stable isotope labeling (*191*) or the AQUA methodology, preparing an isotopically labeled internal standard (*192*).

Unfortunately, the affinity enrichment technique using immobilized cAMP does not directly enrich for the catalytic sub-unit of PKA, for which also many isozymes have been described. Bowen at al. (*193*) reported a similar strategy that may be used to focus on PKA-C isozymes and its splice-variants occurring in the nematode *C. Elegans*. Therefore, the C-subunits were affinity purified using an immobilized PKI (Protein Kinase Inhibitor) peptide. Mass spectrometric analysis revealed several isozymes and splice-variants whose abundance was found to depend significantly on the developmental stage of the nematode (*193*).

2.2.2. Identification of PKA/PKG interactors

In a pioneering study by Lohmann *et al.* (*127*), immobilized cAMP was amended in combination with SDS-PAGE to find that the regulatory subunit of PKA co-purifies with a variety of specific proteins and that this group of specific proteins is different in different tissues. One of the co-purified proteins was identified as MAP2, designated as the first AKAP two years earlier (*26*). The diverse family of AKAPs provides strong spatial resolution for PKA through interaction with the regulatory subunit of the dimer. Through these interactions cAMP is accumulated, in larger multiprotein signaling complexes, often including phosphatases and PDEs, in discrete intracellular compartments.(*25*) With current mass spectrometric techniques, the identification of many different AKAPs in a single sample is achievable (*34, 114*). We performed a similar experiment as Lohmann *et al.*(*127*) but identified all proteins by state-of-the-art LC-MS/MS. In a single experiment on a single mouse ventricular tissue sample, we were able to identify 13 different AKAP families. For several of them multiple splice variants were identified based on distinct isozyme determining

peptide identifications. It was also demonstrated how such an approach can aid in the identification of novel AKAPs. For instance, by probing the cAMP-interactome dataset of protein sequences *in silico* for the presence of the AKAP interaction domains.(*139, 194*) In this way, we designated sphingosine kinase 1 interacting protein (SKIP) as a potential novel AKAP in rat ventricular tissue (*114*).

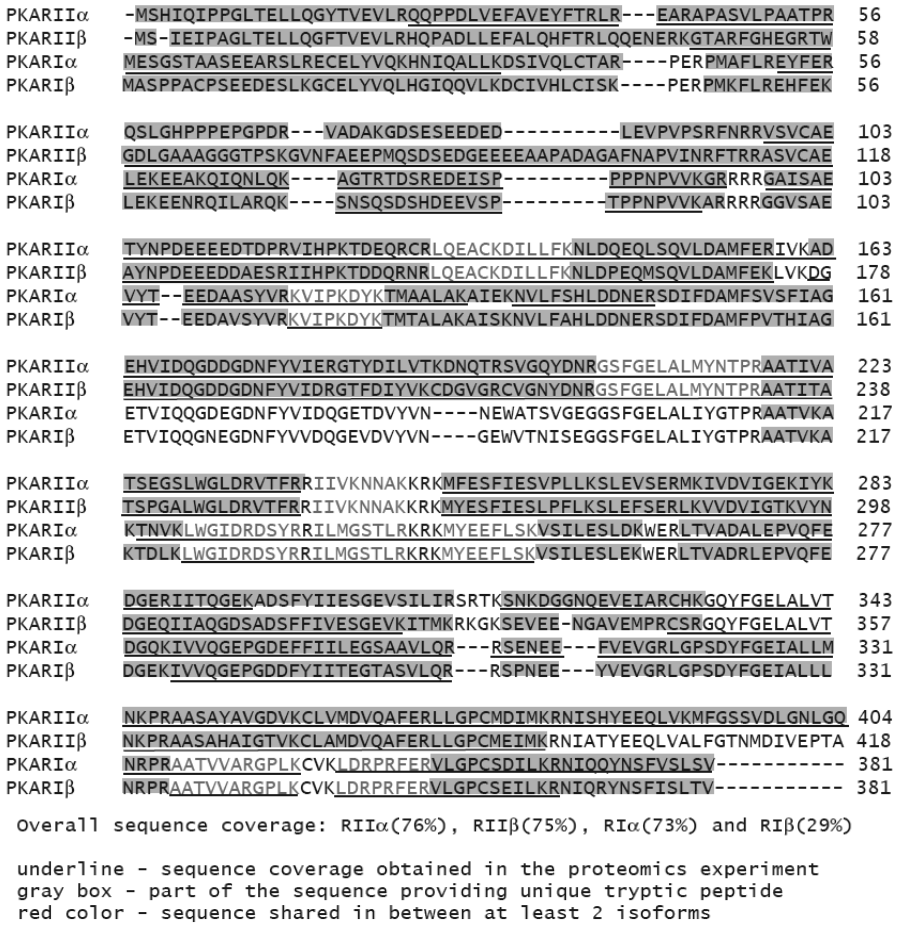

Figure 3. Alignment of the four human PKA regulatory subunits RIα, RIβ, RIIα and RIIβ, together with the extensive sequence coverage obtained in cAMP affinity-based chemical proteomics experiments in human heart tissue (unpublished data), whereby the gray boxed peptide sequences are unique peptides, whereas the red colored boxes represent shared peptide sequences in between at least two of the isozymes [Color Figure can be viewed in the online issue, which is available at www.interscience.wiley.com]

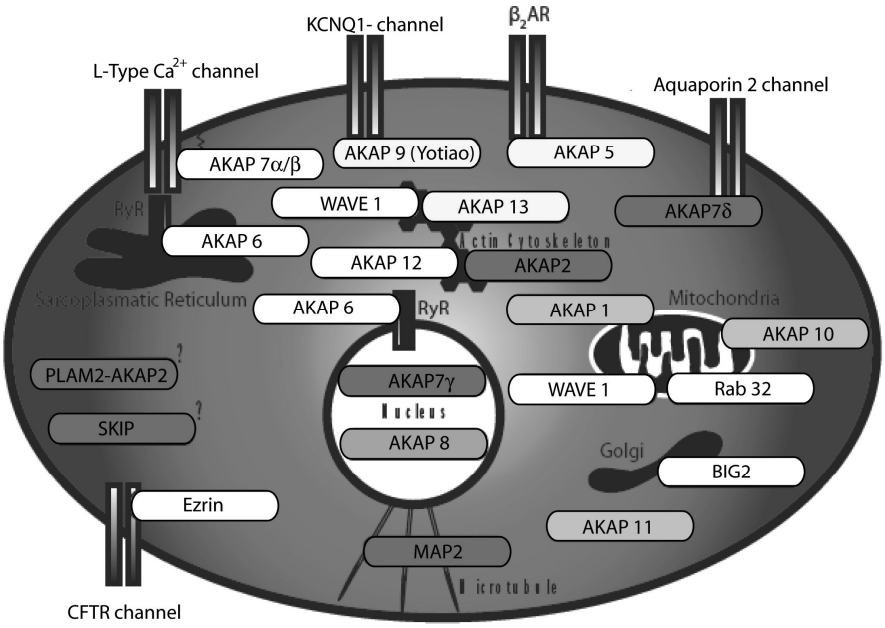

Figure 4. Overview of detected AKAPs in chemical proteomics experiments on mouse ventricular heart tissue, whereby their putative intracellular interaction points are annotated. Adapted from (34). [Color Figure can be viewed in the online issue, which is available at www.interscience.wiley.com]

In Figure 4, an overview of all AKAPs detected in such chemical proteomics experiments on mouse ventricular heart tissue are depicted, whereby their putative intracellular interaction points are annotated. More and more biologists start to use the protein identification power of current LC-MS/MS techniques, often at the exploratory point of an investigation where the characterization of specific interactors of a target protein is required. These unknown interactors are often obtained by different affinity purification methods like chemical proteomics (*195*), genetically tagged proteins (*196*) and immunoprecipitation. Often, the initial identification of an interactor or complex constituent is the starting point for a range of functional biological experiments. In the cyclic nucleotide signaling field this is of particular interest, as the AKAP conundrum shows that specificity of signaling is attained by intracellular localization of specific PKA-AKAP complexes near their targets. A nice example of this latter approach was reported by Schlossmann and co-workers who observed the co-purification of an unknown protein when isolating PKG Iβ by immobilized cGMP and immunoprecipitation (*187*). Initially, mass spectrometry was used for identification of this novel protein that was designated as IRAG. The IP_3-receptor was also found to be part of this complex. Subsequent experiments then showed the function of this complex in the regulation

of intracellular calcium levels. In experiments in our laboratory we were able to co-purify PKG I with IRAG in rat lung tissue; obtaining a high sequence coverage allowing us to identify several phosphorylation sites on IRAG (unpublished data). A potential advantage and disadvantage of the use of immobilized cyclic nucleotide beads is that they cross-react, as both cAMP and cGMP beads enrich both for PKA and PKG. It would be interesting in the future to design beads that would be able to selectively enrich for either PKA or PKG, or even better specific PKA isozymes.

2.2.3. Phosphorylation states of PKA and PKG

Besides performing phosphorylation on substrate proteins, it is known that both PKA and PKG are *in vivo* phosphorylated and have the ability to autophosphorylate (*156, 197*) PKA-C is found autophosphorylated at Thr197 and Ser338, while PKA-RII autophosphorylates at Ser97 (*198*). PKA-RI seems not to autophosphorylate itself (*199*). In addition, PKA-R and PKA-C are subject to heterophosphorylation by other kinases, such as casein kinase II and glycogen synthese kinase 3β (*200*). LC-ESI-MS/MS techniques allow the study of protein phosphorylation due to specific ion fragmentation patterns that occur upon dissociation of the phosphopeptides in tandem MS. In combination with vital phosphopeptide enrichment techniques, such as metal ion affinity resins based on immobilized metal affinity chromatography (IMAC) (*201, 202*) and the more recently introduced use of solid titanium dioxide (TiO_2) particles (*157, 203, 204*) a wide-range analysis of *in vivo* phosphorylation sites has become available. Implementation of these techniques in analytical platforms has increased the abilities to detect phosphorylated peptides tremendously, even when they are quite low abundant, for instance due to sub-stoichiometric phosphorylation events.

The TiO_2-based phosphopeptide enrichment technique was pioneered in our laboratory. In fact, the analysis of PKG's autophosphorylation sites was one of the first biological questions addressed using this new enrichment method (*157*). Bovine PKG Iα was *in vitro* auto-phosphorylated for 0, 10 and 60 minutes. Using the TiO_2 enrichment technique and two different proteases the PKG sequence could be largely covered. From the extracted ion chromatograms the amount of phosphorylation was differentially quantified and the extent of autophosphorylation could be determined. In this study Thr516 and Ser26 were found to be endogenously phosphorylated in PKG Iα purified from bovine lung. Thr516, as mentioned earlier, resides in the activation loop and is required for catalytic activity. Ser50, Thr58 and Ser72 were found to be rapidly autophosphorylated, while autophosphorylation on Ser44, Ser64 and Thr84 showed a slower incorporation. More recently, the mass spectrometric characterization of endogenous mouse ventricular PKG enriched by immobilized cGMP, revealed the presence *in vivo* of a phosphate at Ser 64, Thr84 and Thr516 (*205*). Characterization of PKA-RIα in mouse ventricular tissue resulted in the identification of Ser77 and Ser83, while for PKA RIIα the known Ser97 was found (*34*).

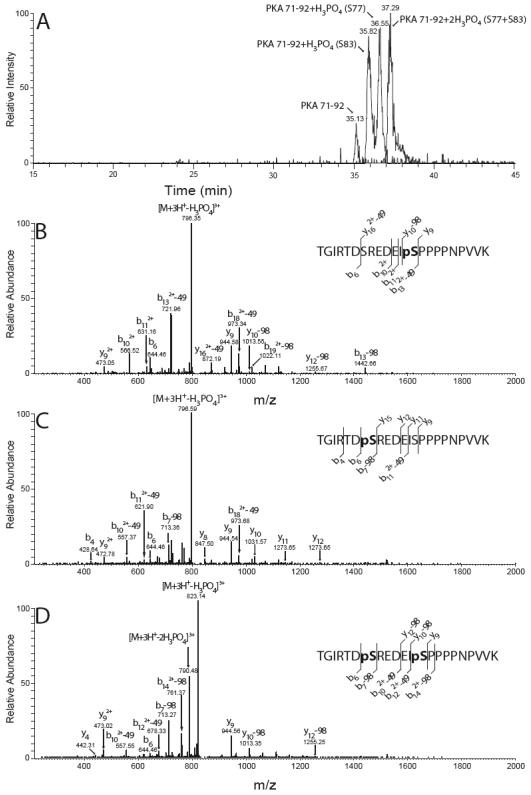

Figure 5. (A) Overlayed Single Ion Chromatograms (SICs) of PKA RIα peptide 71-92 in the non-, singly and doubly phosphorylated form. SICs were generated with precursor masses of the 3^+ ions at m/z 802.09, 828.74 and 855.40 ± 0.02 Da respectively. B) MS/MS spectrum corresponding to peak at 35.82 min. C) tandem MS spectrum of peak at 36.55 D) MS/MS spectrum of doubly phosphorylated peptide with a retention time of 37.29 min. Also depicted are observed b- and y-ions that were crucial for the annotation of the phosphate group at the specified position(s) in the differentially modified peptide 71-92. Adapted from (34).

Interestingly, as illustrated in Figure 5, for PKA-RIα, in mouse ventricular tissue, peptides originating from the amino acids 71-92, containing the phosphorylation sites Ser77 and Ser83, were detected as non-, singly and doubly phosphorylated, revealing that at least 4 differently phosphorylated PKA RIα species are present *in vivo* in mouse heart tissue, adding to the complexity in regulation in the PKA system. Recently more mass spectrometric data on the post-translational modifications of PKA-C have been reported as well (*206*), including two autophosphorylation sites on the Cα-subunit of recombinantly expressed murine PKA. The exact physiological role for most of these phosphorylation events remain to be solved, which is not a simple task.

2.2.4. Phosphorylation by PKA and PKG

Based on an extensive body of work with peptide substrates *in vitro* and mapping of potential physiological phosphorylation sites *in vivo*, PKA is well known to phosphorylate substrates with the general motif R(R/K)X(S/T), whereas the consensus for PKG is (R/K2-3)(X/K)(S/T). In a recent large scale phosphoproteomic dataset obtained from human activated cells (*203*) thousands of phosphopeptides were reported. Evaluation of short protein sequence motifs around the detected sites for agreement with the known PKA consensus motif identified hundreds of putative PKA induced phosphorylation sites (*203*). Similarly, in other large phosphoproteomics datasets (*202, 204*) numerous putative PKA and PKG induced phosphorylation sites can be identified. Huang *et al*. (*207*) reported a more targeted systematic proteomics approach, using stable isotope dimetyl labeling (*208, 209*), whereby quantification depended on MS detection, for the identification of substrates of PKA and PKG, in pregnant rat uteri, using recombinant PKA and PKG. To facilitate detection, exogenous phosphatases were added to the samples to remove intrinsic phosphorylation followed by a heating step to inactivate all enzymes. A total of 61 and 12 substrate candidates were identified *in vitro* for PKA and PKG, respectively, whereby most of these sites contained consensus motifs of each kinase with only a few sites overlapped, indicating a good specificity. Moreover, differential phosphoproteomics analysis using stable isotope dimethyl labeling and MS was performed to detect the change of protein phosphorylation upon kinase stimulation *in vivo*.

It is expected that in the next few years a wealth of new data on phosphoproteins and the specific sites of phosphorylation will become available, both from comprehensive phosphoproteomics analysis as well as more targeted approaches, zooming in on a specific kinase isozyme or substrate. This will certainly help to better understand the specificity of PKA and PKG, and their isozymes, *in vivo*. However, as mentioned above, the functional annotation of this wealth of phosphoproteomics data provides already the next big challenge.

2.3. Mass Spectrometry based Structural Biology

For PKA, primarily through the availability of high-resolution X-ray structures, a wealth of information is available on the structural properties, albeit mostly of individual domains, as described in the introduction. However, to fully understand the molecular function and structural biology of PKA and PKG, one would ideally investigate the dynamic properties of the kinases in solution, which can be attained through a variety of biophysical techniques. To complement crystallographic structures, fluorescence anisotropy (*210, 211*), NMR (*141, 212*) and, most recently, FT-IR (*213*) have been used to probe the dynamical behavior of PKA-R in its binding to PKA-C and AKAPs. Fluorescence anisotropy for instance showed, before the holoenzyme structure was solved, that the flexible linker of PKA-RIα became more ordered upon binding to PKA-C. This was confirmed for PKA-RIIß, by endogenous tryptophan fluorescence.(*214*) FT-IR studies suggested an overall increase in dynamics of both PKA-R and PKA-C in the holoenzyme, compared to the cAMP bound

PKA-R and active PKA-C.(*213*) The fact that cAMP binding stabilizes PKA-R was also obtained by the observed urea unfolding stabilization of 7.1 kcal mol^{-1} upon cAMP-binding (*215*). NMR studies on the N-terminal docking/dimerization (PKA-R 1-44) domain of PKA revealed the different interfaces that PKA-RI and PKA-RII present, thereby explaining the specificity for the individual subtypes of AKAPs (*142, 188, 212*).

2.3.1. Structural properties of PKA probed by mass spectrometry

To complement the above studies and to gain further insight into the structural changes that occur upon ligand binding and/or protein-protein interactions hydrogen/deuterium exchange (HDX) in combination with mass spectrometry has been used to study PKA. Detailed reviews on this technique are available (*216, 217*). Komives and co-workers (*218*) investigated the detailed protein-peptide interface of PKA-C in presence of ATP/Mg^{2+} and PKI(5-24), a strong PKA inhibitor peptide. Matrix assisted laser desorption ionization (MALDI) time of flight (TOF) MS was amended for the analysis (*217, 219, 220*). With the help of the PKA-C crystal structure (*180*), already available at the time, the peptides originating from the ATP and PKI interaction sites could be retrieved and considered for their deuterium incorporation. Clearly, in presence of these molecules, the sites of interaction became less accessible, which was directly indicative of their location within the protein structure. HDX mass spectrometry has also been utilized for other questions into the structural biology of PKA, like the mapping of the interaction surface between PKA-R and PKA-C. The initial report used a double truncation mutant of PKA-RIα (94-244), in presence and absence of cAMP and PKA-C(*221*), and later the experiment was performed with full length PKA-RIα (*222*) and PKA RIIβ (*223, 224*). These analyses validated many important interaction residues on both PKA-R and PKA-C involved in deactivation of PKA, of which a couple were already known from extensive, labor intensive, targeted mutagenesis studies. In addition, the differences indicated that cAMP induced a conformational change over long distance within the protein structure to abolish PKA-C binding.(*221*) All these observations were later confirmed by the first holo-enzyme crystal structure of PKA (*225*). A quite recent very interesting study employing HDX-MS focused on the differences in interactions between PKA-RI and PKA-RII when interacting with an -helical A-kinase binding (AKB) motif from the dual specificity D-AKAP2. Interestingly, it was observed that D-AKAP2 uses two distinct binding modes towards the different PKA-R isozymes (*226*) as schematically depicted in Figure 6. Moreover, HDX-MS was used to evaluate, in combination with other biophysical methods, the kinase-dead mutant of PKA-C, in which Lys72 was replaced with a Histidine (*227*). This mutant was further studied in its unphosphorylated and phosphorylated (at Thr 197) form. Interestingly, the kinase-dead PKA-C could still bind ATP. The HDX-MS results indicated that the small lobe was much more exposed in the mutant, making the kinase less stable. This effect was diminished by the phosphorylation of Thr197, a striking demonstration of the long-distance effect of phosphorylation on the organization of the active site in PKA-C (*227*).

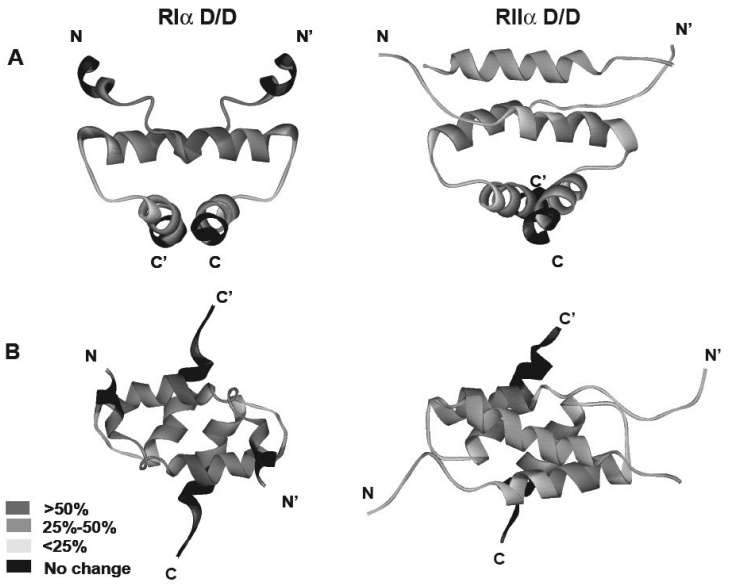

Figure 6. Difference in measured HDX exchange mapped onto the structures of RI and RII D/D domains when interacting with a peptide mimicking the interaction surface of the dual specificity AKAP2. A) Side view and B) View looking down onto the AKAP binding surface. The ligand-induced protected regions are highlighted in red (>50%), orange (25–50%), yellow (<25%), and black (no change). The ligand induces a broader region of protection on the RI surface when compared to that of RII. Adapted from ref (226). [Color Figure can be viewed in the online issue, which is available at www.interscience.wiley.com]

2.3.2. Structural properties of PKG probed by mass spectrometry

With no crystal structural available for PKG it is fair to say that the structural properties of this kinase are much less well understood. Many biophysical techniques have been amended to obtain functional and structural data on PKG. There is for instance NMR data available, but this focuses only on the very N-terminal dimerization part of PKG (*144*). Small angle X-Ray scattering data revealed that cGMP binding to PKG induces a 30% elongation of the protein (*228*). Moreover, FT-IR data suggest that the conformational change induced by cGMP-binding is primarily due to a topographical movement of the structural domains of PKG rather than to secondary structural changes within one or more of the individual domains (*229*). As for PKA, PKG was shown to be stabilized upon cGMP binding, as determined by tryptophan fluorescence unfolding studies(*230*).

Analysis of PKG by limited proteolysis showed that PKG is rapidly cleaved into a dimeric N-terminal fragment and two catalytically active C-terminal fragments (*151*). Later,

this fragment was designated as PKG Δ1-77 (*152*). In these days, it was difficult to deal with the resulting cleavage patterns of limited proteolysis, but with the availability of mass spectrometry today, identification of these protein fragments has become a lot easier, as shown recently (*230*). The differences in observed PKG cleavages in absence and presence of cGMP could be precisely pin-pointed to specific locations within the PKG sequence. Binding of cGMP is essential for PKG activation, however the exact character of the conformational changes induced upon binding are still not fully understood. It is thought that cGMP induces the release of the auto-inhibitory domain from the active site, thereby activating the kinase. Data that supports this, is the observed increase in the proteolytic sensitivity of the N-terminus in the presence of cGMP, indicating that a conformational change has occurred that increases the solvent exposure of this region (*231*) (*230*). Together with targeted mutagenesis data, this led to the hypothesis that PKG is present in a very tight conformation in absence of cGMP (*230*). Before we address recent results using HDX combined with mass spectrometry to investigate in more detail the conformational changes that occur upon cGMP binding/activation of PKG, we describe other alternative mass spectrometric approaches which have recently been used to study the changes in the structure of apo- and holo-PKG, namely native mass spectrometry and ion mobility mass spectrometry

2.3.2.1. Native MS analysis of cGMP binding and co-factor binding to PKG

With soft-electrospray ionization MS, the investigation of large 'native' non-covalent multiprotein assemblies can be achieved (*232*). Often these type of studies are amended for the elucidation of protein complex stoichiometries and stability, and for protein-ligand or protein co-factor interaction analysis (*232-234*). Pinkse *et al.* demonstrated the potential of this technique when applied to PKG Iα (*150*). Native mass spectrometry revealed that wild-type PKG exists solely as a dimeric species in solution and confirmed the cGMP binding stoichiometry as $[PKG_2(cGMP)_4]$ at saturating cGMP concentrations (Figure 7). The native-ESI-MS spectra of PKG revealed a shift of the mass/charge (m/z) envelope to lower m/z upon cGMP binding (*150, 230, 235*), which indicates that PKG picks up more positive charges in the electrospray process when cGMP is bound. This shift in charge distribution can be attributed to a conformational change hinting at a more open character of holo-PKG, corroborating with the observed increased protease susceptibility (*230, 231*) and elongation in small angle X-Ray scattering experiments (*228*). Furthermore, it was shown by native-ESI-MS that binding of Mg^{2+}/ATP could take place in absence of cGMP, reiterating that the auto-inhibitory domain does not block access to this site and that Mg^{2+}-binding is required for ATP binding. cGMP binding seemed to decrease the affinity of ATP for the kinase (*150*). This is likely caused by the observed repositioning of ATP on the small lobe of the catalytic subunit to facilitate hetero-phosphorylation, as observed for PKA (*236, 237*). Pinkse *et al.* (*150*) also showed the elegant simultaneous read-out of up to 8 autophosphorylation events that occur upon binding of cGMP or cAMP to PKG Iα together with Mg^{2+}/ATP. Binding of cGMP to

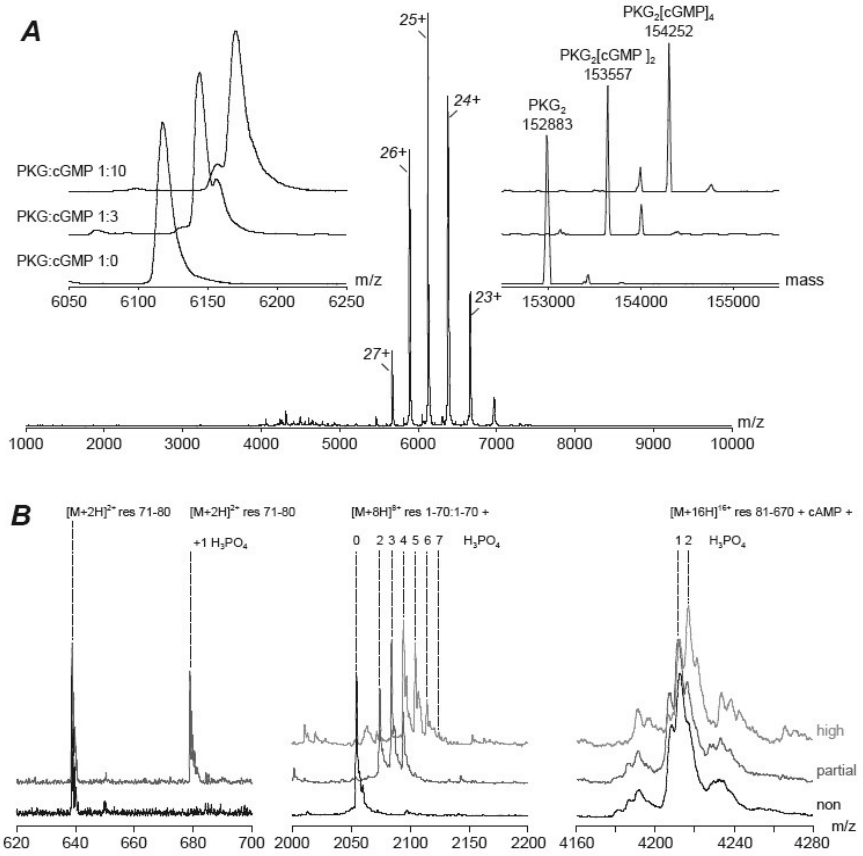

Figure 7. (A) Electrospray ionization mass spectrum of native PKG electrosprayed from an aqueous 200 mM ammonium acetate solution, pH 6.7, at a concentration of 1 μM. The inset on the left shows the changes of the $[M+25H]^{25+}$ signal of dimeric PKG upon addition of cGMP. The inset on the right shows the corresponding convoluted zero-charge spectra of PKG acquired in absence or presence of cGMP, clearly revealing the specific binding of 4 cGMP molecules. (B) ESI MS spectra for partially proteolyzed PKG, which was prior to digestion (from top to bottom) non-, partially- and highly- autophosphorylated. Mass spectra on the left display the low m/z region from m/z 620-700, displaying the double charge molecular ion of residues 71-80. Mass spectra in the middle display the $[M+8H]^{8+}$ of the dimeric N-terminus (residues 1-70). Mass spectra on the right display the $[M+16H]^{16+}$ of the C-terminal residues 81-670. The numbers of phosphate groups present on each of the three proteolytic fragments are listed above each ion signal. Adopted from ref (150).

PKG induces autophosphorylation of PKG at 1-2 residues per monomer, while cAMP binding (cAMP binds to PKG, although higher concentrations are required to saturate) induces hyperphosphorylation of the N-terminal domain with 3-4 events per monomer (*159, 160*). The exact location of the autophosphorylation sites was investigated as well (*157*). Alverdi *et al.* (*235*) used an, on native mass spectrometry based, approach to analyze the difference in global HDX behaviour between intact PKG dimers in their apo- and holo-forms (Figure 8). In this approach, the exchange of both backbone and side-chain hydrogens is monitored in real-time. A significant increase in deuterium incorporation (i.e. approximately 170 more exchanged hydrogens) was observed between apo- and holo-PKG, despite the protection expected from the binding of four cGMP molecules. The significantly higher H/D exchange in holo-PKG is however in good agreement with opening-up of the PKG structure in the presence of cGMP and consistent with the observed higher charging of holo-PKG compared to apo-PKG described above. Moreover, Alverdi *et al.* used ion mobility mass spectrometry on the intact 152 kDa dimeric PKG to investigate the global conformational changes in PKG (Figure 8). This technique relies on the measurement of the collisional cross-section, i.e. the drift time through a collision chamber with neutral gas under a weak electrical field (*238, 239*). The collisional cross-section was found to be directly proportional to the size of the protein or protein complex. In our lab, we investigated the structural changes of PKG upon cGMP-binding by this new technique (*235*). cGMP-binding increased the collisional cross-section thereby again confirming the proposed more open shape of the holo-PKG structure.

2.3.2.2. HDX mass spectrometry analysis of cGMP binding to PKG

In contrast, by using HDX-MALDI-MS, we were able to show more specifically which area's of PKG Iα were impacted by cGMP binding(*235*). Interestingly, binding of the four small cGMP molecules to the large 153 kDa dimeric PKG induced changes in the complete structure, from the very N-terminus to the C-terminus. We observed a higher solvent exposure of the autohinhibitory domain, while the cGMP binding pockets became less solvent accessible. Several regions on the large lobe of the catalytic domain were also more accessible, in line with the proposed binding of the pseudo-substrate stretch of the autoinhibitory domain to the substrate binding region on the large lobe of the catalytic domain. The ATP binding loop on the small lobe of the catalytic domain was not affected, corroborating with the ATP binding studies by Pinkse *et al.* (*150*).

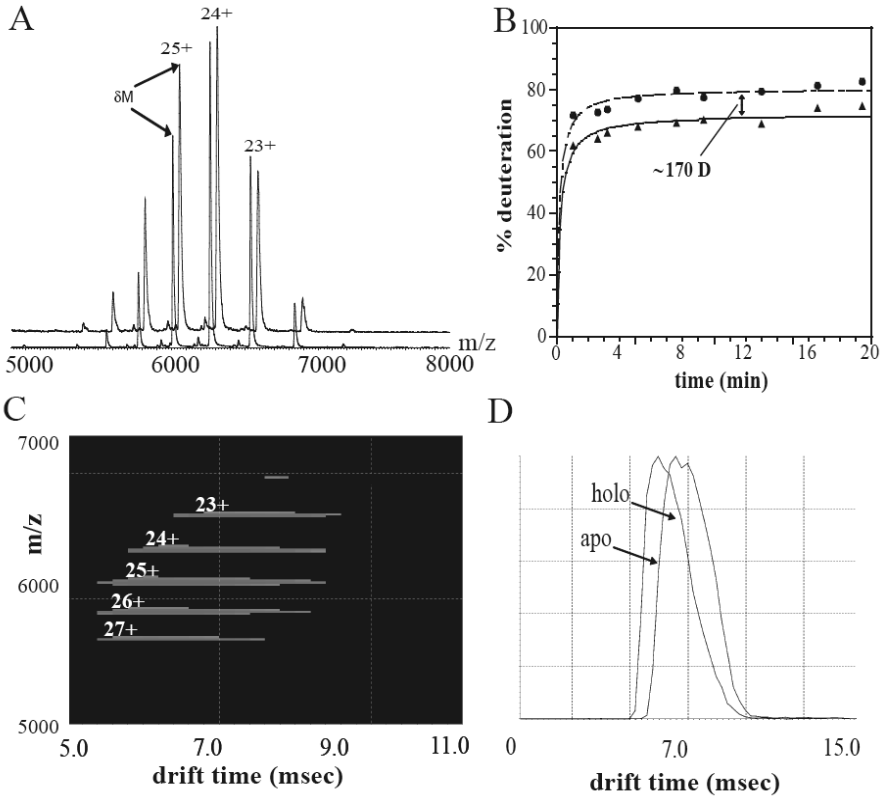

Figure 8. (A) Mass spectra of apo-PKG incubated for 15 minutes in aqueous (H_2O and D_2O, respectively) ammonium acetate. The ion signals originate from PKG dimers. The observed increase in m/z in D_2O, corresponds to a mass shift of about 1200 Da, indicating the number of hydrogens that have been exchanged. (B) Global H/D exchange kinetics of PKG determined by native mass spectrometry. The graph shows the percentage (with standard deviations) of exchanged hydrogens (i.e. incorporated deuteriums) as a function of time for apo (▲), and cGMP-bound (●) PKG. Over the whole time-window holo-PKG had approximately 300 more hydrogen exchanged than apo-PKG. (C) Plot of ion intensities versus drift time inside the ion mobility mass spectrometer of apo-PKG. Red coloring means most intense. (D) Drift time distributions for the $[M+H]^{26+}$ ions of apo- and holo-PKG revealing the shift to longer retention times for holo-PKG. Adapted from (235). [Color Figure can be viewed in the online issue, which is available at www.interscience.wiley.com]

2.4. Outlook

In this review we have attempted to capture the many contributions that a multitude of mass spectrometric techniques, available today, have made to the investigation of two important related cyclic nucleotide signaling kinases PKA and PKG. Mass spectrometry has been used at many different levels in the investigation of these proteins. PKA and PKG have become unique model systems for kinase action and function, and mass spectrometry is still gaining momentum in contributing to our efforts to understand these kinases and their regulation in the cell.We have no doubt that mass spectrometry will continue to provide more insights into their function. Mass spectrometry will be involved in the characterization and detailed mapping of all post-translational modifications on PKA and PKG isozymes, originating from different tissues, species, or even sub-cellular locations. Mass spectrometry based studies will also further map the “interactome” of these kinases. The functional study of the differentially modified isozymes will also involve the use of mass spectrometry, if only to show that these isozymes have different interaction partners. In parallel, structural approaches like HDX-MS, native mass spectrometry and ion mobility will be used to further characterize the local molecular differences within these differentially modified isozymes. Combining all this mass spectrometry based data with other biophysical and biochemical data will help us to unravel the intricate regulation of kinase function in the cell.

References:

1. Manning, G., Whyte, D. B., Martinez, R., Hunter, T., and Sudarsanam, S. (2002) The protein kinase complement of the human genome, *Science 298*, 1912-1934.
2. Sinha, S. C., and Sprang, S. R. (2006) Structures, mechanism, regulation and evolution of class III nucleotidyl cyclases, *Rev Physiol Biochem Pharmacol 157*, 105-140.
3. Furchgott, R. F., and Zawadzki, J. V. (1980) The obligatory role of endothelial cells in the relaxation of arterial smooth muscle by acetylcholine, *Nature 288*, 373-376.
4. Ignarro, L. J., Buga, G. M., Wood, K. S., Byrns, R. E., and Chaudhuri, G. (1987) Endothelium-derived relaxing factor produced and released from artery and vein is nitric oxide, *Proc Natl Acad Sci U S A 84*, 9265-9269.
5. Garbers, D. L. (1992) Guanylyl cyclase receptors and their endocrine, paracrine, and autocrine ligands, *Cell 71*, 1-4.
6. Sandberg, M., Natarajan, V., Ronander, I., Kalderon, D., Walter, U., Lohmann, S. M., and Jahnsen, T. (1989) Molecular cloning and predicted full-length amino acid sequence of the type I beta isozyme of cGMP-dependent protein kinase from human placenta. Tissue distribution and developmental changes in rat, *FEBS Lett 255*, 321-329.
7. Wernet, W., Flockerzi, V., and Hofmann, F. (1989) The cDNA of the two isoforms of bovine cGMP-dependent protein kinase, *FEBS Lett 251*, 191-196.
8. Uhler, M. D. (1993) Cloning and expression of a novel cyclic GMP-dependent protein kinase from mouse brain, *J Biol Chem 268*, 13586-13591.
9. Francis, S. H., Woodford, T. A., Wolfe, L., and Corbin, J. D. (1988) Types I alpha and I beta isozymes of cGMP-dependent protein kinase: alternative mRNA splicing may produce different inhibitory domains, *Second Messengers Phosphoproteins 12*, 301-310.
10. Wolfe, L., Corbin, J. D., and Francis, S. H. (1989) Characterization of a novel isozyme of cGMP-dependent protein kinase from bovine aorta, *J Biol Chem 264*, 7734-7741.
11. Geiselhoringer, A., Gaisa, M., Hofmann, F., and Schlossmann, J. (2004) Distribution of IRAG and cGKI-isoforms in murine tissues, *FEBS Lett 575*, 19-22.
12. Vaandrager, A. B., Ehlert, E. M., Jarchau, T., Lohmann, S. M., and de Jonge, H. R. (1996) N-terminal myristoylation is required for membrane localization of cGMP-dependent protein kinase type II, *J Biol Chem 271*, 7025-7029.
13. Jarchau, T., Hausler, C., Markert, T., Pohler, D., Vanderkerckhove, J., De Jonge, H. R., Lohmann, S. M., and Walter, U. (1994) Cloning, expression, and in situ localization of rat intestinal cGMP-dependent protein kinase II, *Proc Natl Acad Sci U S A 91*, 9426-9430.
14. Taylor, S. S., Kim, C., Vigil, D., Haste, N. M., Yang, J., Wu, J., and Anand, G. S. (2005) Dynamics of signaling by PKA, *Biochim Biophys Acta 1754*, 25-37.

15. Taylor, S. S., Yang, J., Wu, J., Haste, N. M., Radzio-Andzelm, E., and Anand, G. (2004) PKA: a portrait of protein kinase dynamics, *Biochim Biophys Acta 1697*, 259-269.
16. Brandon, E. P., Idzerda, R. L., and McKnight, G. S. (1997) PKA isoforms, neural pathways, and behaviour: making the connection, *Curr Opin Neurobiol 7*, 397-403.
17. Doskeland, S. O., Maronde, E., and Gjertsen, B. T. (1993) The genetic subtypes of cAMP-dependent protein kinase--functionally different or redundant?, *Biochim Biophys Acta 1178*, 249-258.
18. Beebe, S. J., Salomonsky, P., Jahnsen, T., and Li, Y. (1992) The C gamma subunit is a unique isozyme of the cAMP-dependent protein kinase, *J Biol Chem 267*, 25505-25512.
19. Cadd, G. G., Uhler, M. D., and McKnight, G. S. (1990) Holoenzymes of cAMP-dependent protein kinase containing the neural form of type I regulatory subunit have an increased sensitivity to cyclic nucleotides, *J Biol Chem 265*, 19502-19506.
20. Tasken, K., Skalhegg, B. S., Solberg, R., Andersson, K. B., Taylor, S. S., Lea, T., Blomhoff, H. K., Jahnsen, T., and Hansson, V. (1993) Novel isozymes of cAMP-dependent protein kinase exist in human cells due to formation of RI alpha-RI beta heterodimeric complexes, *J Biol Chem 268*, 21276-21283.
21. Skalhegg, B. S., and Tasken, K. (2000) Specificity in the cAMP/PKA signaling pathway. Differential expression,regulation, and subcellular localization of subunits of PKA, *Front Biosci 5*, D678-693.
22. Cadd, G., and McKnight, G. S. (1989) Distinct patterns of cAMP-dependent protein kinase gene expression in mouse brain, *Neuron 3*, 71-79.
23. Cummings, D. E., Brandon, E. P., Planas, J. V., Motamed, K., Idzerda, R. L., and McKnight, G. S. (1996) Genetically lean mice result from targeted disruption of the RII beta subunit of protein kinase A, *Nature 382*, 622-626.
24. Chin, K. V., Yang, W. L., Ravatn, R., Kita, T., Reitman, E., Vettori, D., Cvijic, M. E., Shin, M., and Iacono, L. (2002) Reinventing the wheel of cyclic AMP: novel mechanisms of cAMP signaling, *Ann N Y Acad Sci 968*, 49-64.
25. Wong, W., and Scott, J. D. (2004) AKAP signalling complexes: focal points in space and time, *Nat Rev Mol Cell Biol 5*, 959-970.
26. Theurkauf, W. E., and Vallee, R. B. (1982) Molecular characterization of the cAMP-dependent protein kinase bound to microtubule-associated protein 2, *J Biol Chem 257*, 3284-3290.
27. Lin, R. Y., Moss, S. B., and Rubin, C. S. (1995) Characterization of S-AKAP84, a novel developmentally regulated A kinase anchor protein of male germ cells, *J Biol Chem 270*, 27804.

28. Trendelenburg, G., Hummel, M., Riecken, E. O., and Hanski, C. (1996) Molecular characterization of AKAP149, a novel A kinase anchor protein with a KH domain, *Biochem Biophys Res Commun 225*, 313-319.
29. Huang, L. J., Durick, K., Weiner, J. A., Chun, J., and Taylor, S. S. (1997) Identification of a novel protein kinase A anchoring protein that binds both type I and type II regulatory subunits, *J Biol Chem 272*, 8057-8064.
30. Asirvatham, A. L., Galligan, S. G., Schillace, R. V., Davey, M. P., Vasta, V., Beavo, J. A., and Carr, D. W. (2004) A-kinase anchoring proteins interact with phosphodiesterases in T lymphocyte cell lines, *J Immunol 173*, 4806-4814.
31. Cardone, L., Carlucci, A., Affaitati, A., Livigni, A., DeCristofaro, T., Garbi, C., Varrone, S., Ullrich, A., Gottesman, M. E., Avvedimento, E. V., and Feliciello, A. (2004) Mitochondrial AKAP121 binds and targets protein tyrosine phosphatase D1, a novel positive regulator of src signaling, *Mol Cell Biol 24*, 4613-4626.
32. Furusawa, M., Taira, T., Iguchi-Ariga, S. M., and Ariga, H. (2002) AMY-1 interacts with S-AKAP84 and AKAP95 in the cytoplasm and the nucleus, respectively, and inhibits cAMP-dependent protein kinase activity by preventing binding of its catalytic subunit to A-kinase-anchoring protein (AKAP) complex, *J Biol Chem 277*, 50885-50892.
33. Dong, F., Feldmesser, M., Casadevall, A., and Rubin, C. S. (1998) Molecular characterization of a cDNA that encodes six isoforms of a novel murine A kinase anchor protein, *J Biol Chem 273*, 6533-6541.
34. Scholten, A., van Veen, T. A., Vos, M. A., and Heck, A. J. (2007) Diversity of cAMP-dependent protein kinase isoforms and their anchoring proteins in mouse ventricular tissue, *J Proteome Res 6*, 1705-1717.
35. Vijayaraghavan, S., Liberty, G. A., Mohan, J., Winfrey, V. P., Olson, G. E., and Carr, D. W. (1999) Isolation and molecular characterization of AKAP110, a novel, sperm-specific protein kinase A-anchoring protein, *Mol Endocrinol 13*, 705-717.
36. Carr, D. W., Fujita, A., Stentz, C. L., Liberty, G. A., Olson, G. E., and Narumiya, S. (2001) Identification of sperm-specific proteins that interact with A-kinase anchoring proteins in a manner similar to the type II regulatory subunit of PKA, *J Biol Chem 276*, 17332-17338.
37. Niu, J., Vaiskunaite, R., Suzuki, N., Kozasa, T., Carr, D. W., Dulin, N., and Voyno-Yasenetskaya, T. A. (2001) Interaction of heterotrimeric G13 protein with an A-kinase-anchoring protein 110 (AKAP110) mediates cAMP-independent PKA activation, *Curr Biol 11*, 1686-1690.
38. Brown, P. R., Miki, K., Harper, D. B., and Eddy, E. M. (2003) A-kinase anchoring protein 4 binding proteins in the fibrous sheath of the sperm flagellum, *Biol Reprod 68*, 2241-2248.

39. Lea, I. A., Widgren, E. E., and O'Rand, M. G. (2004) Association of sperm protein 17 with A-kinase anchoring protein 3 in flagella, *Reprod Biol Endocrinol 2*, 57.
40. Bajpai, M., Fiedler, S. E., Huang, Z., Vijayaraghavan, S., Olson, G. E., Livera, G., Conti, M., and Carr, D. W. (2006) AKAP3 selectively binds PDE4A isoforms in bovine spermatozoa, *Biol Reprod 74*, 109-118.
41. Turner, R. M., Johnson, L. R., Haig-Ladewig, L., Gerton, G. L., and Moss, S. B. (1998) An X-linked gene encodes a major human sperm fibrous sheath protein, hAKAP82. Genomic organization, protein kinase A-RII binding, and distribution of the precursor in the sperm tail, *J Biol Chem 273*, 32135-32141.
42. Bregman, D. B., Bhattacharyya, N., and Rubin, C. S. (1989) High affinity binding protein for the regulatory subunit of cAMP-dependent protein kinase II-B. Cloning, characterization, and expression of cDNAs for rat brain P150, *J Biol Chem 264*, 4648-4656.
43. Rosenmund, C., Carr, D. W., Bergeson, S. E., Nilaver, G., Scott, J. D., and Westbrook, G. L. (1994) Anchoring of protein kinase A is required for modulation of AMPA/kainate receptors on hippocampal neurons, *Nature 368*, 853-856.
44. Coghlan, V. M., Perrino, B. A., Howard, M., Langeberg, L. K., Hicks, J. B., Gallatin, W. M., and Scott, J. D. (1995) Association of protein kinase A and protein phosphatase 2B with a common anchoring protein, *Science 267*, 108-111.
45. Klauck, T. M., Faux, M. C., Labudda, K., Langeberg, L. K., Jaken, S., and Scott, J. D. (1996) Coordination of three signaling enzymes by AKAP79, a mammalian scaffold protein, *Science 271*, 1589-1592.
46. Fraser, I. D., Cong, M., Kim, J., Rollins, E. N., Daaka, Y., Lefkowitz, R. J., and Scott, J. D. (2000) Assembly of an A kinase-anchoring protein-beta(2)-adrenergic receptor complex facilitates receptor phosphorylation and signaling, *Curr Biol 10*, 409-412.
47. Dart, C., and Leyland, M. L. (2001) Targeting of an A kinase-anchoring protein, AKAP79, to an inwardly rectifying potassium channel, Kir2.1, *J Biol Chem 276*, 20499-20505.
48. Colledge, M., Dean, R. A., Scott, G. K., Langeberg, L. K., Huganir, R. L., and Scott, J. D. (2000) Targeting of PKA to glutamate receptors through a MAGUK-AKAP complex, *Neuron 27*, 107-119.
49. Altier, C., Dubel, S. J., Barrere, C., Jarvis, S. E., Stotz, S. C., Spaetgens, R. L., Scott, J. D., Cornet, V., De Waard, M., Zamponi, G. W., Nargeot, J., and Bourinet, E. (2002) Trafficking of L-type calcium channels mediated by the postsynaptic scaffolding protein AKAP79, *J Biol Chem 277*, 33598-33603.
50. Brandon, N. J., Jovanovic, J. N., Colledge, M., Kittler, J. T., Brandon, J. M., Scott, J. D., and Moss, S. J. (2003) A-kinase anchoring protein 79/150 facilitates the phosphorylation of GABA(A) receptors by cAMP-dependent protein kinase via selective interaction with receptor beta subunits, *Mol Cell Neurosci 22*, 87-97.

51. Nauert, J. B., Rigas, J. D., and Lester, L. B. (2003) Identification of an IQGAP1/AKAP79 complex in beta-cells, *J Cell Biochem 90*, 97-108.
52. Bauman, A. L., Soughayer, J., Nguyen, B. T., Willoughby, D., Carnegie, G. K., Wong, W., Hoshi, N., Langeberg, L. K., Cooper, D. M., Dessauer, C. W., and Scott, J. D. (2006) Dynamic regulation of cAMP synthesis through anchored PKA-adenylyl cyclase V/VI complexes, *Mol Cell 23*, 925-931.
53. Chai, S., Li, M., Lan, J., Xiong, Z. G., Saugstad, J. A., and Simon, R. P. (2007) A kinase-anchoring protein 150 and calcineurin are involved in regulation of acid-sensing ion channels ASIC1a and ASIC2a, *J Biol Chem 282*, 22668-22677.
54. McCartney, S., Little, B. M., Langeberg, L. K., and Scott, J. D. (1995) Cloning and characterization of A-kinase anchor protein 100 (AKAP100). A protein that targets A-kinase to the sarcoplasmic reticulum, *J Biol Chem 270*, 9327-9333.
55. Dodge, K. L., Khouangsathiene, S., Kapiloff, M. S., Mouton, R., Hill, E. V., Houslay, M. D., Langeberg, L. K., and Scott, J. D. (2001) mAKAP assembles a protein kinase A/PDE4 phosphodiesterase cAMP signaling module, *Embo J 20*, 1921-1930.
56. Marx, S. O., Reiken, S., Hisamatsu, Y., Jayaraman, T., Burkhoff, D., Rosemblit, N., and Marks, A. R. (2000) PKA phosphorylation dissociates FKBP12.6 from the calcium release channel (ryanodine receptor): defective regulation in failing hearts, *Cell 101*, 365-376.
57. Schulze, D. H., Muqhal, M., Lederer, W. J., and Ruknudin, A. M. (2003) Sodium/calcium exchanger (NCX1) macromolecular complex, *J Biol Chem 278*, 28849-28855.
58. Kapiloff, M. S., Jackson, N., and Airhart, N. (2001) mAKAP and the ryanodine receptor are part of a multi-component signaling complex on the cardiomyocyte nuclear envelope, *J Cell Sci 114*, 3167-3176.
59. Pare, G. C., Easlick, J. L., Mislow, J. M., McNally, E. M., and Kapiloff, M. S. (2005) Nesprin-1alpha contributes to the targeting of mAKAP to the cardiac myocyte nuclear envelope, *Exp Cell Res 303*, 388-399.
60. Dodge-Kafka, K. L., Soughayer, J., Pare, G. C., Carlisle Michel, J. J., Langeberg, L. K., Kapiloff, M. S., and Scott, J. D. (2005) The protein kinase A anchoring protein mAKAP coordinates two integrated cAMP effector pathways, *Nature 437*, 574-578.
61. Michel, J. J., Townley, I. K., Dodge-Kafka, K. L., Zhang, F., Kapiloff, M. S., and Scott, J. D. (2005) Spatial restriction of PDK1 activation cascades by anchoring to mAKAPalpha, *Mol Cell 20*, 661-672.
62. Fraser, I. D., Tavalin, S. J., Lester, L. B., Langeberg, L. K., Westphal, A. M., Dean, R. A., Marrion, N. V., and Scott, J. D. (1998) A novel lipid-anchored A-kinase Anchoring Protein facilitates cAMP-responsive membrane events, *Embo J 17*, 2261-2272.

63. Trotter, K. W., Fraser, I. D., Scott, G. K., Stutts, M. J., Scott, J. D., and Milgram, S. L. (1999) Alternative splicing regulates the subcellular localization of A-kinase anchoring protein 18 isoforms, *J Cell Biol 147*, 1481-1492.
64. Gray, P. C., Johnson, B. D., Westenbroek, R. E., Hays, L. G., Yates, J. R., 3rd, Scheuer, T., Catterall, W. A., and Murphy, B. J. (1998) Primary structure and function of an A kinase anchoring protein associated with calcium channels, *Neuron 20*, 1017-1026.
65. Tibbs, V. C., Gray, P. C., Catterall, W. A., and Murphy, B. J. (1998) AKAP15 anchors cAMP-dependent protein kinase to brain sodium channels, *J Biol Chem 273*, 25783-25788.
66. Henn, V., Edemir, B., Stefan, E., Wiesner, B., Lorenz, D., Theilig, F., Schmitt, R., Vossebein, L., Tamma, G., Beyermann, M., Krause, E., Herberg, F. W., Valenti, G., Bachmann, S., Rosenthal, W., and Klussmann, E. (2004) Identification of a novel A-kinase anchoring protein 18 isoform and evidence for its role in the vasopressin-induced aquaporin-2 shuttle in renal principal cells, *J Biol Chem 279*, 26654-26665.
67. Coghlan, V. M., Langeberg, L. K., Fernandez, A., Lamb, N. J., and Scott, J. D. (1994) Cloning and characterization of AKAP 95, a nuclear protein that associates with the regulatory subunit of type II cAMP-dependent protein kinase, *J Biol Chem 269*, 7658-7665.
68. Akileswaran, L., Taraska, J. W., Sayer, J. A., Gettemy, J. M., and Coghlan, V. M. (2001) A-kinase-anchoring protein AKAP95 is targeted to the nuclear matrix and associates with p68 RNA helicase, *J Biol Chem 276*, 17448-17454.
69. Arsenijevic, T., Degraef, C., Dumont, J. E., Roger, P. P., and Pirson, I. (2004) A novel partner for D-type cyclins: protein kinase A-anchoring protein AKAP95, *Biochem J 378*, 673-679.
70. Steen, R. L., Cubizolles, F., Le Guellec, K., and Collas, P. (2000) A kinase-anchoring protein (AKAP)95 recruits human chromosome-associated protein (hCAP)-D2/Eg7 for chromosome condensation in mitotic extract, *J Cell Biol 149*, 531-536.
71. Eide, T., Tasken, K. A., Carlson, C., Williams, G., Jahnsen, T., Tasken, K., and Collas, P. (2003) Protein kinase A-anchoring protein AKAP95 interacts with MCM2, a regulator of DNA replication, *J Biol Chem 278*, 26750-26756.
72. Kamada, S., Kikkawa, U., Tsujimoto, Y., and Hunter, T. (2005) A-kinase-anchoring protein 95 functions as a potential carrier for the nuclear translocation of active caspase 3 through an enzyme-substrate-like association, *Mol Cell Biol 25*, 9469-9477.
73. Arsenijevic, T., Degraef, C., Dumont, J. E., Roger, P. P., and Pirson, I. (2006) G1/S Cyclins interact with regulatory subunit of PKA via A-kinase anchoring protein, AKAP95, *Cell Cycle 5*, 1217-1222.

74. Yang, Y., Mahaffey, C. L., Berube, N., and Frankel, W. N. (2006) Interaction between fidgetin and protein kinase A-anchoring protein AKAP95 is critical for palatogenesis in the mouse, *J Biol Chem 281*, 22352-22359.
75. Dirksen, E. H., Pinkse, M. W., Rijkers, D. T., Cloos, J., Liskamp, R. M., Slijper, M., and Heck, A. J. (2006) Investigating the dynamic nature of the interactions between nuclear proteins and histones upon DNA damage using an immobilized peptide chemical proteomics approach, *J Proteome Res 5*, 2380-2388.
76. Schmidt, P. H., Dransfield, D. T., Claudio, J. O., Hawley, R. G., Trotter, K. W., Milgram, S. L., and Goldenring, J. R. (1999) AKAP350, a multiply spliced protein kinase A-anchoring protein associated with centrosomes, *J Biol Chem 274*, 3055-3066.
77. Witczak, O., Skalhegg, B. S., Keryer, G., Bornens, M., Tasken, K., Jahnsen, T., and Orstavik, S. (1999) Cloning and characterization of a cDNA encoding an A-kinase anchoring protein located in the centrosome, AKAP450, *Embo J 18*, 1858-1868.
78. Takahashi, M., Shibata, H., Shimakawa, M., Miyamoto, M., Mukai, H., and Ono, Y. (1999) Characterization of a novel giant scaffolding protein, CG-NAP, that anchors multiple signaling enzymes to centrosome and the golgi apparatus, *J Biol Chem 274*, 17267-17274.
79. Westphal, R. S., Tavalin, S. J., Lin, J. W., Alto, N. M., Fraser, I. D., Langeberg, L. K., Sheng, M., and Scott, J. D. (1999) Regulation of NMDA receptors by an associated phosphatase-kinase signaling complex, *Science 285*, 93-96.
80. Takahashi, M., Mukai, H., Oishi, K., Isagawa, T., and Ono, Y. (2000) Association of immature hypophosphorylated protein kinase cepsilon with an anchoring protein CG-NAP, *J Biol Chem 275*, 34592-34596.
81. Marx, S. O., Kurokawa, J., Reiken, S., Motoike, H., D'Armiento, J., Marks, A. R., and Kass, R. S. (2002) Requirement of a macromolecular signaling complex for beta adrenergic receptor modulation of the KCNQ1-KCNE1 potassium channel, *Science 295*, 496-499.
82. Steadman, B. T., Schmidt, P. H., Shanks, R. A., Lapierre, L. A., and Goldenring, J. R. (2002) Transforming acidic coiled-coil-containing protein 4 interacts with centrosomal AKAP350 and the mitotic spindle apparatus, *J Biol Chem 277*, 30165-30176.
83. Sillibourne, J. E., Milne, D. M., Takahashi, M., Ono, Y., and Meek, D. W. (2002) Centrosomal anchoring of the protein kinase CK1delta mediated by attachment to the large, coiled-coil scaffolding protein CG-NAP/AKAP450, *J Mol Biol 322*, 785-797.
84. Shanks, R. A., Larocca, M. C., Berryman, M., Edwards, J. C., Urushidani, T., Navarre, J., and Goldenring, J. R. (2002) AKAP350 at the Golgi apparatus. II. Association of AKAP350 with a novel chloride intracellular channel (CLIC) family member, *J Biol Chem 277*, 40973-40980.

85. Takahashi, M., Yamagiwa, A., Nishimura, T., Mukai, H., and Ono, Y. (2002) Centrosomal proteins CG-NAP and kendrin provide microtubule nucleation sites by anchoring gamma-tubulin ring complex, *Mol Biol Cell 13*, 3235-3245.
86. Keryer, G., Di Fiore, B., Celati, C., Lechtreck, K. F., Mogensen, M., Delouvee, A., Lavia, P., Bornens, M., and Tassin, A. M. (2003) Part of Ran is associated with AKAP450 at the centrosome: involvement in microtubule-organizing activity, *Mol Biol Cell 14*, 4260-4271.
87. Tu, H., Tang, T. S., Wang, Z., and Bezprozvanny, I. (2004) Association of type 1 inositol 1,4,5-trisphosphate receptor with AKAP9 (Yotiao) and protein kinase A, *J Biol Chem 279*, 19375-19382.
88. Huang, L. J., Durick, K., Weiner, J. A., Chun, J., and Taylor, S. S. (1997) D-AKAP2, a novel protein kinase A anchoring protein with a putative RGS domain, *Proc Natl Acad Sci U S A 94*, 11184-11189.
89. Gisler, S. M., Madjdpour, C., Bacic, D., Pribanic, S., Taylor, S. S., Biber, J., and Murer, H. (2003) PDZK1: II. an anchoring site for the PKA-binding protein D-AKAP2 in renal proximal tubular cells, *Kidney Int 64*, 1746-1754.
90. Lester, L. B., Coghlan, V. M., Nauert, B., and Scott, J. D. (1996) Cloning and characterization of a novel A-kinase anchoring protein. AKAP 220, association with testicular peroxisomes, *J Biol Chem 271*, 9460-9465.
91. Schillace, R. V., and Scott, J. D. (1999) Association of the type 1 protein phosphatase PP1 with the A-kinase anchoring protein AKAP220, *Curr Biol 9*, 321-324.
92. Tanji, C., Yamamoto, H., Yorioka, N., Kohno, N., Kikuchi, K., and Kikuchi, A. (2002) A-kinase anchoring protein AKAP220 binds to glycogen synthase kinase-3beta (GSK-3beta) and mediates protein kinase A-dependent inhibition of GSK-3beta, *J Biol Chem 277*, 36955-36961.
93. Lin, X., Tombler, E., Nelson, P. J., Ross, M., and Gelman, I. H. (1996) A novel src- and ras-suppressed protein kinase C substrate associated with cytoskeletal architecture, *J Biol Chem 271*, 28430-28438.
94. Erlichman, J., Gutierrez-Juarez, R., Zucker, S., Mei, X., and Orr, G. A. (1999) Developmental expression of the protein kinase C substrate/binding protein (clone 72/SSeCKS) in rat testis identification as a scaffolding protein containing an A-kinase-anchoring domain which is expressed during late-stage spermatogenesis, *Eur J Biochem 263*, 797-805.
95. Fan, G., Shumay, E., Wang, H., and Malbon, C. C. (2001) The scaffold protein gravin (cAMP-dependent protein kinase-anchoring protein 250) binds the beta 2-adrenergic receptor via the receptor cytoplasmic Arg-329 to Leu-413 domain and provides a mobile scaffold during desensitization, *J Biol Chem 276*, 24005-24014.

96. Lin, X., and Gelman, I. H. (2002) Calmodulin and cyclin D anchoring sites on the Src-suppressed C kinase substrate, SSeCKS, *Biochem Biophys Res Commun 290*, 1368-1375.
97. Wassler, M. J., Foote, C. I., Gelman, I. H., and Shur, B. D. (2001) Functional interaction between the SSeCKS scaffolding protein and the cytoplasmic domain of beta1,4-galactosyltransferase, *J Cell Sci 114*, 2291-2300.
98. Willoughby, D., Wong, W., Schaack, J., Scott, J. D., and Cooper, D. M. (2006) An anchored PKA and PDE4 complex regulates subplasmalemmal cAMP dynamics, *Embo J 25*, 2051-2061.
99. Tao, J., Wang, H. Y., and Malbon, C. C. (2007) Src docks to A-kinase anchoring protein gravin, regulating beta2-adrenergic receptor resensitization and recycling, *J Biol Chem 282*, 6597-6608.
100. Diviani, D., Soderling, J., and Scott, J. D. (2001) AKAP-Lbc anchors protein kinase A and nucleates Galpha 12-selective Rho-mediated stress fiber formation, *J Biol Chem 276*, 44247-44257.
101. Klussmann, E., Edemir, B., Pepperle, B., Tamma, G., Henn, V., Klauschenz, E., Hundsrucker, C., Maric, K., and Rosenthal, W. (2001) Ht31: the first protein kinase A anchoring protein to integrate protein kinase A and Rho signaling, *FEBS Lett 507*, 264-268.
102. Diviani, D., Abuin, L., Cotecchia, S., and Pansier, L. (2004) Anchoring of both PKA and 14-3-3 inhibits the Rho-GEF activity of the AKAP-Lbc signaling complex, *Embo J 23*, 2811-2820.
103. Park, B., Nguyen, N. T., Dutt, P., Merdek, K. D., Bashar, M., Sterpetti, P., Tosolini, A., Testa, J. R., and Toksoz, D. (2002) Association of Lbc Rho guanine nucleotide exchange factor with alpha-catenin-related protein, alpha-catulin/CTNNAL1, supports serum response factor activation, *J Biol Chem 277*, 45361-45370.
104. Lewis, T. E., Milam, T. D., Klingler, D. W., Rao, P. S., Jaggi, M., Smith, D. J., Hemstreet, G. P., and Balaji, K. C. (2005) Tissue transglutaminase interacts with protein kinase A anchor protein 13 in prostate cancer, *Urol Oncol 23*, 407-412.
105. Kultgen, P. L., Byrd, S. K., Ostrowski, L. E., and Milgram, S. L. (2002) Characterization of an A-kinase anchoring protein in human ciliary axonemes, *Mol Biol Cell 13*, 4156-4166.
106. Dransfield, D. T., Bradford, A. J., Smith, J., Martin, M., Roy, C., Mangeat, P. H., and Goldenring, J. R. (1997) Ezrin is a cyclic AMP-dependent protein kinase anchoring protein, *Embo J 16*, 35-43.
107. Sun, F., Hug, M. J., Lewarchik, C. M., Yun, C. H., Bradbury, N. A., and Frizzell, R. A. (2000) E3KARP mediates the association of ezrin and protein kinase A with the cystic fibrosis transmembrane conductance regulator in airway cells, *J Biol Chem 275*, 29539-29546.

108. Lamprecht, G., Weinman, E. J., and Yun, C. H. (1998) The role of NHERF and E3KARP in the cAMP-mediated inhibition of NHE3, *J Biol Chem 273*, 29972-29978.
109. Westphal, R. S., Soderling, S. H., Alto, N. M., Langeberg, L. K., and Scott, J. D. (2000) Scar/WAVE-1, a Wiskott-Aldrich syndrome protein, assembles an actin-associated multi-kinase scaffold, *Embo J 19*, 4589-4600.
110. Suetsugu, S., Miki, H., and Takenawa, T. (1999) Identification of two human WAVE/SCAR homologues as general actin regulatory molecules which associate with the Arp2/3 complex, *Biochem Biophys Res Commun 260*, 296-302.
111. Ibarra, N., Pollitt, A., and Insall, R. H. (2005) Regulation of actin assembly by SCAR/WAVE proteins, *Biochem Soc Trans 33*, 1243-1246.
112. Alto, N. M., Soderling, J., and Scott, J. D. (2002) Rab32 is an A-kinase anchoring protein and participates in mitochondrial dynamics, *J Cell Biol 158*, 659-668.
113. Lacana, E., Maceyka, M., Milstien, S., and Spiegel, S. (2002) Cloning and characterization of a protein kinase A anchoring protein (AKAP)-related protein that interacts with and regulates sphingosine kinase 1 activity, *J Biol Chem 277*, 32947-32953.
114. Scholten, A., Poh, M. K., van Veen, T. A., van Breukelen, B., Vos, M. A., and Heck, A. J. (2006) Analysis of the cGMP/cAMP interactome using a chemical proteomics approach in mammalian heart tissue validates sphingosine kinase type 1-interacting protein as a genuine and highly abundant AKAP, *J Proteome Res 5*, 1435-1447.
115. Li, H., Adamik, R., Pacheco-Rodriguez, G., Moss, J., and Vaughan, M. (2003) Protein kinase A-anchoring (AKAP) domains in brefeldin A-inhibited guanine nucleotide-exchange protein 2 (BIG2), *Proc Natl Acad Sci U S A 100*, 1627-1632.
116. Xu, K. F., Shen, X., Li, H., Pacheco-Rodriguez, G., Moss, J., and Vaughan, M. (2005) Interaction of BIG2, a brefeldin A-inhibited guanine nucleotide-exchange protein, with exocyst protein Exo70, *Proc Natl Acad Sci U S A 102*, 2784-2789.
117. Ishizaki, R., Shin, H. W., Iguchi-Ariga, S. M., Ariga, H., and Nakayama, K. (2006) AMY-1 (associate of Myc-1) localization to the trans-Golgi network through interacting with BIG2, a guanine-nucleotide exchange factor for ADP-ribosylation factors, *Genes Cells 11*, 949-959.
118. Togawa, A., Morinaga, N., Ogasawara, M., Moss, J., and Vaughan, M. (1999) Purification and cloning of a brefeldin A-inhibited guanine nucleotide-exchange protein for ADP-ribosylation factors, *J Biol Chem 274*, 12308-12315.
119. Schillace, R. V., Andrews, S. F., Liberty, G. A., Davey, M. P., and Carr, D. W. (2002) Identification and characterization of myeloid translocation gene 16b as a novel a kinase anchoring protein in T lymphocytes, *J Immunol 168*, 1590-1599.
120. Kussel-Andermann, P., El-Amraoui, A., Safieddine, S., Hardelin, J. P., Nouaille, S., Camonis, J., and Petit, C. (2000) Unconventional myosin VIIA is a novel A-kinase-anchoring protein, *J Biol Chem 275*, 29654-29659.

121. Kussel-Andermann, P., El-Amraoui, A., Safieddine, S., Nouaille, S., Perfettini, I., Lecuit, M., Cossart, P., Wolfrum, U., and Petit, C. (2000) Vezatin, a novel transmembrane protein, bridges myosin VIIA to the cadherin-catenins complex, *Embo J 19*, 6020-6029.
122. El-Amraoui, A., Schonn, J. S., Kussel-Andermann, P., Blanchard, S., Desnos, C., Henry, J. P., Wolfrum, U., Darchen, F., and Petit, C. (2002) MyRIP, a novel Rab effector, enables myosin VIIa recruitment to retinal melanosomes, *EMBO Rep 3*, 463-470.
123. Goehring, A. S., Pedroja, B. S., Hinke, S. A., Langeberg, L. K., and Scott, J. D. (2007) MyRIP anchors protein kinase A to the exocyst complex, *J Biol Chem*.
124. Diviani, D., Langeberg, L. K., Doxsey, S. J., and Scott, J. D. (2000) Pericentrin anchors protein kinase A at the centrosome through a newly identified RII-binding domain, *Curr Biol 10*, 417-420.
125. Chen, D., Purohit, A., Halilovic, E., Doxsey, S. J., and Newton, A. C. (2004) Centrosomal anchoring of protein kinase C betaII by pericentrin controls microtubule organization, spindle function, and cytokinesis, *J Biol Chem 279*, 4829-4839.
126. Miller, P., Walter, U., Theurkauf, W. E., Vallee, R. B., and De Camilli, P. (1982) Frozen tissue sections as an experimental system to reveal specific binding sites for the regulatory subunit of type II cAMP-dependent protein kinase in neurons, *Proc Natl Acad Sci U S A 79*, 5562-5566.
127. Lohmann, S. M., DeCamilli, P., Einig, I., and Walter, U. (1984) High-affinity binding of the regulatory subunit (RII) of cAMP-dependent protein kinase to microtubule-associated and other cellular proteins, *Proc Natl Acad Sci U S A 81*, 6723-6727.
128. Anhe, G. F., Torrao, A. S., Nogueira, T. C., Caperuto, L. C., Amaral, M. E., Medina, M. C., Azevedo-Martins, A. K., Carpinelli, A. R., Carvalho, C. R., Curi, R., Boschero, A. C., and Bordin, S. (2006) ERK3 associates with MAP2 and is involved in glucose-induced insulin secretion, *Mol Cell Endocrinol 251*, 33-41.
129. Reynolds, J. G., McCalmon, S. A., Tomczyk, T., and Naya, F. J. (2007) Identification and mapping of protein kinase A binding sites in the costameric protein myospryn, *Biochim Biophys Acta 1773*, 891-902.
130. Benson, M. A., Tinsley, C. L., and Blake, D. J. (2004) Myospryn is a novel binding partner for dysbindin in muscle, *J Biol Chem 279*, 10450-10458.
131. Kouloumenta, A., Mavroidis, M., and Capetanaki, Y. (2007) Proper perinuclear localization of the TRIM-like protein myospryn requires its binding partner desmin, *J Biol Chem*.
132. Gronholm, M., Vossebein, L., Carlson, C. R., Kuja-Panula, J., Teesalu, T., Alfthan, K., Vaheri, A., Rauvala, H., Herberg, F. W., Tasken, K., and Carpen, O. (2003) Merlin links to the cAMP neuronal signaling pathway by anchoring the RIbeta subunit of protein kinase A, *J Biol Chem 278*, 41167-41172.

133. Alfthan, K., Heiska, L., Gronholm, M., Renkema, G. H., and Carpen, O. (2004) Cyclic AMP-dependent protein kinase phosphorylates merlin at serine 518 independently of p21-activated kinase and promotes merlin-ezrin heterodimerization, *J Biol Chem 279*, 18559-18566.
134. Russell, M. A., Lund, L. M., Haber, R., McKeegan, K., Cianciola, N., and Bond, M. (2006) The intermediate filament protein, synemin, is an AKAP in the heart, *Arch Biochem Biophys 456*, 204-215.
135. Lim, C. J., Han, J., Yousefi, N., Ma, Y., Amieux, P. S., McKnight, G. S., Taylor, S. S., and Ginsberg, M. H. (2007) Alpha4 integrins are type I cAMP-dependent protein kinase-anchoring proteins, *Nat Cell Biol 9*, 415-421.
136. Liu, S., Thomas, S. M., Woodside, D. G., Rose, D. M., Kiosses, W. B., Pfaff, M., and Ginsberg, M. H. (1999) Binding of paxillin to alpha4 integrins modifies integrin-dependent biological responses, *Nature 402*, 676-681.
137. Obar, R. A., Dingus, J., Bayley, H., and Vallee, R. B. (1989) The RII subunit of cAMP-dependent protein kinase binds to a common amino-terminal domain in microtubule-associated proteins 2A, 2B, and 2C, *Neuron 3*, 639-645.
138. Rubino, H. M., Dammerman, M., Shafit-Zagardo, B., and Erlichman, J. (1989) Localization and characterization of the binding site for the regulatory subunit of type II cAMP-dependent protein kinase on MAP2, *Neuron 3*, 631-638.
139. Carr, D. W., Stofko-Hahn, R. E., Fraser, I. D., Bishop, S. M., Acott, T. S., Brennan, R. G., and Scott, J. D. (1991) Interaction of the regulatory subunit (RII) of cAMP-dependent protein kinase with RII-anchoring proteins occurs through an amphipathic helix binding motif, *J Biol Chem 266*, 14188-14192.
140. Lester, L. B., Langeberg, L. K., and Scott, J. D. (1997) Anchoring of protein kinase A facilitates hormone-mediated insulin secretion, *Proc Natl Acad Sci U S A 94*, 14942-14947.
141. Newlon, M. G., Roy, M., Morikis, D., Hausken, Z. E., Coghlan, V., Scott, J. D., and Jennings, P. A. (1999) The molecular basis for protein kinase A anchoring revealed by solution NMR, *Nat Struct Biol 6*, 222-227.
142. Newlon, M. G., Roy, M., Hausken, Z. E., Scott, J. D., and Jennings, P. A. (1997) The A-kinase anchoring domain of type IIalpha cAMP-dependent protein kinase is highly helical, *J Biol Chem 272*, 23637-23644.
143. Newlon, M. G., Roy, M., Morikis, D., Carr, D. W., Westphal, R., Scott, J. D., and Jennings, P. A. (2001) A novel mechanism of PKA anchoring revealed by solution structures of anchoring complexes, *Embo J 20*, 1651-1662.
144. Atkinson, R. A., Saudek, V., Huggins, J. P., and Pelton, J. T. (1991) 1H NMR and circular dichroism studies of the N-terminal domain of cyclic GMP dependent protein kinase: a leucine/isoleucine zipper, *Biochemistry 30*, 9387-9395.

145. Landgraf, W., Hofmann, F., Pelton, J. T., and Huggins, J. P. (1990) Effects of cyclic GMP on the secondary structure of cyclic GMP dependent protein kinase and analysis of the enzyme's amino-terminal domain by far-ultraviolet circular dichroism, *Biochemistry 29*, 9921-9928.
146. Richie-Jannetta, R., Francis, S. H., and Corbin, J. D. (2003) Dimerization of cGMP-dependent protein kinase Ibeta is mediated by an extensive amino-terminal leucine zipper motif, and dimerization modulates enzyme function, *J Biol Chem 278*, 50070-50079.
147. Gamm, D. M., Francis, S. H., Angelotti, T. P., Corbin, J. D., and Uhler, M. D. (1995) The type II isoform of cGMP-dependent protein kinase is dimeric and possesses regulatory and catalytic properties distinct from the type I isoforms, *J Biol Chem 270*, 27380-27388.
148. Ruth, P., Landgraf, W., Keilbach, A., May, B., Egleme, C., and Hofmann, F. (1991) The activation of expressed cGMP-dependent protein kinase isozymes I alpha and I beta is determined by the different amino-termini, *Eur J Biochem 202*, 1339-1344.
149. Vaandrager, A. B., Edixhoven, M., Bot, A. G., Kroos, M. A., Jarchau, T., Lohmann, S., Genieser, H. G., and de Jonge, H. R. (1997) Endogenous type II cGMP-dependent protein kinase exists as a dimer in membranes and can Be functionally distinguished from the type I isoforms, *J Biol Chem 272*, 11816-11823.
150. Pinkse, M. W., Heck, A. J., Rumpel, K., and Pullen, F. (2004) Probing noncovalent protein-ligand interactions of the cGMP-dependent protein kinase using electrospray ionization time of flight mass spectrometry, *J Am Soc Mass Spectrom 15*, 1392-1399.
151. Monken, C. E., and Gill, G. N. (1980) Structural analysis of cGMP-dependent protein kinase using limited proteolysis, *J Biol Chem 255*, 7067-7070.
152. Heil, W. G., Landgraf, W., and Hofmann, F. (1987) A catalytically active fragment of cGMP-dependent protein kinase. Occupation of its cGMP-binding sites does not affect its phosphotransferase activity, *Eur J Biochem 168*, 117-121.
153. Kemp, B. E., and Pearson, R. B. (1991) Intrasteric regulation of protein kinases and phosphatases, *Biochim Biophys Acta 1094*, 67-76.
154. Busch, J. L., Bessay, E. P., Francis, S. H., and Corbin, J. D. (2002) A conserved serine juxtaposed to the pseudosubstrate site of type I cGMP-dependent protein kinase contributes strongly to autoinhibition and lower cGMP affinity, *J Biol Chem 277*, 34048-34054.
155. Yuasa, K., Michibata, H., Omori, K., and Yanaka, N. (2000) Identification of a conserved residue responsible for the autoinhibition of cGMP-dependent protein kinase Ialpha and beta, *FEBS Lett 466*, 175-178.
156. Aitken, A., Hemmings, B. A., and Hofmann, F. (1984) Identification of the residues on cyclic GMP-dependent protein kinase that are autophosphorylated in the presence of cyclic AMP and cyclic GMP, *Biochim Biophys Acta 790*, 219-225.

157. Pinkse, M. W., Uitto, P. M., Hilhorst, M. J., Ooms, B., and Heck, A. J. (2004) Selective isolation at the femtomole level of phosphopeptides from proteolytic digests using 2D-NanoLC-ESI-MS/MS and titanium oxide precolumns, *Anal Chem 76*, 3935-3943.
158. Smith, J. A., Francis, S. H., Walsh, K. A., Kumar, S., and Corbin, J. D. (1996) Autophosphorylation of type Ibeta cGMP-dependent protein kinase increases basal catalytic activity and enhances allosteric activation by cGMP or cAMP, *J Biol Chem 271*, 20756-20762.
159. Hofmann, F., Gensheimer, H. P., and Gobel, C. (1985) cGMP-dependent protein kinase. Autophosphorylation changes the characteristics of binding site 1, *Eur J Biochem 147*, 361-365.
160. Landgraf, W., Hullin, R., Gobel, C., and Hofmann, F. (1986) Phosphorylation of cGMP-dependent protein kinase increases the affinity for cyclic AMP, *Eur J Biochem 154*, 113-117.
161. Ruth, P., Pfeifer, A., Kamm, S., Klatt, P., Dostmann, W. R., and Hofmann, F. (1997) Identification of the amino acid sequences responsible for high affinity activation of cGMP kinase Ialpha, *J Biol Chem 272*, 10522-10528.
162. Landgraf, W., and Hofmann, F. (1989) The amino terminus regulates binding to and activation of cGMP-dependent protein kinase, *Eur J Biochem 181*, 643-650.
163. MacMillan-Crow, L. A., and Lincoln, T. M. (1994) High-affinity binding and localization of the cyclic GMP-dependent protein kinase with the intermediate filament protein vimentin, *Biochemistry 33*, 8035-8043.
164. Casteel, D. E., Zhuang, S., Gudi, T., Tang, J., Vuica, M., Desiderio, S., and Pilz, R. B. (2002) cGMP-dependent protein kinase I beta physically and functionally interacts with the transcriptional regulator TFII-I, *J Biol Chem 277*, 32003-32014.
165. Yuasa, K., Omori, K., and Yanaka, N. (2000) Binding and phosphorylation of a novel male germ cell-specific cGMP-dependent protein kinase-anchoring protein by cGMP-dependent protein kinase Ialpha, *J Biol Chem 275*, 4897-4905.
166. Vaandrager, A. B., Smolenski, A., Tilly, B. C., Houtsmuller, A. B., Ehlert, E. M., Bot, A. G., Edixhoven, M., Boomaars, W. E., Lohmann, S. M., and de Jonge, H. R. (1998) Membrane targeting of cGMP-dependent protein kinase is required for cystic fibrosis transmembrane conductance regulator Cl- channel activation, *Proc Natl Acad Sci U S A 95*, 1466-1471.
167. Takio, K., Wade, R. D., Smith, S. B., Krebs, E. G., Walsh, K. A., and Titani, K. (1984) Guanosine cyclic 3',5'-phosphate dependent protein kinase, a chimeric protein homologous with two separate protein families, *Biochemistry 23*, 4207-4218.
168. Weber, I. T., Takio, K., Titani, K., and Steitz, T. A. (1982) The cAMP-binding domains of the regulatory subunit of cAMP-dependent protein kinase and the

catabolite gene activator protein are homologous, *Proc Natl Acad Sci U S A 79*, 7679-7683.

169. Shabb, J. B., and Corbin, J. D. (1992) Cyclic nucleotide-binding domains in proteins having diverse functions, *J Biol Chem 267*, 5723-5726.
170. Shabb, J. B., Buzzeo, B. D., Ng, L., and Corbin, J. D. (1991) Mutating protein kinase cAMP-binding sites into cGMP-binding sites. Mechanism of cGMP selectivity, *J Biol Chem 266*, 24320-24326.
171. Shabb, J. B., Ng, L., and Corbin, J. D. (1990) One amino acid change produces a high affinity cGMP-binding site in cAMP-dependent protein kinase, *J Biol Chem 265*, 16031-16034.
172. Steinberg, R. A., Gorman, K. B., Ogreid, D., Doskeland, S. O., and Weber, I. T. (1991) Mutations that alter the charge of type I regulatory subunit and modify activation properties of cyclic AMP-dependent protein kinase from S49 mouse lymphoma cells, *J Biol Chem 266*, 3547-3553.
173. Herberg, F. W., Taylor, S. S., and Dostmann, W. R. (1996) Active site mutations define the pathway for the cooperative activation of cAMP-dependent protein kinase, *Biochemistry 35*, 2934-2942.
174. Dostmann, W. R., and Taylor, S. S. (1991) Identifying the molecular switches that determine whether (Rp)-cAMPS functions as an antagonist or an agonist in the activation of cAMP-dependent protein kinase I, *Biochemistry 30*, 8710-8716.
175. Knighton, D. R., Zheng, J. H., Ten Eyck, L. F., Ashford, V. A., Xuong, N. H., Taylor, S. S., and Sowadski, J. M. (1991) Crystal structure of the catalytic subunit of cyclic adenosine monophosphate-dependent protein kinase, *Science 253*, 407-414.
176. Sicheri, F., and Kuriyan, J. (1997) Structures of Src-family tyrosine kinases, *Curr Opin Struct Biol 7*, 777-785.
177. Dostmann, W. R., Nickl, C., Thiel, S., Tsigelny, I., Frank, R., and Tegge, W. J. (1999) Delineation of selective cyclic GMP-dependent protein kinase Ialpha substrate and inhibitor peptides based on combinatorial peptide libraries on paper, *Pharmacol Ther 82*, 373-387.
178. Tegge, W., Frank, R., Hofmann, F., and Dostmann, W. R. (1995) Determination of cyclic nucleotide-dependent protein kinase substrate specificity by the use of peptide libraries on cellulose paper, *Biochemistry 34*, 10569-10577.
179. Zheng, J., Knighton, D. R., ten Eyck, L. F., Karlsson, R., Xuong, N., Taylor, S. S., and Sowadski, J. M. (1993) Crystal structure of the catalytic subunit of cAMP-dependent protein kinase complexed with MgATP and peptide inhibitor, *Biochemistry 32*, 2154-2161.
180. Zheng, J., Trafny, E. A., Knighton, D. R., Xuong, N. H., Taylor, S. S., Ten Eyck, L. F., and Sowadski, J. M. (1993) 2.2 A refined crystal structure of the catalytic subunit

of cAMP-dependent protein kinase complexed with MnATP and a peptide inhibitor, *Acta Crystallogr D Biol Crystallogr 49*, 362-365.

181. Pfeifer, A., Ruth, P., Dostmann, W., Sausbier, M., Klatt, P., and Hofmann, F. (1999) Structure and function of cGMP-dependent protein kinases, *Rev Physiol Biochem Pharmacol 135*, 105-149.
182. Chestukhin, A., Litovchick, L., Schourov, D., Cox, S., Taylor, S. S., and Shaltiel, S. (1996) Functional malleability of the carboxyl-terminal tail in protein kinase A, *J Biol Chem 271*, 10175-10182.
183. Feil, R., Kellermann, J., and Hofmann, F. (1995) Functional cGMP-dependent protein kinase is phosphorylated in its catalytic domain at threonine-516, *Biochemistry 34*, 13152-13158.
184. Hanks, S. K., and Hunter, T. (1995) Protein kinases 6. The eukaryotic protein kinase superfamily: kinase (catalytic) domain structure and classification, *Faseb J 9*, 576-596.
185. Reimann, E. M., Walsh, D. A., and Krebs, E. G. (1971) Purification and properties of rabbit skeletal muscle adenosine 3',5'-monophosphate-dependent protein kinases, *J Biol Chem 246*, 1986-1995.
186. Skalhegg, B. S., Tasken, K., Hansson, V., Huitfeldt, H. S., Jahnsen, T., and Lea, T. (1994) Location of cAMP-dependent protein kinase type I with the TCR-CD3 complex, *Science 263*, 84-87.
187. Schlossmann, J., Ammendola, A., Ashman, K., Zong, X., Huber, A., Neubauer, G., Wang, G. X., Allescher, H. D., Korth, M., Wilm, M., Hofmann, F., and Ruth, P. (2000) Regulation of intracellular calcium by a signalling complex of IRAG, IP3 receptor and cGMP kinase Ibeta, *Nature 404*, 197-201.
188. Gold, M. G., Lygren, B., Dokurno, P., Hoshi, N., McConnachie, G., Tasken, K., Carlson, C. R., Scott, J. D., and Barford, D. (2006) Molecular basis of AKAP specificity for PKA regulatory subunits, *Mol Cell 24*, 383-395.
189. Daub, H., Godl, K., Brehmer, D., Klebl, B., and Muller, G. (2004) Evaluation of kinase inhibitor selectivity by chemical proteomics, *Assay Drug Dev Technol 2*, 215-224.
190. Bauer, A., and Kuster, B. (2003) Affinity purification-mass spectrometry. Powerful tools for the characterization of protein complexes, *Eur J Biochem 270*, 570-578.
191. Heck, A. J., and Krijgsveld, J. (2004) Mass spectrometry-based quantitative proteomics, *Expert Rev Proteomics 1*, 317-326.
192. Kirkpatrick, D. S., Gerber, S. A., and Gygi, S. P. (2005) The absolute quantification strategy: a general procedure for the quantification of proteins and post-translational modifications, *Methods 35*, 265-273.

193. Bowen, L. C., Bicknell, A. V., Tabish, M., Clegg, R. A., Rees, H. H., and Fisher, M. J. (2006) Expression of multiple isoforms of the cAMP-dependent protein kinase (PK-A) catalytic subunit in the nematode, Caenorhabditis elegans, *Cell Signal 18*, 2230-2237.
194. Carr, D. W., Hausken, Z. E., Fraser, I. D., Stofko-Hahn, R. E., and Scott, J. D. (1992) Association of the type II cAMP-dependent protein kinase with a human thyroid RII-anchoring protein. Cloning and characterization of the RII-binding domain, *J Biol Chem 267*, 13376-13382.
195. Katayama, H., and Oda, Y. (2007) Chemical proteomics for drug discovery based on compound-immobilized affinity chromatography, *J Chromatogr B Analyt Technol Biomed Life Sci*.
196. Gavin, A. C., Bosche, M., Krause, R., Grandi, P., Marzioch, M., Bauer, A., Schultz, J., Rick, J. M., Michon, A. M., Cruciat, C. M., Remor, M., Hofert, C., Schelder, M., Brajenovic, M., Ruffner, H., Merino, A., Klein, K., Hudak, M., Dickson, D., Rudi, T., Gnau, V., Bauch, A., Bastuck, S., Huhse, B., Leutwein, C., Heurtier, M. A., Copley, R. R., Edelmann, A., Querfurth, E., Rybin, V., Drewes, G., Raida, M., Bouwmeester, T., Bork, P., Seraphin, B., Kuster, B., Neubauer, G., and Superti-Furga, G. (2002) Functional organization of the yeast proteome by systematic analysis of protein complexes, *Nature 415*, 141-147.
197. Shoji, S., Titani, K., Demaille, J. G., and Fischer, E. H. (1979) Sequence of two phosphorylated sites in the catalytic subunit of bovine cardiac muscle adenosine 3':5'-monophosphate-dependent protein kinase, *J Biol Chem 254*, 6211-6214.
198. Rangel-Aldao, R., and Rosen, O. M. (1976) Mechanism of self-phosphorylation of adenosine 3':5'-monophosphate-dependent protein kinase from bovine cardiac muscle, *J Biol Chem 251*, 7526-7529.
199. Taylor, S. S., Buechler, J. A., and Yonemoto, W. (1990) cAMP-dependent protein kinase: framework for a diverse family of regulatory enzymes, *Annu Rev Biochem 59*, 971-1005.
200. Carmichael, D. F., Geahlen, R. L., Allen, S. M., and Krebs, E. G. (1982) Type II regulatory subunit of cAMP-dependent protein kinase. Phosphorylation by casein kinase II at a site that is also phosphorylated in vivo, *J Biol Chem 257*, 10440-10445.
201. Andersson, L., and Porath, J. (1986) Isolation of phosphoproteins by immobilized metal (Fe3+) affinity chromatography, *Anal Biochem 154*, 250-254.
202. Villen, J., Beausoleil, S. A., Gerber, S. A., and Gygi, S. P. (2007) Large-scale phosphorylation analysis of mouse liver, *Proc Natl Acad Sci U S A 104*, 1488-1493.
203. Olsen, J. V., Blagoev, B., Gnad, F., Macek, B., Kumar, C., Mortensen, P., and Mann, M. (2006) Global, in vivo, and site-specific phosphorylation dynamics in signaling networks, *Cell 127*, 635-648.

204. Benschop, J. J., Mohammed, S., O'Flaherty, M., Heck, A. J., Slijper, M., and Menke, F. L. (2007) Quantitative Phosphoproteomics of Early Elicitor Signaling in Arabidopsis, *Mol Cell Proteomics 6*, 1198-1214.
205. Scholten, A. *Unpublished Results*.
206. Gesellchen, F., Bertinetti, O., and Herberg, F. W. (2006) Analysis of posttranslational modifications exemplified using protein kinase A, *Biochim Biophys Acta 1764*, 1788-1800.
207. Huang, S. Y., Tsai, M. L., Chen, G. Y., Wu, C. J., and Chen, S. H. (2007) A systematic MS-based approach for identifying in vitro substrates of PKA and PKG in rat uteri, *J Proteome Res 6*, 2674-2684.
208. Hsu, J. L., Huang, S. Y., and Chen, S. H. (2006) Dimethyl multiplexed labeling combined with microcolumn separation and MS analysis for time course study in proteomics, *Electrophoresis 27*, 3652-3660.
209. Hsu, J. L., Huang, S. Y., Chow, N. H., and Chen, S. H. (2003) Stable-isotope dimethyl labeling for quantitative proteomics, *Anal Chem 75*, 6843-6852.
210. Li, F., Gangal, M., Jones, J. M., Deich, J., Lovett, K. E., Taylor, S. S., and Johnson, D. A. (2000) Consequences of cAMP and catalytic-subunit binding on the flexibility of the A-kinase regulatory subunit, *Biochemistry 39*, 15626-15632.
211. Li, F., Gangal, M., Juliano, C., Gorfain, E., Taylor, S. S., and Johnson, D. A. (2002) Evidence for an internal entropy contribution to phosphoryl transfer: a study of domain closure, backbone flexibility, and the catalytic cycle of cAMP-dependent protein kinase, *J Mol Biol 315*, 459-469.
212. Banky, P., Roy, M., Newlon, M. G., Morikis, D., Haste, N. M., Taylor, S. S., and Jennings, P. A. (2003) Related protein-protein interaction modules present drastically different surface topographies despite a conserved helical platform, *J Mol Biol 330*, 1117-1129.
213. Yu, S., Mei, F. C., Lee, J. C., and Cheng, X. (2004) Probing cAMP-dependent protein kinase holoenzyme complexes I alpha and II beta by FT-IR and chemical protein footprinting, *Biochemistry 43*, 1908-1920.
214. Zawadzki, K. M., Pan, C. P., Barkley, M. D., Johnson, D., and Taylor, S. S. (2003) Endogenous tryptophan residues of cAPK regulatory subunit type IIbeta reveal local variations in environments and dynamics, *Proteins 51*, 552-561.
215. Leon, D. A., Dostmann, W. R., and Taylor, S. S. (1991) Unfolding of the regulatory subunit of cAMP-dependent protein kinase I, *Biochemistry 30*, 3035-3040.
216. Wales, T. E., and Engen, J. R. (2006) Hydrogen exchange mass spectrometry for the analysis of protein dynamics, *Mass Spectrom Rev 25*, 158-170.
217. Hotchko, M., Anand, G. S., Komives, E. A., and Ten Eyck, L. F. (2006) Automated extraction of backbone deuteration levels from amide H/2H mass spectrometry experiments, *Protein Sci 15*, 583-601.

218. Mandell, J. G., Falick, A. M., and Komives, E. A. (1998) Identification of protein-protein interfaces by decreased amide proton solvent accessibility, *Proc Natl Acad Sci U S A 95*, 14705-14710.
219. Mandell, J. G., Falick, A. M., and Komives, E. A. (1998) Measurement of amide hydrogen exchange by MALDI-TOF mass spectrometry, *Anal Chem 70*, 3987-3995.
220. Truhlar, S. M., Croy, C. H., Torpey, J. W., Koeppe, J. R., and Komives, E. A. (2006) Solvent accessibility of protein surfaces by amide H/2H exchange MALDI-TOF mass spectrometry, *J Am Soc Mass Spectrom 17*, 1490-1497.
221. Anand, G. S., Hughes, C. A., Jones, J. M., Taylor, S. S., and Komives, E. A. (2002) Amide H/2H exchange reveals communication between the cAMP and catalytic subunit-binding sites in the R(I)alpha subunit of protein kinase A, *J Mol Biol 323*, 377-386.
222. Anand, G. S., Law, D., Mandell, J. G., Snead, A. N., Tsigelny, I., Taylor, S. S., Ten Eyck, L. F., and Komives, E. A. (2003) Identification of the protein kinase A regulatory RIalpha-catalytic subunit interface by amide H/2H exchange and protein docking, *Proc Natl Acad Sci U S A 100*, 13264-13269.
223. Hamuro, Y., Zawadzki, K. M., Kim, J. S., Stranz, D. D., Taylor, S. S., and Woods, V. L., Jr. (2003) Dynamics of cAPK type IIbeta activation revealed by enhanced amide H/2H exchange mass spectrometry (DXMS), *J Mol Biol 327*, 1065-1076.
224. Zawadzki, K. M., Hamuro, Y., Kim, J. S., Garrod, S., Stranz, D. D., Taylor, S. S., and Woods, V. L., Jr. (2003) Dissecting interdomain communication within cAPK regulatory subunit type IIbeta using enhanced amide hydrogen/deuterium exchange mass spectrometry (DXMS), *Protein Sci 12*, 1980-1990.
225. Kim, C., Xuong, N. H., and Taylor, S. S. (2005) Crystal structure of a complex between the catalytic and regulatory (RIalpha) subunits of PKA, *Science 307*, 690-696.
226. Burns-Hamuro, L. L., Hamuro, Y., Kim, J. S., Sigala, P., Fayos, R., Stranz, D. D., Jennings, P. A., Taylor, S. S., and Woods, V. L., Jr. (2005) Distinct interaction modes of an AKAP bound to two regulatory subunit isoforms of protein kinase A revealed by amide hydrogen/deuterium exchange, *Protein Sci 14*, 2982-2992.
227. Iyer, G. H., Garrod, S., Woods, V. L., Jr., and Taylor, S. S. (2005) Catalytic independent functions of a protein kinase as revealed by a kinase-dead mutant: study of the Lys72His mutant of cAMP-dependent kinase, *J Mol Biol 351*, 1110-1122.
228. Wall, M. E., Francis, S. H., Corbin, J. D., Grimes, K., Richie-Jannetta, R., Kotera, J., Macdonald, B. A., Gibson, R. R., and Trewhella, J. (2003) Mechanisms associated with cGMP binding and activation of cGMP-dependent protein kinase, *Proc Natl Acad Sci U S A 100*, 2380-2385.
229. Zhao, J., Trewhella, J., Corbin, J., Francis, S., Mitchell, R., Brushia, R., and Walsh, D. (1997) Progressive cyclic nucleotide-induced conformational changes in the cGMP-

dependent protein kinase studied by small angle X-ray scattering in solution, *J Biol Chem 272*, 31929-31936.

230. Scholten, A., Fuss, H., Heck, A. J., and Dostmann, W. R. (2007) The hinge region operates as a stability switch in cGMP-dependent protein kinase Ialpha, *Febs J 274*, 2274-2286.
231. Chu, D. M., Corbin, J. D., Grimes, K. A., and Francis, S. H. (1997) Activation by cyclic GMP binding causes an apparent conformational change in cGMP-dependent protein kinase, *J Biol Chem 272*, 31922-31928.
232. Heck, A. J., and Van Den Heuvel, R. H. (2004) Investigation of intact protein complexes by mass spectrometry, *Mass Spectrom Rev 23*, 368-389.
233. van den Heuvel, R. H., and Heck, A. J. (2004) Native protein mass spectrometry: from intact oligomers to functional machineries, *Curr Opin Chem Biol 8*, 519-526.
234. Benesch, J. L., Ruotolo, B. T., Simmons, D. A., and Robinson, C. V. (2007) Protein Complexes in the Gas Phase: Technology for Structural Genomics and Proteomics, *Chem Rev*.
235. Alverdi, V., Mazon, H., Hemrika, W., Scholten, A., Van den Heuvel, R. H., and Heck, A. J. (2007) *Submitted*.
236. Adams, J. A., and Taylor, S. S. (1993) Phosphorylation of peptide substrates for the catalytic subunit of cAMP-dependent protein kinase, *J Biol Chem 268*, 7747-7752.
237. Bhatnagar, D., Roskoski, R., Jr., Rosendahl, M. S., and Leonard, N. J. (1983) Adenosine cyclic 3',5'-monophosphate dependent protein kinase: a new fluorescence displacement titration technique for characterizing the nucleotide binding site on the catalytic subunit, *Biochemistry 22*, 6310-6317.
238. Wyttenbach, T., and Bowers, M. T. (2007) Intermolecular interactions in biomolecular systems examined by mass spectrometry, *Annu Rev Phys Chem 58*, 511-533.
239. Valentine, S. J., Liu, X., Plasencia, M. D., Hilderbrand, A. E., Kurulugama, R. T., Koeniger, S. L., and Clemmer, D. E. (2005) Developing liquid chromatography ion mobility mass spectometry techniques, *Expert Rev Proteomics 2*, 553-565.

Chapter 3

Selectivity in enrichment of PKA RI and RII isoforms and their interactors using modified cAMP affinity resins

Thin Thin Aye[1,2]
Shabaz Mohammed[1,2]
Henk W.P. van den Toorn[1,2]
Toon A.B. Van Veen[3]
Marcel A. G. van der Heyden[3]
Arjen Scholten[1,2]
Albert J. R. Heck[1,2]

[1]Department of Biomolecular Mass Spectrometry and Proteomic Group, Bijvoet Center for Biomolecular Research and Utrecht Institute for Pharmaceutical Sciences, Utrecht University, Sorbonnelaan 16, 3584 CA Utrecht, the Netherlands
[2]Netherland Proteomics Centre, The Netherlands
[3]Department of Medical Physiology, University Medical Centre Utrecht, Yalelaan 50, 3584 CM Utrecht, The Netherlands

Mol Cell Proteomics. 2009 May;8(5):1016-28.

Abstract

cAMP regulates cellular functions primarily by activating PKA. The involvement of PKAs in various signaling pathways occurring simultaneously in different cellular compartments necessitates stringent spatial and temporal regulation. This specificity is largely achieved by binding of PKA to protein scaffolds, whereby a distinct group of proteins called A kinase anchoring proteins (AKAPs) play a dominant role. AKAPs are a diverse family of proteins that all bind via a small PKA binding domain to the regulatory subunits of PKA. The binding affinities between PKA and several AKAPs can be different for different isoforms of the regulatory subunits of PKA. Here we employ a combination of affinity chromatography and mass spectrometry-based quantitative proteomics to investigate specificity in PKA-AKAP interactions. Three different immobilized cAMP analogues were used to enrich for PKA and its interacting proteins from several systems; HEK293 and RCC10 cells and rat lung and testis tissues. Stable isotope labeling was used to confidently identify and differentially quantify target proteins and their preferential binding affinity for the three different cAMP analogs. We were able to enrich all four isoforms of the regulatory subunits of PKA, and concomitantly identify more than ten AKAPs. A selective enrichment of the PKA RI isoforms could be achieved; which allowed us to unravel which AKAPs bind preferentially to the RI or RII regulatory domains of PKA. Of the twelve AKAPs detected, seven preferentially bound to RII, whereas the remaining five displayed at least dual-specificity with a potential preference for RI. For some of these AKAPs our data provides the first insights into their specificity.

3.1. Introduction

cAMP is an ubiquitous second messenger that transduces signals from a variety of hormones, neurotransmitters and inflammatory mediators to regulate a large number of key cellular processes. cAMP can influence cell growth, differentiation and movement as well as regulating specialized actions unique to specific cell types. The principal target of cAMP is protein kinase A (PKA). Several other proteins such as cyclic nucleotide gated channels (CNG) (*1*), phosphodiesterases (PDE)(*2*) and guanine nucleotide exchange factors (Epac)(*3*) bind cAMP. Interestingly, localized pools of cAMP regulate defined physiological events. It appears that for such events a supramolecular complex is required that comprises of the appropriate effector system together with signal termination enzymes such as PDEs and phosphatases (PPs) that are sequestered by scaffolding proteins(*4*). Some of the best-described scaffolding proteins are the so-called A-kinase Anchoring Proteins (AKAPs), which all bind specifically to the N-terminal dimerization domain of the PKA regulatory domain. The organization of a few of these individual supramolecular complexes containing PKA/AKAPs/PDE etc. have been described(*4*), numerous more of such complexes are expected to exist.

The regulatory domains of mammalian PKAs exist in several isoforms such as RIα, RIβ, RIIα and RIIβ, which are all encoded by separate genes. The two major isoforms i.e. RI and RII differ in molecular weight, isoelectric point, amino acid sequence, phosphorylation status, tissue distribution and sub-cellular localization. RI and RII subunits are known to bind to AKAPs with distinct levels of affinity adding another level of intracellular organization for PKA and also facilitating the diversity of the cAMP mediated signal transduction pathways. Although the PKA-R isoforms differ in functionality, they share a similar overall organization i.e. a dimerization domain, the catalytic subunits inhibitor region and two cAMP binding domains. The two cAMP binding domains differ in cAMP binding kinetics and are known as site A and site B respectively (*5*). Both sites share considerable sequence identity, as a result of a tandem gene duplication, and have conserved phosphate binding cassettes (PBC) that can be considered as signature motif for cAMP binding. The relative orientation of these two sites is nonetheless, quite different in RI and RII. Additionally, the A and B sites have different binding affinity to cAMP derivatives. Site A has a preference for N6-substituted analogs while Site B is preferred by C2- and C8-substituted analogs (*6*).

Protein kinase A has been studied for a long time (*7, 8*). One of the important goals therein is to develop different cAMP analogs that can result in specific binding, activation and/or inhibition for each individual cAMP interaction site of the RI and RII isoforms (*9*). This can help to decipher in detail, specific cyclic nucleotide signaling pathways(*10*). To fully interpret such pathways, analogs should ideally not cross-activate (or inhibit) with other cAMP regulated proteins such as the before mentioned PDEs, EPAC, CNG and the cGMP-dependent protein kinase (PKG). Although the latter is mainly activated by cGMP, it also binds to cAMP (*11, 12*). It has been suggested that cGMP and cAMP can cross-activate their respective kinase (*13*). This cross-talk between PKA and PKG hampers, to some degree, the study of these proteins individually, as dissecting the individual pathways of PKA and PKG requires specific binders, activators or inhibitors (*9, 14*). Compared to PKA, PKG is involved in quite different signalling pathways, such as the well-characterized nitric oxide mediated relaxation of smooth muscle cells (*15*).

The development of synthetic cAMP and cGMP analogs as tools to unravel specific signal transduction pathways requires the sensitive identification and characterization of their cyclic nucleotide interacting proteins. These proteins are typically relatively low abundant, and therefore specific enrichment techniques are essential to study these so-called cyclic-nucleotide interactomes. In recent years such affinity enrichment techniques have been coupled to sensitive mass spectrometric identification of the enriched proteins, nowadays often referred to as chemical proteomics. Chemical proteomics using small molecules as baits, i.e. messenger molecules, drugs or metabolites, becomes more and more widely used to selectively isolate target proteins from whole cell lysates enabling the analysis of protein subcomplexes and/or signaling pathways (*16, 17*).

In the present study we compare the properties of three cAMP analogues immobilized individually on agarose beads, for enrichment, isolation and detection of cyclic nucleotide interacting proteins and their interaction partners, like AKAPs, directly from a crude lysate of cells and tissue. To quantify differential affinity, we use a common strategy in proteomics, namely stable isotope labeling, whereby we introduce the label via reductive amination (*18-20*). Most interestingly, a very selective enrichment of PKA RI isoforms can be achieved by using cAMP-agarose beads in which the hydroxyl group at the 2' position on the ribose was replaced with a methoxyl-group. This allows us to distinguish which AKAPs bind preferentially to the RI or RII isoforms. Therefore, this approach provides an elegant tool to further decipher specific cyclic nucleotide signaling pathways.

3.2. Experimental procedures

3.2.1. Materials

The cAMP coupled agarose beads were purchased from BIOLOG (Bremen, Germany). The amount of immobilized cyclic nucleotide on the beads was ~6 µmol/mL. Protease inhibitor cocktail was from Roche Diagnostics (Almere, The Netherlands). All other chemicals were purchased from commercial sources and were of analysis grade, unless stated otherwise. Isotope labeled CD_2O formaldehyde (20% solution in D_2O) was from Sigma-Aldich (Milwaukee, USA). The rabbit polyclonal PKA RIα, RIIα antibodies and HRP-conjugated secondary antibody were from Santa Cruz Biotechnology Inc. (California, USA). High purity water, obtained from a Milli-Q system (Millipore, Bedford, MA USA), was used for all experiments.

3.2.2. Tissue and cell lysate preparation

Lysate and tissue preparation protocols were largely as described previously (*17, 21*). Briefly, HEK293 cells ($1.5x10^6$ cells/mL) were lysed by dounce homogenization and were left on ice for 10 min. The soluble fraction was taken after centrifugation at 20,800g for 10 min. The yield was approximately 8 mg of protein, as determined by Bradford assay. For the tissue sample, approximately 800 mg of tissue was pulverized in a custom made steel mortar which was pre-cooled with liquid nitrogen. Subsequently, 1 mL of ice-cold lysis buffer (50mM K_2HPO_4, pH 7.0, 150mM NaCl. 0.1% Tween 20, Protease Inhibitor cocktail) was added and the sample was left at room temperature for 5 min. These treated tissue samples were stored on ice for another 10 min. followed by the same procedure as that for HEK293 cells. The final yield of protein was approximately 80 mg.

3.2.3. Pull-down assay

Prior to pull-down, a 50 µL dry volume of immobilized cAMP beads (~300 nmol of cAMP) were washed with 1 mL of PBS buffer (50mM K_2HPO_4, 150mM NaCl). For control, beads blocked by ethanolamine were used in a parallel identical pulldown procedure. Prior to

the pull-down assays, tissue and cell lysates were incubated with 10 mM ADP/GDP and incubated for 15 min at 4 ^{o}C in order to reduce non-specific binding, mainly contributed by ADP and GDP binding proteins(*17, 21*). cAMP agarose beads were added to the lysate in the volume ratio of 1:100 beads to lysate ratio. The lysate-bead suspension was incubated for 2 hours at 4 ^{o}C by rotary shaking. The supernatant was collected as unbound fraction (UF). The bead bound fraction (BF), was washed in several steps with in total 12 mL of lysis buffer to further reduce non-specific binding. Then the bound fraction was eluted with 90µl of 8M Urea for denaturing. After digestion with lysine-C (Roche Diagnostics, Almere, The Netherlands) for 4 hr at 37 ^{o}C, reduction and alkylation of the peptides were performed in 2M urea, followed by further digestion by trypsin (Roche Diagnostics, Almere, The Netherlands). The dual protease digestion procedure resulted in the detection of more peptides. Reproducibility of the pull down experiments was evaluated in the rat testis tissue. The ratio's observed in this duplicate experiment were reproducible as they were within an experimental error of 10% (Supplemental Table S1).

3.2.4. Stable isotope labeling strategy

The resulting peptides were desalted, dried *in-vacuo* and re-suspended in 100 µL of triethylammonium bicarbonate (100 µM). Subsequently, 4 µL formaldehyde-H_2 (4% v/v in water for light-labeling) was added, vortexed for 2 minutes followed by the addition of 4 µL of freshly prepared sodium cyanoborohydride (600 mM). The resultant mixture was vortexed for 5 min. at RT. 16 µL of ammonium hydroxide (1% in water) was added to consume the excess formaldehyde, and 5% formic acid (in water) was added to acidify the solution. For perdeutero-methylation labeling, formaldehyde-D2 (4% v/v in water) was used. The light 4H- and heavy 4D- di-methyl labeled samples were mixed in 1:1 ratio based on the total protein input material for the pull down and dried *in vacuum*, and then re-dissolved in 5% ACN containing 0.1 formic acid, prior to preparation for mass spectrometric analysis.

3.2.5. Protein identification and quantification

For mass spectrometric analysis peptides were injected onto a nano-scale liquid chromatography system. Therefore, an Agilent 1100 series LC system was equipped with an 20 mm Aqua C18 (Phenomenex, Torrance, CA) trapping column (packed in-house, i.d., 100 µm; resin, 5 µm) and a 250 mm ReproSil-Pur C18-AQ f analytical column (packed in-house, i.d., 50 µm; resin, 3 µm). Trapping was performed at 5 µL/min for 10 min and elution was achieved with a gradient of 0-32% B in 60 min, 32-40% B in 5 min, 40-100% B in 2 min and 100% B for 2 min leading to a total analysis time of 90 minutes. The flow rate was passively split from 0.4 ml/min to 100 nl/min when performing the elution analysis. Nanospray was achieved using a distally coated fused silica emitter (New Objective, Cambridge, MA) (o.d., 360 µm; i.d., 20 µm, tip i.d. 10 µm) biased to 1.8 kV. The LC system was coupled to a 7

Tesla Finnigan LTQ-FT ICR mass spectrometer (Thermo Electron, Bremen, Germany). Briefly, the mass spectrometer was operated in the data-dependent mode to automatically switch between MS and MS/MS acquisition. Survey full scan MS spectra were acquired from m/z 350 to m/z 1500 in the FT-ICR with a resolution of R=100,000 at m/z 400 after accumulation to a target value of 2,000,000 in the linear ion trap. The five most intense ions were fragmented in the linear ion trap using collisionally induced dissociation at a target value of 10,000. Spectra were processed with Bioworks 3.3 (Thermo, Bremen, Germany) and the subsequent data analysis was carried out using the Mascot (version 2.1.0) software platform (Matrix Science, London, UK) against the IPI-Rat database version 3.19 (44845 protein sequences; 23003239 residues) allowing 1 missed cleavages, carbamidomethyl (C) as fixed modification, 'light' and 'heavy' methylation of peptide N-termini and lysine residues and oxidation (M) as variable modifications. The peptide tolerance was set to 10 ppm and the MS/MS tolerance to 0.9 Da. Proteins were organized using the scaffold software package (www.proteomesoftware.com). Quantification was performed using MSQuant which is a modified version of 1.4.2a (http://msquant.sourceforge.net/). Peptide ratios between the monoisotopic peaks of "normal" and "heavy" forms of the peptide were calculated and averaged over consecutive MS cycles for the duration of their respective LC-MS peaks in the total ion chromatogram using only FT-MS scans heavy and light labeled peptides were found to co-elute. All data presented in this manuscript is available in the pride database (http://www.ebi.ac.uk/pride) under the PRIDE experiment accession numbers: 3706-3714 and project title name *Selectivity in enrichment of PKA isoforms and their interactors*.

3.2.6. Immunoblotting

After separating the affinity purified proteins from HEK293 cells on a 1D SDS-PAGE gel, they were transferred to nitrocellulose membranes. Blocking was performed using a solution of TBS (pH7.5) containing 5% non-fat milk powder. The membranes were then respectively incubated with the PKA RIα (goat polyclonal antibody, PKA Iα reg (C-14): sc-18800, Santa Cruz Biotechnology, USA) in a dilution ratio of 1:100, and PKA RIIα (rabbit polyclonal antibody, PKA IIα reg (M-20): sc-30666, Santa Cruz Biotechnology, USA) in a ratio of 1:100 for 1 h at room temperature. The membranes were washed for 40 min., changing the TBS buffer every 10 min, and then incubated with an HRP-conjugated secondary antibody (sc-2004 and sc-2768, Santa Cruz Biotechnology, USA) in a dilution ratio of 1:1000 for 1h at room temperature. After washing the membrane with TBS buffer, the membrane was subjected to chemiluminescence detection according to the manufacturer's protocol (ECL, Amersham Bioscience).

3.3. Results

For the affinity purification of cAMP interacting proteins, various cAMP analogs are available. These cAMP analogs can be immobilized to beads using different coupling

positions and different linkers. Here we chose to use agarose beads on which cAMP is immobilized via an aminohexylamino spacer that is attached to either the 8-position of the imidazole ring or 2-position of the pyrimidine ring in the adenine moiety (referred to further on as **C8** for the 8-position linked cAMP analog; and **C2** for the 2-position linked cAMP analog). We took a long chain spacer, as it is expected that the conformational flexibility of the ligand is also increased by increasing the chain length. In addition, we selected 8AHA-2'-O-Me-cAMP-agarose beads (further referred to as **C8_OCH$_3$**) in which the hydroxyl group at the 2' position on the ribose is replaced with a methoxyl-group. This modified cAMP analogue, which is thought to have specific activation characteristics for EPAC1(*22*), is linked to the agarose beads via a similar 1,6-diaminohexyl spacer at the C8-position of the adenine ring. Finally, as a negative control we used beads that were blocked by ethanolamine. The chemical structures of the cAMP analogues immobilized on the beads are shown schematically in Figure 1A.

3.3.1. Differential affinity enrichment of the cAMP beads visualized by 1D gel analysis

In the first experiment, we divided rat lung tissue lysate into four equal aliquots. These four samples were individually incubated with the four different, above-mentioned, affinity beads. Following incubation and affinity purification, the enriched proteins were separated using SDS-PAGE. As shown in Figure 1B, the gel obtained with the control ethanolamine blocked beads (EtOH) did not show any significant protein bands in contrast to protein bands that were pulled-down using the C8 beads, C2 beads and C8_OCH$_3$ beads, respectively. These three lanes clearly show the high degree of selectivity obtained using our specific enrichment, comparable to results reported previously (*17*). Although the three gel lanes show high similarity, there are also striking differences, especially in the molecular weight region where the PKA RI and RII subunits are expected. To confidently identify these differences, we cut each of the four lanes into 20 equal pieces and subjected them to LC-MS analysis. The resulting mass spectra were analyzed using MASCOT and organized using the Scaffold software package. For confident identifications we set a threshold at a minimum of 3 unique peptides with a peptide Mascot score of 30 ($p<0.05$). Using these strict settings, we identified 56 proteins in the C8 dataset, 62 proteins for the C2 gel lane, 40 proteins for the C8_OCH$_3$ sample (Supplemental Table S2), and no significant proteins in the control lane for the ethanolamine blocked beads. The number of proteins detected is relatively low, but, as illustrated in Supplemental Table S2, very specific. A large fraction of proteins are 'real' cyclic nucleotide binding proteins or interactors thereof. We attribute this to the fact that we are able to significantly reduce 'non-specific' binding proteins by pre-clearing the lysates with ADP/GDP(*17*). To confidently determine the relative affinity purification levels of each protein with each of the four types of beads we chose to use isotope labeling by chemical reductive dimethylation labeling (*18-20*).

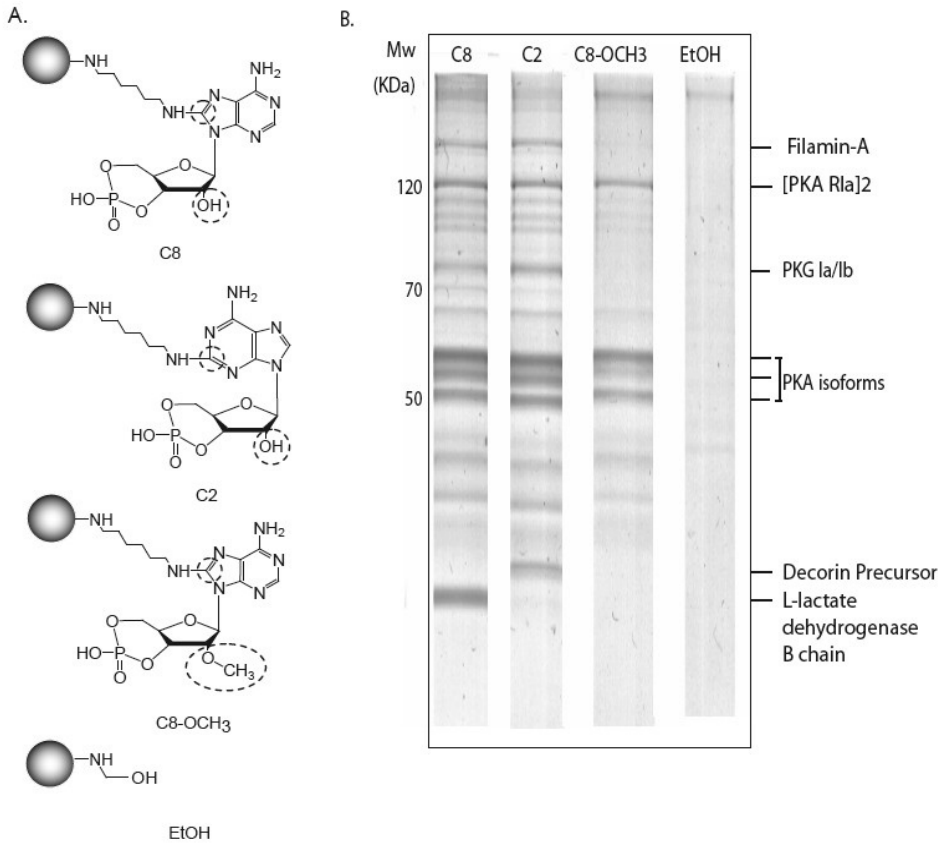

Figure 1. (A). The chemical structures of the modified immobilized cAMP analogues beads. (B) SDS-page gels (Coomassie stained) of rat lung tissue incubated with C8 (lane 1), C2 (lane 2), C8_OCH3 (lane 3) and EtOH control (lane 4) beads. The triplet bands around 50 kDa originate from the PKA-R isoforms, whereas the band at ~75 kDa is PKG.

3.3.2. Differential affinity enrichment determined by stable isotope labeling based quantitative proteomics

Stable isotope labeling in combination with mass spectrometry is a very elegant approach to quantify differential protein expression (*23, 24*). To differentially quantify the protein abundance in each pull-down fraction using the four different affinity beads, we designed an experiment as depicted schematically in Figure 2 and in more detail in Supplemental Figure S1. Following the affinity pull-down, we digested all proteins in-solution and chemically labeled the tryptic peptides originating from the pull-down with C8 beads with perdeutero-formaldehyde. In individual experiments, the peptides originating

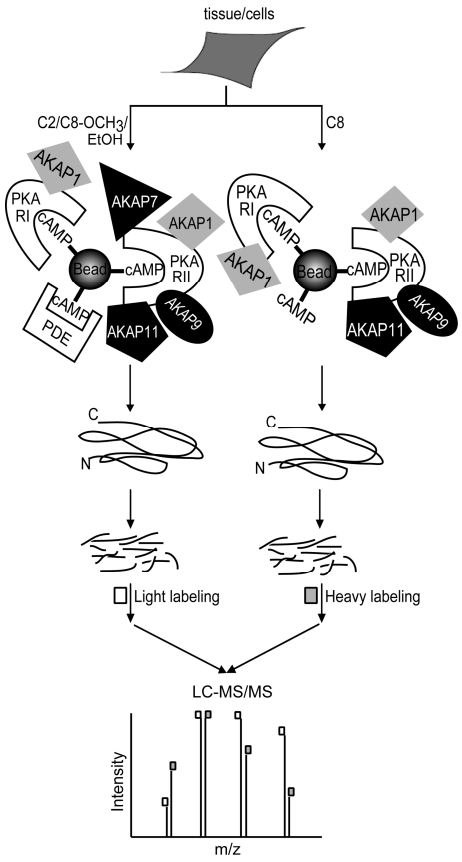

Figure 2. Following the parallel affinity enrichments using C8 and C2 beads, proteins were digested in-solution with LysC and trypsin, respectively. The tryptic peptides originating from the pull-down using the C8 beads were chemically labeled using CD_2O ('heavy-label') whereas those originating from C2 beads (and also C8_OCH_3 and EtOH beads) were labeled with CH_2O ('light-label'). Each set of CD_2O and CH_2O labeled samples were mixed in a 1:1 ratio (Supplemental Figure S1) and then analyzed by LC-coupled nanospray LTQ-FT-ICR mass spectrometry for protein identification and quantification.

from the pull-downs using C2, the C8_OCH_3 and the ethanolamine blocked beads were chemically labeled using normal formaldehyde. In dimethyl labeling, formaldehyde reacts with the N-terminus and the α-amino group of lysine residues of a peptide, which are subsequently reduced with sodium cyanoborohydride to generate secondary amino groups that are relatively more reactive than their original primary amino groups. Subsequently, each of these species reacts with another formaldehyde moiety to produce a dimethyl substituted tertiary amino group adding 28 (CH_2O, "light") or 32 Da (CD_2O, "heavy") in mass for each N-terminus or lysine residue in each peptide (*18-20*). We mixed the "heavy" labeled sample obtained with the C8 beads, with one of the other three "light" labeled samples. Each set of two labeled samples were mixed in a 1:1 ratio and then analyzed by LC-coupled nanospray LTQ-FT-ICR based mass spectrometry for protein identification and quantification.

In Figure 3, an illustrative example of our quantitative analysis is given, whereby MS spectra (upper panel) and extracted ion chromatograms (lower panel) are depicted in which the "light" (dashed line) and "heavy" (solid line) of individual peptide pairs can be distinguis-

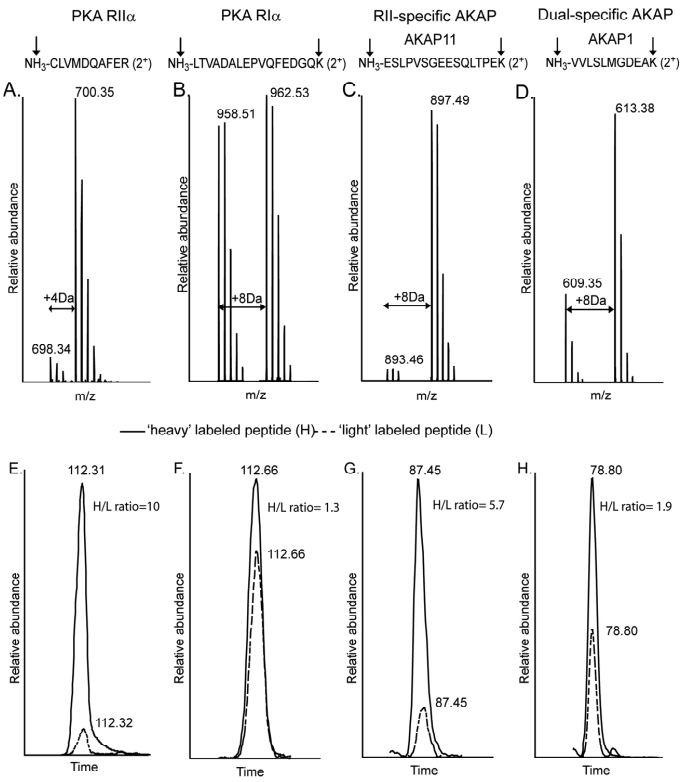

Figure 3. MS spectra (upper panels, A-D) and extracted ion chromatograms (lower panels, E-H) of peptides originating from proteins in the affinity-enriched HEK293 cell lysate are depicted. The upper panel shows that each detected peptide exists as a pair with a typical 2Da m/z difference for doubly charged peptides that have no lysine residues whereas a 4Da m/z difference is observed for doubly charged peptides with one lysine residue. Labeling sites are indicated by the arrows. In the lower panel, the heavy-labeled peptides (peptides which are enriched by C8) are in solid line and light-labeled peptides (peptides which are enriched by C8-OCH_3) are in dashed line. Each individual peptide pair is used for the assessment of differential binding affinities.

hed. Each peptide is detected as a pair with a typical mass difference of 4 Da per amine group, i.e. for the N-terminus and each lysine residue present in the peptide. For instance, in the doubly charged peptide of CLVMDVQAFER (Figure 3A), formaldehyde dimethylates the N-terminus generating a m/z difference of 2 which is corresponding to a mass difference of 4 Da between the light- and heavy- labeled peptide. It has been reported that hydrogen-based isotopes can have an isotopic effect during LC separation in which the heavy and light tags

show a partial separation which can obviously reduce the accuracy of quantification. However, as shown in Figure 3E, F, G and H, both the light- and heavy-labeled peptide ions co-elute, indicating that such an isotopic effect turns out to be negligible. This is possibly due to deuterium labeling occurring on charged amino residues, which may reduce the differential interaction of hydrogen and deuterium based methyl labels with the RP-HPLC stationary phase(*19*).

We performed affinity enrichments with three different immobilized cAMP beads in the lysates of HEK293 cells, RCC10 cells, rat lung and rat testis tissue. We selected these four systems as literature predicted that they may contain quite a diversity of cAMP interacting proteins. A summary of proteins detected, together with the number of identified and quantified peptides, with each of the four beads (i.e. C8, C2, C8_OCH_3, EtOH) with different samples is given in Supplemental Tables S3A-I. All peptide pairs used for differential quantification are listed in this summary together with their ratios. The protein differential binding ratio was calculated by averaging over all peptide pairs measured for that particular protein. In the remainder of the paper we do not further discuss the results with the ethanolamine blocked beads, as for all proteins discussed below, we were not able to detect them using these beads underscoring the selectivity of our affinity-purifications.

In our pull-downs, we enriched most specifically for the isoforms of the regulatory domain of PKA, represented by the triplet dark bands on the 1D gel of Figure 1. We detected all four described PKA-R isoforms. Figure 4A illustrates the differential enrichment of PKA RIIα in the affinity pull-downs with the three beads (i.e. C8, C2 and C8_OCH_3). White bars indicate the relative abundance of PKA RIIα pulled down with C8 *versus* C2 beads; while grey bars depict the relative abundance of PKA RIIα recovered with the C8 *versus* C8_OCH_3 beads. The C8 to C2 ratios are close to 1, irrespective of the origin of the sample (i.e. rat lung tissue, rat testis tissue, HEK293 cells or RCC10 cells), indicating that both C8 and C2 beads have equal binding specificity towards PKA RIIα. In sharp contrast, the averaged ratios are 5 and higher for the C8 versus C8_OCH_3 pairs, again irrespective of the origin of the sample, indicating that the C8 beads have substantial higher affinity for PKA RIIα than the C8_OCH_3 beads. PKA RIIβ displays similar patterns as observed for PKA RIIα as illustrated in Supplemental Figure S2A.

Figure 4B shows that PKA RIα has no substantial binding specificity for either C8 or C2 beads, as revealed by the ratios (~ 1) (Note the different scale of the y-axis in Figure 4B, compared to 4A). However, in sharp contrast to the results obtained for RII, the binding specificity ratio of C8 to C8_OCH3 is also close to 1, indicating that the C8_OCH3 beads have similar affinity for PKA RIα compared to C8. Similarly, PKA RIβ that we observed in HEK293 and RCC10 exhibits a C8/C8_OCH_3 specificity ratio of approximately one as well, proving that PKA RIβ binds to C8 and C8_OCH_3 with similar specificity as well. It was shown in (Supplemental Figure S2B).

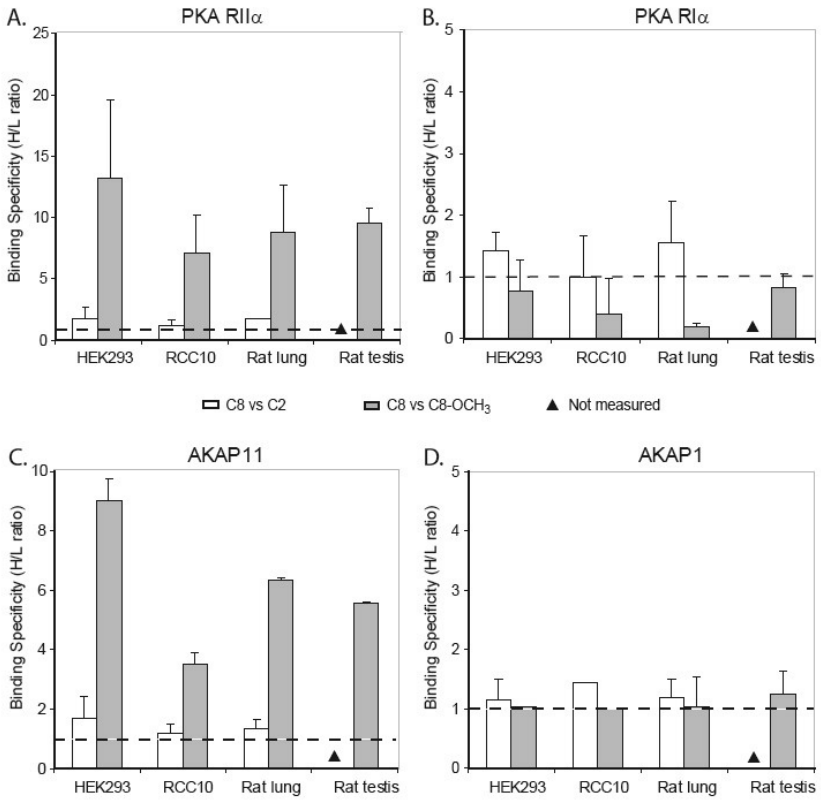

Figure 4. The ratios were measured in two cell lysates (i.e. HEK293 and RCC10) and two tissue lysates (i.e. rat lung and rat testis tissue) for A. PKA RIIα, B. PKA RIα, and their secondary binding proteins, C. AKAP11 and D. AKAP1. The binding specificity ratios of C8 versus C2 are in white and C8 versus C8_OCH$_3$ are in grey.

In addition to the primary binders of cAMP, we enriched for several secondary binders, primarily many of the expected A kinase anchoring proteins. The enrichment ratio's of AKAP11 and AKAP1 which were identified in all four biological systems, are depicted in Figure 4C and D respectively. In Figure 4C, the measured enrichment patterns of AKAP11 are shown, which are markedly similar to PKA RII shown in Figure 4A. There is no significant difference between the C8 and C2 beads but lower enrichment when C8_OCH$_3$ beads are used. We attribute this similarity in patterns to the fact that AKAP11 is a PKA RII targeting AKAP. In contrast, AKAP1 exhibited a quite different pattern, as it was found to be equally enriched using the C8, C2 or C8_OCH$_3$ beads (Figure 4D). This can be rationalized by AKAP1's ability to bind equally well to RI and RII meaning that it is a dual specificity

AKAP. Other examples are shown in Supplemental Figure 3, which reveals that AKAP7 is RII-specific and AKAP2 is dual specific.

Next to the two AKAPs shown in Figure 4C and D, we detected and determined differential binding patterns for a further 10 AKAPs in the 4 different samples. Figure 5 summarizes all results for C8 versus C8-OCH_3 on a ^{2}log scale. For each AKAP, the peptides detected in the four samples (HEK293, RCC10, Rat lung tissue and Rat testis tissue) were pooled into one data set and the mean ratios and their standard deviations were calculated. The PKA isoforms, RIIα and RIIβ (white bars on the left) show a ^{2}log ratio of 3.2 (stdev =0.12) and 3.9 (stdev =0.17) whereas RIα and RIβ have similar ^{2}log ratios of -0.79 (stdev =0.20) and -0.89 (stdev =0.16), respectively. Furthermore, 6 AKAPs have similar ratios compared to the RII isoforms:AKAP5, AKAP7, AKAP9, AKAP11, MAP2 and AKAP14 (dark grey bars), indicating they are RII specific AKAPs, in agreement with literature data for AKAP5(*25*), AKAP7(*26*), AKAP11(*27*) and MAP2(*28*).

On the other hand, AKAP1 (light grey bars) had average ratios of around 1 indicating that it has similar binding affinities to both RI and RII, so it can be classified as dual specificity AKAP. AKAP10 (D-AKAP2) was also observed as a dual specificity AKAP with a binding pattern similar to AKAP1. Although we only identified one quantifiable peptide of AKAP10 (SIEQDAVNTFTK, Supplemental Table S3I), the peptide was identified with high confidence (mascot score of 59, mascot delta score to the next best hit of 47). A manual annotation of the tandem MS spectrum of this peptide is provided in Supplemental Figure 4. Additionally, we performed a BLAST analysis of the peptide sequence against the non-redundant NCBI database in order to verify the specificity of this peptide referring to AKAP10. The quantitation was manually inspected in the raw data by extracted ion chromatograms of the heavy and light versions of this peptide. This showed ample intensity to confidently quantitate this peptide (Supplemental Figure 4). In agreement, AKAP1(*25, 29*), AKAP10(*30*), AKAP3 (*31*) and AKAP4(*32*) have been reported as dual specificity AKAPs previously. In the case of AKAP3 and AKAP4, it seems to be dual specificity with a preferred binding to RII, as the average binding specificity ratios of 1.1 and 0.64 respectively are slightly higher than that of other dual specificity AKAPs in this dataset. In addition to the enrichment of PKA R isoforms and their binding proteins, we also attained enrichment of PKG. This kinase is known to cross-react with cAMP (Supplemental Figure S2C). Although PKG was identified with good sequence coverage, we were not able to unambiguously differentiate between the known isoforms (Iα or Iβ) due to the lack of unique peptides in the quantitative experiment.

In the qualitative experiment in rat lung tissue, detailed in Supplemental Table S2, we identified peptides of both PKG I isoforms. In our experiments PKG was pulled down with equal efficiency by C8 and C2 beads with a ratio of 1.2 (HEK293 cell lysate) and 1.6 (Rat lung tissue lysate). In sharp contrast, the C8_OCH_3 beads exhibited poor levels of PKG enrichment with a ratio of >100 (Supplemental Figure S2C).

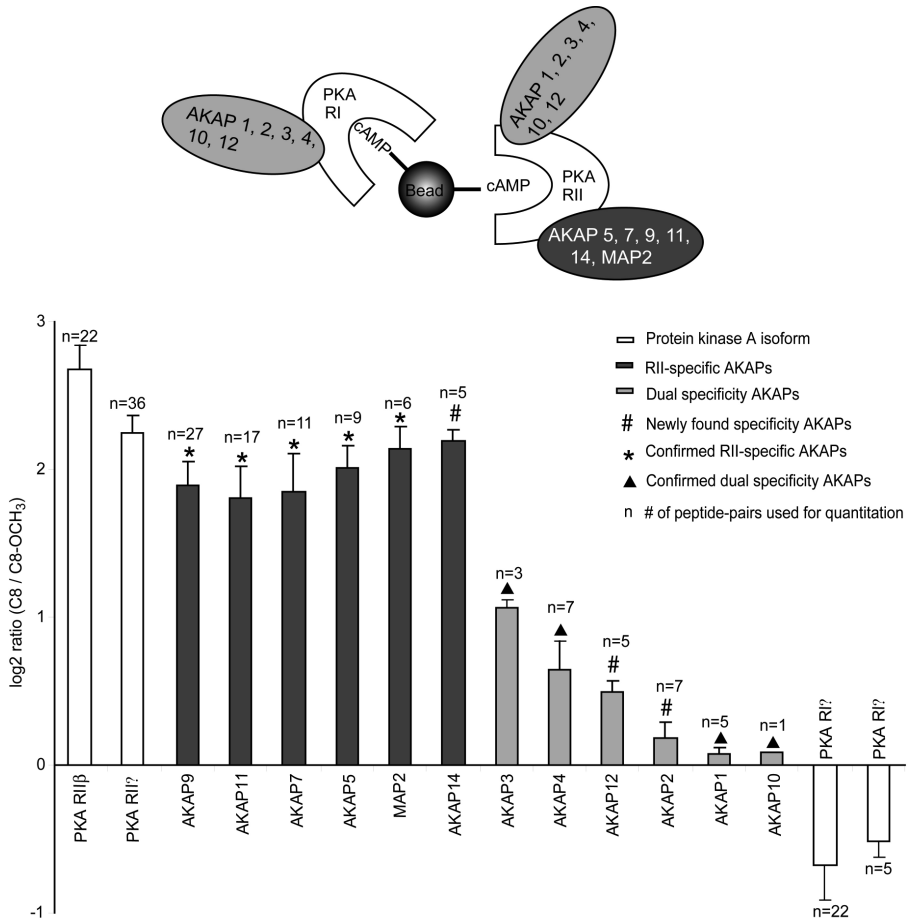

Figure 5. Overview of averaged binding specificity ratios of all AKAPs affinity purified in the four studied lysates of HEK293, RCC10, rat lung and rat testis tissue. The protein ratios are calculated by pooling all peptide pairs detected in each tissue for a certain protein. The overall standard deviation was calculated over all spectra in the pool. For comparison, all averaged ratios are depicted on a ^{2}log scale. The number of spectra which were used for the average ratios are shown.

Therefore, it seems that cAMP modification at the ribose moiety is detrimental for binding to PKG, as recently confirmed in an *in vitro* binding assay with recombinant PKG(*9*). Besides PKG, IRAG, a known PKG Iβ binding protein(*33*), could be detected and displayed a differential enrichment pattern similar to that of PKG (Supplemental Table S3I), also with a strikingly lower enrichment using the C8_OCH_3 beads, confirming that IRAG is likely enriched as secondary binder to PKG. Furthermore, we enriched and detected PDE2A and

PDE10A. PDE2A was found to be less enriched using the C8 beads compared to the C2 beads (data not shown), consistent with earlier reports that an unmodified C8 position in cAMP is essential for phosphodiesterase interactions (*17, 34*). We validated some of the observed differential enrichment characteristics especially for the isoforms RIα and RIIα of PKA (Figure 6A) by Western blotting with isoform specific antibodies, taking the HEK293 cells as test-sample. As shown in Figure 6A, PKA RII bound to the C8 beads with approximately 2.5-fold higher specificity than to the C8_OCH_3 beads, in agreement with our chemical proteomics data. Using the RI specific antibodies, western blotting analysis confirmed that there is no significant selectivity between C8 and C8_OCH_3 beads. To confirm the differential enrichment observed for PKG, we performed pull-downs with recombinant PKG (rPKG). The same amount of rPKG was incubated with the three different beads and the amounts of bound and unbound protein were visualized by SDS-PAGE.

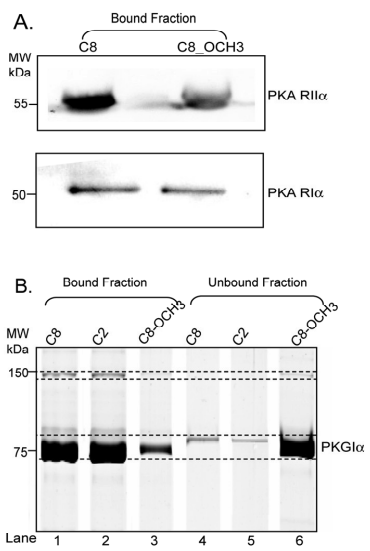

Figure 6. Validation of quantitative chemical proteomics approach. A. Western Blot analysis of PKA RIα and PKA RIIα affinity enriched from HEK293 cells by the C8 and C8_OCH_3 beads, respectively. B. Affinity pull-down assays using recombinant PKGIα, visualized using SDS gels in which analysis of PKG bound to the bead fractions is shown in lane 1, 2 and 3. The unbound fractions are depicted in lane 4, 5 and 6.

These results are shown in Figure 6B, with lane 1, 2 and 3 showing the relative amount of PKG bound to the C8, C2 and C8_OCH_3 beads respectively. The fraction of unbound protein is depicted in the lanes 4, 5 and 6 for C8, C2 and C8_OCH_3 beads respectively. The results clearly confirm that PKG binds to C8 and C2 beads with similar affinities, whereas the binding to the C8_OCH_3 beads is significantly less, confirming our chemical proteomics data. Overall these validation experiments on PKA RI & RII and PKG reveal good agreement with the quantitative proteomics experiments, providing confidence to the latter approach for the quantification of the binding ratios of the other proteins.

3.3.3. Background proteins can be bead-specific

In our affinity pull-downs we also detected some high abundance "background" proteins such as actin, hemoglobin, alpha 2-globulin, L-lactose dehydrogenase B-chain and glyceraldehyde-3-phosphate dehydrogenase (GAPDH). When analyzing the differential binding behavior of these proteins we observed that actin, hemoglobin and alpha 2-globulin were equally abundant no matter which of the four beads (C8, C2, C8_OCH_3 and control beads) we used. Remarkably, several "background" proteins revealed also to some extent specific enrichments. For instance, L-lactose dehydrogenase B-chain bound to C8 beads with a relative affinity ratio of 100, compared to C2. GAPDH was enriched by the C8 beads with a relative affinity ratio of 4:1 to both C2 and C8_OCH_3. Finally, various ribosomal proteins were found to be preferentially enriched using the C2 beads (Supplemental Table S2).

3.4. Discussions

To gain further insights into the protein scaffolds involved in cAMP/PKA directed signaling, such protein complexes are best analyzed and compared in a large set of different cellular and tissue samples. Recently, we introduced methodology to identify at a medium-large scale different cAMP/PKA linked scaffolds in a qualitative way identifying several AKAPs present in heart tissue (*17, 21*). For this, we applied specific enrichment of PKA-AKAP complexes using immobilized cAMP. Although these studies gave good insight in the presence of over 14 different AKAPs in heart tissue and also allowed the identification of a novel potential AKAP, it did not provide any detailed information on the PKA-isoform specificity of these AKAPs. A way to address this would be to make use of cAMP analogues that have a specificity for RI over RII or vice versa, however these were poorly recognized thus far (*9*). In this study we discovered that immobilized C8_OCH3 binds much weaker to the PKA RII than the PKA RI isoforms. By applying a quantitative MS approach, using differential stable isotope labeling, we now show we can evaluate AKAPs for their PKA RI/RII specificity in a variety of tissues, making use of the differential co-enrichment of the AKAPs with either RI or RII.

In summary, the enrichment characteristics of three differently immobilized cAMP-analogues were probed in HEK293 cells, RCC10 cells, rat lung and rat testis tissue. These tissues were chosen as they were expected to contain a wide variety of different AKAPs. Stable isotope dimethyl labeling at the peptide level was applied to quantify the enrichment characteristics on the different beads. For each specifically binding protein an affinity ratio could be calculated based on the comparison of mass spectra peak intensities. We were able to enrich and relatively quantify all 4 different isoforms of the regulatory subunits of PKA, about a dozen of AKAPs and several other primary (PKG, PDE) and secondary protein binders of cAMP. Below we will discuss in some more detail the different classes of affinity enriched proteins focusing first on the primary bait proteins, followed by the AKAPs, which are secondary binding proteins.

3.4.1. Primary Binding Proteins

Our quantitative proteomics data clearly indicated that both RII isoforms (RIIα and RIIβ) bind equally well to C8 and C2 cAMP beads. In contrast, RII seems to have a much lower affinity towards the C8_OCH_3 beads (Figure 4A). The two beads have the same linking position at C8 but in the latter the 2'-OH is methylated. Detailed structural studies on cAMP bound PKA RI and RII(*35, 36*), point out that the cAMP-binding domains of RI and RII are highly conserved. Also the residues interacting directly with the 2'-OH seem to be similarly oriented in RI and RII. The invariant Gly (G204/334 for RIIα and G220/349 for RIIβ) and Glu (E205/335 and E221/350 for RIIα and RIIβ, respectively) bind to the 2'OH of the ribose moiety by forming an H-bond. This would point out that the modification at 2'OH ribose moiety (C8_OCH_3) likely reduces the binding to RII by disruption of the H-bond. Intriguingly, the same interactions were revealed for RI in which both the Gly (G201/325 for RIα and RIβ) and the Glu (E202/326 for RIα and RIβ) residue are conserved. (*36*). This means that the formation of the H-bond is apparently not solely responsible for diminishing the binding of RII to our C8_OCH_3 beads. This observation hints at different interactions in RI and RII that help to stabilize their complex with cAMP, and especially with 2'-methoxy-cAMP. We attribute this partly to possible different stacking interactions of cAMP with RI and RII. A sequence alignment between RI and RII reveals that the key hydrophobic residues required for this stacking interaction such as Val (V184), Val (V186), Val (V302), Val (V315), Leu (L318), Ile (I327) and Ser (S375) in RI are differently positioned and poorly conserved in RII in which the aligned residues are Ile (I183), Val (V185), Ile (I305), Ile (I324), Cys (C327), Leu (L336) and Glu (E384). These variable residues between the two isoforms could influence binding specificity to cAMP. Detailed molecular structures of the two regulatory isoforms bound to the different cAMP analogs would be required to validate the above speculations and possibly point to other differences in the cAMP binding domains of RI and RII.

Another known primary bait protein for the beads is PKG. Our results indicate that PKG binds equally well to C8 and C2, however binding to C8_OCH_3 is dramatically reduced (Supplemental Figure S2C). Interestingly, the PKG H-bonding residues: Arg (R177/R403), Gly (G167/G393) and Glu (E168/E394) are conserved with respect to PKA RII. The data on PKG suggest that the ribose 2'OH moiety related H-bonding is even more crucial for binding of PKG than PKA RII. Additionally, we enriched for two phosphodiesterases; PDE2A3 in rat lung tissue and PDE10A in rat testis tissue. PDE2A3 was found to bind C2 with an approximately 10-fold higher than C8 in binding specificity, indicating that hydrophobic binding between the imidazole ring of cAMP is stronger than that to the pyrimidine ring, both of which are required for cyclic nucleotide discrimination. Very recently the affinities of a range of widely used cyclic nucleotides and derivatives were tested on all subtypes of PKA

and PKG, as well as on Epac1 and 6 types of PDE's.(*9*) This study by Poppe et al. shed light on the potential promiscuity of cyclic nucleotide derivatives when applying them as pharmacological tools. The results obtained by Poppe et al. on recombinant proteins *in vitro* are completely consistent with our findings *invivo*. The non-linked version of C8_OCH_3 binds to PKA RI with higher affinity than to RII, while it does not seem to bind to PKG at all.

3.4.2. Secondary Binding proteins

In the cell PKA is localized through interaction of the regulatory domains with the family of distinct but functionally homologous AKAPs. Through an extensive body of work it has now been established that some AKAPs prefer to bind the RII regulatory subunit while others have dual-specificity for both RI and RII. To some extent the amino acid residues that play a role in whether an AKAP protein binds preferentially RII or displays dual specificity have been defined by extensive mutagenesis studies and biochemical analysis (*29, 37-40*).

As described above we observed distinct binding specificities for C8 and C8_OCH_3 beads, which can be further exploited as a discriminating factor to establish the preference of the secondary AKAP binders for RI or RII. In other words, we can differentiate between RII specific and dual specific AKAPs depending on the measured binding specificity ratios between the pull-downs performed with the C8 and C8_OCH_3 beads. AKAPs with a ratio significantly similar to RII isoforms were considered RII-specific AKAPs. We detected in total 12 AKAPs, of which 6 could be classified as preferentially binding to the RII regulatory subunit of PKA, whereas the remaining 6 were considered to be dual-specificity AKAPs (Figure 5). In cases where prior literature is available our data confirmed reported specificities of AKAPs providing the validation of our method. However, for a number of AKAPs no information is available about their specificity. Below we discuss for each detected AKAP our findings in the context of literature data.

3.4.2.1. RII specific AKAPs

Our data clearly shows that AKAP5 is an RII-binding protein. AKAP5 was shown to be an RIIβ binding AKAP by deletion experiments and site-directed mutagenesis(*41*) revealing that several amino acid residues at the C-terminus with long aliphatic side chains play a central role. The microtubule-associated protein MAP2 was the first protein shown to co-purify with RII(*28, 42*). In our experiments, we identified MAP2c in testis tissue and MAP2a/b in HEK293, as based on unique peptide identifiers of these splice isoforms. The binding specificity ratios of these two isoforms clearly confirm that both are RII-specific AKAPs. AKAP11, which we detected in all our cells and tissues, is a clear RII-specific binding AKAP. This protein is known to be expressed abundantly in human testis(*43*). The peptide Ht31 which is an AKAP-PKA anchoring antagonist, has been successfully used to block RII-AKAP11 interactions, suggesting that AKAP11 may bind RII in a manner similar to other AKAPs(*27*). AKAP9, which was relatively abundant in HEK293 and RCC10 cells, is

also a clear RII-specific AKAP (Figure 5). Using a yeast two-hybrid screen Feliciello *et. al.* showed that the RII regulatory subunits of PKA bind *in vitro* Yotiao (AKAP9) with nanomolar affinity (*Kd* 50-90 nM) (*44*). Of AKAP7, identified in our experiments (Supplemental Figure 3), at least four splice variants have been reported. Our initial 1D gel analyses indicated that in our systems AKAP7 had a molecular weight of around 40 kDa indicating that it is likely the γ or δ isoform, which we were unfortunately unable to distinguish based on the detected peptides. Hundsrucker *et. al.* showed that AKAP7δ is a high affinity RIIα binding protein with a *Kd* value of 31 nM (*26*). In contrast, yeast two-hybrid analysis and co-immunoprecipitation studies(*45*) showed that AKAP7γ binds also to the RI subunit. Based on these studies, it seems likely that we mainly enriched for AKAP7δ, being a specific RII-binding AKAP. Finally we clearly show, for the first time, that AKAP14 preferentially binds to RII. Although relatively little information has been reported about AKAP14, sequence analysis indicates that this protein is closely related to TAKAP-80 which is exclusively expressed in testis(*46*). In line, we detected this protein only in rat testis.

3.4.2.2. Dual specificity AKAPs

Our data confirm that AKAP1, AKAP10, AKAP2, and AKAP12 have dual specificity. Huang *et al.*, (*29*) identified D-AKAP1 (AKAP1) as a fragment from a yeast two hybrid screen based on specific interaction with the RI portion of Ret/ptc2 which includes most of the RI/RII binding domain. The interacting regions on both RI and RII are localized to their N-termini. AKAP10 (D-AKAP2) has been well studied and shown to display dual specificity (Kd ~ 2 and 48nM for RII and RI respectively) (*47-49*), in agreement with our analysis. AKAP2 (AKAP-KL) isoforms contain a 20-residue domain (aa 586-605) that binds RII with nanomolar affinity (*Kd* ~ 10nM) and a partial AKAP2 protein isoform (aa 354-741) that includes the putative tethering site that binds both RIIα and RIIβ (*50, 51*). Although AKAP2 is known to bind RII, our data showed that AKAP2 seems to have dual specificity based on the observed ratio profile (Supplemental Figure 3). AKAP12 (Gravin), a 250 kDa AKAP, was originally identified as a cytoplasmic antigen recognized by myasthenia gravis sera. Our data establish for the first time that AKAP12 is a dual specific AKAP. Studies *in vitro* revealed that the residue stretch 1526–1780 of AKAP12 binds RII with nanomolar binding affinity(*52*).

AKAP3 appears to be expressed specifically in spermatoids and spermatozoa and as expected in our experiments we only detected it in rat testis. AKAP3 has been reported to bind to both RII and RI (*31*) which is in agreement with our finding. In the sequence of AKAP3, an RII-binding domain has been identified (residues 124-141), which is conserved between the human, murine and bovine AKAP3 (*31*). In an earlier study, AKAP4 has been reported as an RII-binding protein(*53, 54*). Nonetheless, our finding is consistent with Vijayaraghavan *et. al.*(*31*) in which AKAP4 is reported as dual specificity AKAP. Our data

indicate that both proteins display dual specificity however with a preference to bind to RII since the specificity ratios are slightly different than for the other dual specificity AKAPs (Figure 5). It is possible that some residues required for RII-binding are different although there is a significant homology between the putative RII-binding domains of AKAP3 and AKAP4 (i.e. 12 of 18 amino acids are identical). These differences in the core of the binding domain might contribute to the observed different binding specificity.

3.5. Conclusion

We combined a chemical proteomics approach with stable isotope labeling and mass spectrometry to enrich specifically for cAMP interacting proteins, directly from cell or tissue lysates. cAMP-agarose affinity resins with 3 different derivatives of cAMP were used to probe their selectivity in the enrichment; C2, C8 and C8_OCH_3. Stable isotope labeling facilitated the identification of unspecifically binding background proteins and allowed us to probe the differential binding behavior of relevant proteins to the different analogues directly in tissue. Our data revealed that all PKA regulatory isoforms have a similar affinity for C8 and C2 beads. In contrast, RII isoforms have a significant lower affinity for the C8_OCH_3 beads, whereas the RI isoforms seem to be unaffected by this small chemical modification. We employed this effect to monitor the specificity of secondary binding proteins to the PKA RI and RII isoforms with our LC-MS stable isotope labeling method as read out. In four different input lyastes we detected 12 main AKAP families, of which 6 were observed to have specificity for the PKA RII isoform, whereas the other 6 displayed dual specificity for both RI and RII. Besides confirming previously reported PKA-AKAP specificities, also the specificity of other PKA-AKAP complexes was elucidated. We have observed for the first time that AKAP14 has RII-specificity whereas AKAP2 and AKAP 12 are dual specific AKAPs (# in Figure 5). In conclusion, our chemical proteomics screen sheds new light on nature's complex diversity in signaling mechanisms, as each AKAP, and each isoform thereof, may direct different PKA-isoforms to different compartments of the cell, providing the basis of the complex multifunctional platform of this single kinase.

In general, our data reveal that chemical biology approaches, combined with stable isotope labeling and mass spectrometry, provide comprehensive ways to study the interplay between small molecules and target proteins which can be applied to complex biological systems, such as total cell or mammalian tissue lysates.

3.6. Acknowledgements

Support from the Netherlands Proteomics Centre is kindly acknowledged (www.netherlandsproteomicscentre.nl). TAV is funded by a Technology Foundation Grant (STW program DPTE, grant UGT.6746).

References:

1. Bradley, J., Reisert, J., and Frings, S. (2005) Regulation of cyclic nucleotide-gated channels, *Curr Opin Neurobiol 15*, 343-349.
2. McConnachie, G., Langeberg, L. K., and Scott, J. D. (2006) AKAP signaling complexes: getting to the heart of the matter, *Trends Mol Med 12*, 317-323.
3. de Rooij, J., Zwartkruis, F. J., Verheijen, M. H., Cool, R. H., Nijman, S. M., Wittinghofer, A., and Bos, J. L. (1998) Epac is a Rap1 guanine-nucleotide-exchange factor directly activated by cyclic AMP, *Nature 396*, 474-477.
4. Wong, W., and Scott, J. D. (2004) AKAP signalling complexes: focal points in space and time, *Nat Rev Mol Cell Biol 5*, 959-970.
5. Ogreid, D., and Doskeland, S. O. (1980) Protein kinase II has two distinct binding sites for cyclic AMP, only one of which is detectable by the conventional membrane-filtration method, *FEBS Lett 121*, 340-344.
6. Ogreid, D., Ekanger, R., Suva, R. H., Miller, J. P., and Doskeland, S. O. (1989) Comparison of the two classes of binding sites (A and B) of type I and type II cyclic-AMP-dependent protein kinases by using cyclic nucleotide analogs, *Eur J Biochem 181*, 19-31.
7. Taylor, S. S., Kim, C., Vigil, D., Haste, N. M., Yang, J., Wu, J., and Anand, G. S. (2005) Dynamics of signaling by PKA, *Biochim Biophys Acta 1754*, 25-37.
8. Scholten, A., Aye, T. T., and Heck, A. J. (2008) A multi-angular mass spectrometric view at cyclic nucleotide dependent protein kinases: In vivo characterization and structure/function relationships, *Mass Spectrom Rev*.
9. Poppe, H., Rybalkin, S. D., Rehmann, H., Hinds, T. R., Tang, X. B., Christensen, A. E., Schwede, F., Genieser, H. G., Bos, J. L., Doskeland, S. O., Beavo, J. A., and Butt, E. (2008) Cyclic nucleotide analogs as probes of signaling pathways, *Nat Methods 5*, 277-278.
10. Schwede, F., Maronde, E., Genieser, H., and Jastorff, B. (2000) Cyclic nucleotide analogs as biochemical tools and prospective drugs, *Pharmacol Ther 87*, 199-226.
11. Landgraf, W., Hullin, R., Gobel, C., and Hofmann, F. (1986) Phosphorylation of cGMP-dependent protein kinase increases the affinity for cyclic AMP, *Eur J Biochem 154*, 113-117.
12. Pohler, D., Butt, E., Meissner, J., Muller, S., Lohse, M., Walter, U., Lohmann, S. M., and Jarchau, T. (1995) Expression, purification, and characterization of the cGMP-dependent protein kinases I beta and II using the baculovirus system, *FEBS Lett 374*, 419-425.
13. Pelligrino, D. A., and Wang, Q. (1998) Cyclic nucleotide crosstalk and the regulation of cerebral vasodilation, *Prog Neurobiol 56*, 1-18.
14. Dostman, W. R. (2003) Inhibitors of cyclic nucleotide-dependent protein kinases, *In Handbook of cllular signaling, Bradshow; Dennis, Eds. Academic Press 2*, 487-493.

15. Lincoln, T. M., Dey, N., and Sellak, H. (2001) Invited review: cGMP-dependent protein kinase signaling mechanisms in smooth muscle: from the regulation of tone to gene expression, *J Appl Physiol 91*, 1421-1430.
16. Kim, E., and Park, J. M. (2003) Identification of novel target proteins of cyclic GMP signaling pathways using chemical proteomics, *J Biochem Mol Biol 36*, 299-304.
17. Scholten, A., Poh, M. K., van Veen, T. A., van Breukelen, B., Vos, M. A., and Heck, A. J. (2006) Analysis of the cGMP/cAMP interactome using a chemical proteomics approach in mammalian heart tissue validates sphingosine kinase type 1-interacting protein as a genuine and highly abundant AKAP, *J Proteome Res 5*, 1435-1447.
18. Boersema, P. J., Aye, T. T., Veen, T. A. B. v., Heck, A. J. R., and Mohammed, S. (2008) Triplex protein quantification based on stable isotope labelling by peptide dimethylation applied to cell and tissue lysates, *Proteomics in press*.
19. Hsu, J. L., Huang, S. Y., Chow, N. H., and Chen, S. H. (2003) Stable-isotope dimethyl labeling for quantitative proteomics, *Anal Chem 75*, 6843-6852.
20. Raijmakers, R., Berkers, C. R., de Jong, A., Ovaa, H., Heck, A. J., and Mohammed, S. (2008) Automated online sequential isotope labeling for protein quantitation applied to proteasome tissue-specific diversity, *Mol Cell Proteomics 7*, 1755-1762.
21. Scholten, A., van Veen, T. A., Vos, M. A., and Heck, A. J. (2007) Diversity of cAMP-dependent protein kinase isoforms and their anchoring proteins in mouse ventricular tissue, *J Proteome Res 6*, 1705-1717.
22. Christensen, A. E., Selheim, F., de Rooij, J., Dremier, S., Schwede, F., Dao, K. K., Martinez, A., Maenhaut, C., Bos, J. L., Genieser, H. G., and Doskeland, S. O. (2003) cAMP analog mapping of Epac1 and cAMP kinase. Discriminating analogs demonstrate that Epac and cAMP kinase act synergistically to promote PC-12 cell neurite extension, *J Biol Chem 278*, 35394-35402.
23. Bantscheff, M., Schirle, M., Sweetman, G., Rick, J., and Kuster, B. (2007) Quantitative mass spectrometry in proteomics: a critical review, *Anal Bioanal Chem 389*, 1017-1031.
24. Heck, A. J., and Krijgsveld, J. (2004) Mass spectrometry-based quantitative proteomics, *Expert Rev Proteomics 1*, 317-326.
25. Herberg, F. W., Maleszka, A., Eide, T., Vossebein, L., and Tasken, K. (2000) Analysis of A-kinase anchoring protein (AKAP) interaction with protein kinase A (PKA) regulatory subunits: PKA isoform specificity in AKAP binding, *J Mol Biol 298*, 329-339.
26. Hundsrucker, C., Krause, G., Beyermann, M., Prinz, A., Zimmermann, B., Diekmann, O., Lorenz, D., Stefan, E., Nedvetsky, P., Dathe, M., Christian, F., McSorley, T., Krause, E., McConnachie, G., Herberg, F. W., Scott, J. D., Rosenthal, W., and Klussmann, E. (2006) High-affinity AKAP7delta-protein kinase A interaction yields novel protein kinase A-anchoring disruptor peptides, *Biochem J 396*, 297-306.

27. Lester, L. B., Coghlan, V. M., Nauert, B., and Scott, J. D. (1996) Cloning and characterization of a novel A-kinase anchoring protein. AKAP 220, association with testicular peroxisomes, *J Biol Chem 271*, 9460-9465.
28. Rubino, H. M., Dammerman, M., Shafit-Zagardo, B., and Erlichman, J. (1989) Localization and characterization of the binding site for the regulatory subunit of type II cAMP-dependent protein kinase on MAP2, *Neuron 3*, 631-638.
29. Huang, L. J., Durick, K., Weiner, J. A., Chun, J., and Taylor, S. S. (1997) Identification of a novel protein kinase A anchoring protein that binds both type I and type II regulatory subunits, *J Biol Chem 272*, 8057-8064.
30. Huang, L. J., Durick, K., Weiner, J. A., Chun, J., and Taylor, S. S. (1997) D-AKAP2, a novel protein kinase A anchoring protein with a putative RGS domain, *Proc Natl Acad Sci U S A 94*, 11184-11189.
31. Vijayaraghavan, S., Liberty, G. A., Mohan, J., Winfrey, V. P., Olson, G. E., and Carr, D. W. (1999) Isolation and molecular characterization of AKAP110, a novel, sperm-specific protein kinase A-anchoring protein, *Mol Endocrinol 13*, 705-717.
32. Miki, K., and Eddy, E. M. (1998) Identification of tethering domains for protein kinase A type Ialpha regulatory subunits on sperm fibrous sheath protein FSC1, *J Biol Chem 273*, 34384-34390.
33. Ammendola, A., Geiselhoringer, A., Hofmann, F., and Schlossmann, J. (2001) Molecular determinants of the interaction between the inositol 1,4,5-trisphosphate receptor-associated cGMP kinase substrate (IRAG) and cGMP kinase Ibeta, *J Biol Chem 276*, 24153-24159.
34. Xu, R. X., Rocque, W. J., Lambert, M. H., Vanderwall, D. E., Luther, M. A., and Nolte, R. T. (2004) Crystal structures of the catalytic domain of phosphodiesterase 4B complexed with AMP, 8-Br-AMP, and rolipram, *J Mol Biol 337*, 355-365.
35. Diller, T. C., Madhusudan, Xuong, N. H., and Taylor, S. S. (2001) Molecular basis for regulatory subunit diversity in cAMP-dependent protein kinase: crystal structure of the type II beta regulatory subunit, *Structure 9*, 73-82.
36. Kim, C., Xuong, N. H., and Taylor, S. S. (2005) Crystal structure of a complex between the catalytic and regulatory (RIalpha) subunits of PKA, *Science 307*, 690-696.
37. Carr, D. W., Stofko-Hahn, R. E., Fraser, I. D., Bishop, S. M., Acott, T. S., Brennan, R. G., and Scott, J. D. (1991) Interaction of the regulatory subunit (RII) of cAMP-dependent protein kinase with RII-anchoring proteins occurs through an amphipathic helix binding motif, *J Biol Chem 266*, 14188-14192.
38. Newlon, M. G., Roy, M., Morikis, D., Hausken, Z. E., Coghlan, V., Scott, J. D., and Jennings, P. A. (1999) The molecular basis for protein kinase A anchoring revealed by solution NMR, *Nat Struct Biol 6*, 222-227.

39. Miki, K., and Eddy, E. M. (1999) Single amino acids determine specificity of binding of protein kinase A regulatory subunits by protein kinase A anchoring proteins, *J Biol Chem 274*, 29057-29062.
40. Banky, P., Newlon, M. G., Roy, M., Garrod, S., Taylor, S. S., and Jennings, P. A. (2000) Isoform-specific differences between the type Ialpha and IIalpha cyclic AMP-dependent protein kinase anchoring domains revealed by solution NMR, *J Biol Chem 275*, 35146-35152.
41. Hausken, Z. E., Dell'Acqua, M. L., Coghlan, V. M., and Scott, J. D. (1996) Mutational analysis of the A-kinase anchoring protein (AKAP)-binding site on RII. Classification Of side chain determinants for anchoring and isoform selective association with AKAPs, *J Biol Chem 271*, 29016-29022.
42. Obar, R. A., Dingus, J., Bayley, H., and Vallee, R. B. (1989) The RII subunit of cAMP-dependent protein kinase binds to a common amino-terminal domain in microtubule-associated proteins 2A, 2B, and 2C, *Neuron 3*, 639-645.
43. Reinton, N., Collas, P., Haugen, T. B., Skalhegg, B. S., Hansson, V., Jahnsen, T., and Tasken, K. (2000) Localization of a novel human A-kinase-anchoring protein, hAKAP220, during spermatogenesis, *Dev Biol 223*, 194-204.
44. Feliciello, A., Cardone, L., Garbi, C., Ginsberg, M. D., Varrone, S., Rubin, C. S., Avvedimento, E. V., and Gottesman, M. E. (1999) Yotiao protein, a ligand for the NMDA receptor, binds and targets cAMP-dependent protein kinase II(1), *FEBS Lett 464*, 174-178.
45. Brown, R. L., August, S. L., Williams, C. J., and Moss, S. B. (2003) AKAP7gamma is a nuclear RI-binding AKAP, *Biochem Biophys Res Commun 306*, 394-401.
46. Mei, X., Singh, I. S., Erlichman, J., and Orr, G. A. (1997) Cloning and characterization of a testis-specific, developmentally regulated A-kinase-anchoring protein (TAKAP-80) present on the fibrous sheath of rat sperm, *Eur J Biochem 246*, 425-432.
47. Burns-Hamuro, L. L., Hamuro, Y., Kim, J. S., Sigala, P., Fayos, R., Stranz, D. D., Jennings, P. A., Taylor, S. S., and Woods, V. L., Jr. (2005) Distinct interaction modes of an AKAP bound to two regulatory subunit isoforms of protein kinase A revealed by amide hydrogen/deuterium exchange, *Protein Sci 14*, 2982-2992.
48. Burns, L. L., Canaves, J. M., Pennypacker, J. K., Blumenthal, D. K., and Taylor, S. S. (2003) Isoform specific differences in binding of a dual-specificity A-kinase anchoring protein to type I and type II regulatory subunits of PKA, *Biochemistry 42*, 5754-5763.
49. Kinderman, F. S., Kim, C., von Daake, S., Ma, Y., Pham, B. Q., Spraggon, G., Xuong, N. H., Jennings, P. A., and Taylor, S. S. (2006) A dynamic mechanism for AKAP binding to RII isoforms of cAMP-dependent protein kinase, *Mol Cell 24*, 397-408.

50. Dong, F., Feldmesser, M., Casadevall, A., and Rubin, C. S. (1998) Molecular characterization of a cDNA that encodes six isoforms of a novel murine A kinase anchor protein, *J Biol Chem 273*, 6533-6541.
51. Glantz, S. B., Li, Y., and Rubin, C. S. (1993) Characterization of distinct tethering and intracellular targeting domains in AKAP75, a protein that links cAMP-dependent protein kinase II beta to the cytoskeleton, *J Biol Chem 268*, 12796-12804.
52. Nauert, J. B., Klauck, T. M., Langeberg, L. K., and Scott, J. D. (1997) Gravin, an autoantigen recognized by serum from myasthenia gravis patients, is a kinase scaffold protein, *Curr Biol 7*, 52-62.
53. Carrera, A., Gerton, G. L., and Moss, S. B. (1994) The major fibrous sheath polypeptide of mouse sperm: structural and functional similarities to the A-kinase anchoring proteins, *Dev Biol 165*, 272-284.
54. Visconti, P. E., Johnson, L. R., Oyaski, M., Fornes, M., Moss, S. B., Gerton, G. L., and Kopf, G. S. (1997) Regulation, localization, and anchoring of protein kinase A subunits during mouse sperm capacitation, *Dev Biol 192*, 351-363.

Chapter 4

Proteome-wide protein concentrations in the human heart

Thin Thin Aye[1,2,5]
Arjen Scholten[1,2,5]
Nadia Taouatas[1,2]
Andras Varro[4]
Toon A.B. Van Veen[3]
Marc A. Vos[3]
Albert J. R. Heck[1,2]

[1]Biomolecular Mass Spectrometry and Proteomics Group, Bijvoet Center for Biomolecular Research and Utrecht Institute for Pharmaceutical Sciences, Utrecht University, Padualaan 8, 3584 CH Utrecht, The Netherlands
[2] Netherlands Proteomics Centre, The Netherlands
[3] Department of Medical Physiology, University Medical Centre Utrecht, Yalelaan 50, 3584 CM Utrecht, The Netherlands
[4] Department of Pharmacology & Pharmacotherapy, Faculty of Medicine, University of Szeged, Hungary

[5] These authors contributed equally to this work

Mol Biosyst. 2010 Jul 1. [Epub ahead of print]

Summary

The largest component of the human heart, the left ventricle (LV), plays a major role in delivering blood throughout the body. Therefore, an in-depth detailed quantitative proteome analysis of the human LV is a valuable resource. For this purpose, a multifaceted proteomics approach combining differential sample fractionations (gel, strong cation exchange (SCX)), enzymatic digestions (trypsin, chymotrypsin, LysN), and peptide fragmentation techniques (CID and ETcaD) was used to enhance protein sequence coverage, identification confidence and quantitative abundance determination. Using stringent criteria, 3,584 distinct proteins could be identified from the latest well-annotated Swissprot database (23,000 entries). Commutatively, the over 130,000 identified MS/MS spectra were used to assess concentrations of each identified LV protein through a combination of spectral counting methods. Among the most concentrated proteins, many currently used biomarkers for detection of myocardial infarction reside. These cardiac leakage markers have a good diagnostic power, but their prognostic potential seems limited. Discovery of markers that represent etiological determinants of cardiac disease require a shift of focus towards the signaling proteome. Therefore, a protein-class centered quantitative analysis of kinases, phosphatases and GTPases was adopted. These comparative analyses revealed many cardiac involved kinases (PKA, CaMKII, ERK) to reside among the most abundant signaling proteins, and also to mediate many observed *in vivo* phosphorylation sites. The abundance chart of signaling proteins may assist in identifying novel functional pathways, for instance through the abundant, but relatively little known, kinases STK38L and OXSR1. The obtained protein concentration library also indentifies signaling based, putative biomarkers with concentrations likely to be detectable in plasma.

4.1. Introduction

Cardiovascular diseases are one of the major causes of death in the Western world. Since proteins, and their posttranslational modifications, are the final functional entities that determine (dys)function, it would be beneficial to have a comprehensive view of the cardiovascular proteome and its dynamic nature related to specific disease anomalies. The emerging field of cardiovascular proteomics (1,2) aims to unravel the molecular basis of cardiovascular function, to allow the development of novel therapeutic interventions and to improve diagnosis and prognosis.

Currently, a number of successful protein diagnostics have emerged from the cardiac proteome. The most definitive of these is targeted at the increased plasma levels of cardiac troponin, which is a primary indicator of myocardial infarction (3). The success of markers such as cardiac troponin relies on their high abundance in heart tissue, but also on their leakage from the tissue into the plasma. However, significant leakage occurs mainly after the myocardium is severely damaged by an infarction, making troponin only useful as biomarker when serious effects have been initiated. It would therefore be highly advantageous to expand

the palette of biomarkers towards a set that can predict events at an earlier stage than myocardial infarction. For this, focus needs to be shifted to proteins that are showing dysfunctional characteristics at that early stage. Potentially these proteins would then also pose as interesting treatment targets.

The major challenge is to identify these for a range of cardiac events that are different in timescale, physical size and relative effects of genes. These challenges can be addressed in a two-stage approach; 1) comparative whole proteome analysis on a small set of samples, followed by 2) a targeted protein analysis on a small subset of proteins in a large cohort of samples. At present, two larger data repositories of proteins expressed in human LV have been reported by using either a 2D gel-based approach (4), or shotgun proteomics (5). Both studies produced a very large number of putative biomarkers for cardiomyopathy, indicative of the large changes in the proteome at the late stage of the disease.

Here, we focus largely on signaling proteins (kinases and phosphatases) to investigate the potential of this category of proteins as a novel source of biomarkers, assuming that alterations in their abundance, or modification, are more likely to play a role in the onset of cardiovascular diseases. Several protein kinases and phosphatases tightly control the heart contraction processes by transmitting signals from the receptor to the nucleus of the cell (6). In line with our hypothesis, several animal models have been developed, using for instance kinase knock-outs or kinase-dead mutants, that confirm their crucial role in heart (dys)function (7). Not surprisingly, kinase-mediated signaling pathways have become promising new targets for therapeutic interventions. Evidently, clinically useable biomarkers should be detectable in plasma, albeit that they might visualize themselves as candidates more readily when analyzed close to the source, i.e. in heart tissue. Therefore, as a first step we set-out to chart quantitatively the signaling proteome of the healthy LV by comparing kinases, phosphatases and GTPases in terms of their abundance, and hence their potential as useful biomarkers detectable in plasma.

We adopted a multiplexed approach in which several parameters of the proteomics analysis work-flow were varied to increase protein coverage, and more importantly, sequence coverage of, and confidence in protein identifications. To expand the proteome coverage we varied several parameters: (i) protein *versus* peptide separation, (ii) proteases for digestion and (iii) peptide fragmentation methods.

Determining protein concentrations is one of the most important parameters in quantitative proteomics, because the kinetics and dynamics of the proteome are depicted in terms of changes in the concentrations of proteins in particular compartments. For instance, the concentration of cardiac myoglobin in serum is increased from 3-90 ng/ml to 200-1000 ng/ml during myocardial infarction (8). But also, the concentration of several isoforms of the pivotal contractile kinase cAMP-dependent protein kinase alters when the heart transforms to dilated cardiomyopathy (9). In order to estimate protein concentration, spectral counting can be used as a relatively straightforward, yet reliable index (10-12). Lu *et al*. demonstrated that

spectral counts show a strong linear correlation with absolute protein abundance with a dynamic range over 3 orders of magnitude using their APEX software (12). Recently, APEX was shown to correlate very well to absolute protein concentrations as established through single reaction monitoring experiments (13). With the above mentioned multi-pronged analysis of the human LV proteome we intend to optimize the likelihood of identifying multiple unique peptides from each protein, to increase both qualitative coverage, but also enable the more accurate estimation of individual protein concentrations.

Our annotation provides a valuable resource for the identification of potential novel marker proteins and therapeutic targets, by drawing attention to the absolute protein abundance of kinases, phosphateses and GTPases. From each of these protein classes many of the most abundant members were identified. Many of these proteins have been implicated in cardiac function, but also several have no prior cardiac context. The most abundant signaling proteins of the LV have a high potential as 'early biomarkers' for CVD as their concentration in plasma is likely accessible, and their involvement in CVD is more etiological than the currently used tissue leakage markers.

4.2. Results and Discussion

4.2.1. Work flow

Here we aim to provide a high-confidence semi-quantitative absolute protein abundance map of the healthy human LV. To effectively identify and characterize the proteins extracted from this tissue, we performed 260 complementary LC-MS/MS runs in which three protease digestions (Trypsin, LysC/chymotrypsin and Lys-N), two separation methods (in-gel and SCX), and two different peptide fragmentation techniques (CAD and ETcaD) were applied. A summary of the multiple analytical strategies employed in this study is given in Figure 1. In all experiments, four different methods (A-D) were used in which method A, C and D were again sub-divided into two experiments, resulting in a total of seven different datasets (I-VII). We note here at the beginning that although our experimental design makes it tempting to compare the individual contributions of each of the datasets in terms of total proteins and peptides, we avoided these types of comparisons as the individual methods had several variables changed at the time (e.g. mass spectrometer settings and/or SCX parameters). A detailed description of the complete data analysis procedure, including data filtering processes, is described in Supplemental Figure 1.

4.2.2. Data Organization

MS/MS spectra were extracted from the individual LC-MS/MS runs and subsequently searched against the human Swissprot database (v56.2, released september 23, 2008, 20328 human sequences) being the most reliable, non-redundant annotation to date. All seven datasets together generated 130,019 spectra resulting in the identification of 38,111 unique peptides (with a false discovery rate < 1%) belonging to 3,584 unique protein identifications.

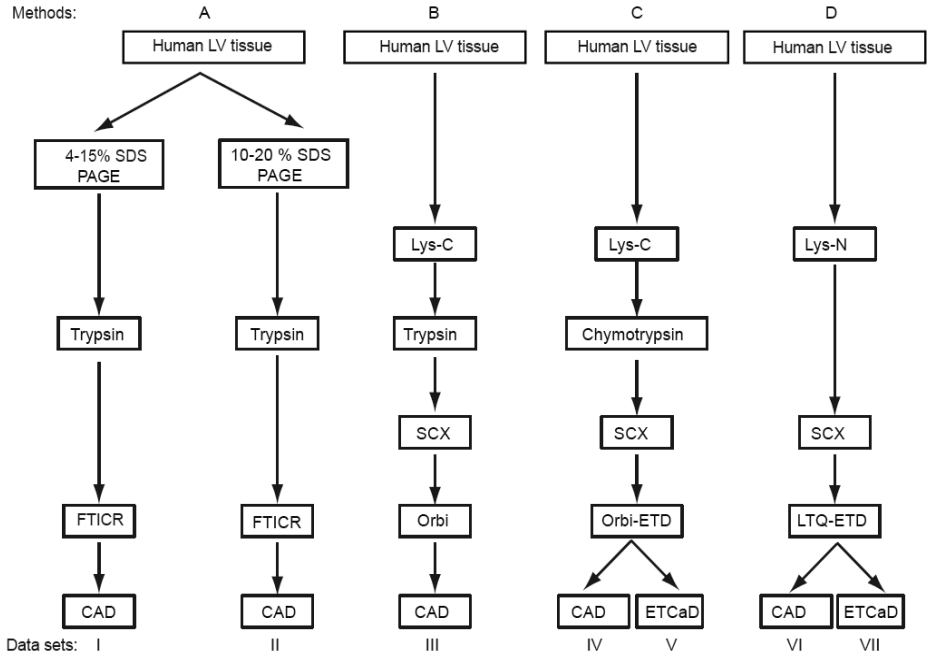

Figure 1. The seven large scale LC-MS/MS datasets (I-VII) from human LV are categorized in 4 methods. The parallel experiments were conducted with different separation methods, multiple enzymatic protein digestions and peptide fragmentation techniques. Method A is sub-divided into two sub-categories (dataset I and II) for two types of 1D-SDS PAGE gels used. Method C is sub-divided into two sub-categories (dataset IV and V) for the two different peptide fragmentation techniques i.e CAD and ETcaD. Similarly, method D is also sub-divided into two datasets (VI and VII).

The total number of identified proteins, peptides and spectra in each dataset are summarized in Table 1 (A detailed list is presented in Supplemental Table 1). It is typically assumed that a minimum of 2 unique peptides are required to identify a protein with high confidence. Hence, we extracted the proteins that met the ≥2 unique peptides criteria from the combination of seven datasets. In this way, a final high quality dataset consisting of 2,306 proteins was achieved (Supplemental Table 2).

4.2.3. Contribution of the different methods

An overlap analysis between the four methods at the protein level showed that only 520 proteins (22.5%) were found to be unambiguously detected by all four methods (Figure 2A). As expected the less in-depth analyses of the methods using Lys-N and Lys-C/Chymotrypsin yielded little additional proteins, although evidently significant additional distinct peptides.

Table 1. Summary of protein, peptide and spectral counts. Total number of detected proteins in each of the human LV tissue datasets using Trypsin-ingel (method A), Trypsin-in solution (method B), LysC/chymotrypsin (method C) and Lys-N (method D).

Method		Separation technique	Proteases	MS analysis	Fragmentation Methods	Peptide cutoff <1% FDR		
						# of proteins	# of peptides	# of spectra
A	I	In-gel (4-15%)	Trypsin	LTQ-FTICR	CAD	2254	12834	45320
	II	In-gel (10-20%)	Trypsin	LTQ-FTICR	CAD	1245	4200	13490
B	III	SCX	Trypsin	Orbi-trap	CAD	2471	11275	38452
C	IV	SCX	Chymotrypsin	Orbi-trap	CAD	738	2171	8391
	V	SCX	Chymotrypsin	Orbi-trap	ETcaD	833	2700	12415
D	VI	SCX	Lys-N	LTQ-ETD	CAD	862	2366	5283
	VII	SCX	Lys-N	LTQ-ETD	ETcaD	920	2565	6669
Total						**3584**	**38111**	**130019**

To investigate whether this poor overlap was an effect of the four different proteases covering different parts of the proteome, or the different depth of analysis achieved in the 4 methods, we performed a similar overlap analysis applied to the top200 most abundant proteins in each dataset (A-D) (Figure 2B) as ranked by their spectral count index F_{abb} (Supplemental Table 3). F_{abb} is a spectral counting index introduced by us previously (14). It is described in detail in the Materials and Methods, and currently one of the different spectral counting indexes used (15).

Somewhat surprisingly, the overlap analysis showed that only 50% of protein identifications were in common between the four top200 datasets. For instance, Troponin T was observed as the 35th most abundant protein in the LysN dataset (method D) while its rank was way lower in the other datasets (i.e. 139th in trypsin in-gel (method A), 64th in trypsin-IS (method B), and it is even out of the top 200 at a 301st position in the chymotrypsin dataset (method C)). Our data therefore suggests that using only trypsin as protease and a single sample preparation method can heavily bias abundance calculations based on spectral counts, even for robustly identified proteins after exhaustive analysis. This is illustrated further in Supplemental Figure 2, where the relative sequence coverage for the top500 proteins was compiled in a heat map for the methods A-D. The data in Supplemental Figure 2 reveals that each method contributes distinct quantitative information for classes of proteins within the top500. Comparing spectral coverage for each individual protein, retrieved by using different proteomics workflows (A-D), clearly indicates that protein abundance estimations based on spectral counts are to some extent method-dependent.

4.2.4. Absolute protein concentration map of the human LV

We now aimed to use the combined spectral count data for absolute protein concentration determination, which was shown previously to correlate well with single

reaction monitoring based absolute quantitation of protein concentrations (13). For this we used the APEX software package (12), instead of the F_{abb} index (14). APEX and F_{abb} are two

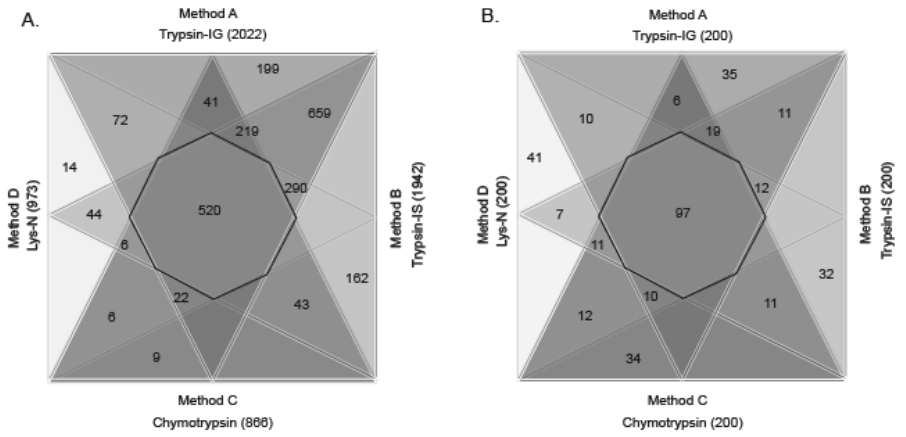

Figure 2. (A) Venn diagram showing the overlap of the high quality 2306 non-redundant proteins between the four methods of data acquisition outlined in Figure 1 and table 1. (B) Venn diagram showing the overlap between the top 200 ranked proteins in each individual method dataset.

different spectral counting indices, whereby the former is more applicable for absolute quantification, however it is presently only amendable for trypsin generated data.Therefore, we first investigated the correlation between $APEX_{trypsin}$ and F_{abb} (14) with the trypsin data (method A and B) using typical default settings, i.e. using unique spectral counts as basis for $APEX_{trypsin}$ and identified spectra as basis for F_{abb}. First the spectral counts observed in each data set were normalized to the total amount in method A-I. Then the F_{abb} values were calculated for method A and B, using the sum of spectral counts over these three datasets. This showed a good linear correlation, however deviation from this correlation was observed for the high abundant proteins with very high spectral counts (Figure 3A).

We hypothesize that the origin of this deviation lie in the fact that for these highly abundant proteins all identifiable unique peptides are depleted and only more redundant spectra can be added after exhaustive analysis. Therefore we adapted our F_{abb} calculation to use unique spectral counts (termed $F_{abb,uni}$), instead of identified spectral counts, and found now a very good linear correlation between $APEX_{trypsin}$ and $F_{abb,uni}$ over the whole dynamic range (Figure 3B). This correlation was used as calibration for all subsequent protein concentration calculations, including the data from method C and D, which, as mentioned above, could not be analyzed directly by the APEX software. First for each protein, the amounts of unique spectra observed in each method were normalized to the total amount in

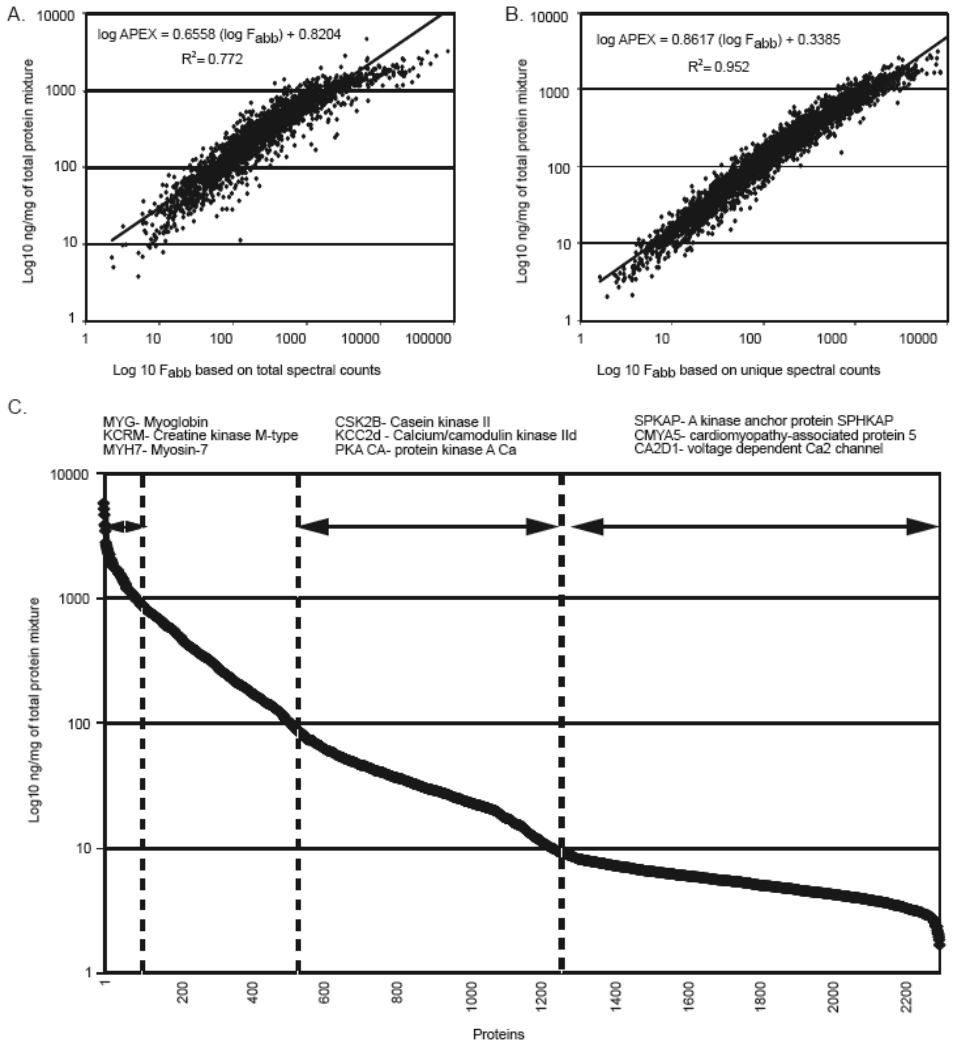

Figure 3. (A) Correlation of protein abundance estimations by APEX vs. F_{abb} based on total spectral counts. 2277 proteins from the method A and B (trypsin based) datasets are plotted. (B) Correlation of the same 2277 protein abundances estimated by APEX vs. $F_{abb,uni}$ based on unique spectral counts, which enhances the correlation between the methods significantly. (C) Absolute protein abundance chart based on absolute protein concentrations (ng/mg of total protein concentration) that reveals that the dynamic range of the analysis spans 4 orders of magnitude. Typical classes of proteins are depicted in relation to their concentration in LV tissue.

method A-I. Subsequently, the average amount of unique spectra over each method (A, B, C and D) was used to calculate the $F_{abb,uni}$. These values were converted to a corresponding

APEX value using the observed linear correlation equation in Figure 3B. These values were then averaged to yield an $APEX_{overall}$ value, which was used to calculate the absolute protein concentration as described in the methods for $APEX_{trypsin}$. The final result of the $APEX_{overall}$ concentration calculations using all data are shown in Supplemental Table 4. In Figure 3C, at the high abundance end, we observed typical high abundant LV proteins such as myoglobin (4.36 µg/mg), and malate-dehydrogenase (3.22 µg/mg), and a large selection of cytoskeletal (muscle) proteins. At the lower abundance end, typical proteins belonging to signaling modules reside, such as several A-kinase anchoring proteins i.e AKAP12 (24.4 ng/mg), SPHKAP (2.8 ng/mg) and myospryn (2.1 ng/mg) (16). The top 50 of LV proteins showed a concentration ranging from 2-4 µg/mg, indicating that these seem to belong to a small selection of relatively high abundant proteins. Supplemental Figure 3 depicts that among the top-200 most abundant LV proteins, most of the currently used biomarkers for CVD reside. This correlation is likely related to their robust quantitation in plasma after tissue damage due to myocardial infarction, so-called tissue-leakage markers. Clear examples within this category include creatine kinase M-type (3.25 µg/mg), Myosin-binding protein C (2.43 µg/mg), myosin-7 (2.18 µg/mg) and cardiac troponin C (1.45 µg/mg).

4.2.5. LV and plasma proteome; overlap and differences

Cardiac tissue is rich in vasculature, therefore plasma contamination is unavoidable and should be evaluated. Illustrative is the observation of classical plasma proteins, such as two hemoglobin isoforms (4.03 and 3.93 µg/mg, respectively), albumin (2.40 µg/mg) and several isoforms of apolipoproteins (range from 4.46 ng-1.5 µg/mg). To further characterize potential contamination, an overlap analysis between our LV proteome and the recently compiled human plasma proteome (17) was conducted. First, the IPI annotated human plasma proteome was converted to identifications in the here used less redundant Swissprot database. Then these plasma proteins were ranked by their calculated $F_{abb,uni}$ based on their reported amount of unique peptides. For the overlapping proteome (447 proteins, Figure 4), the rank within the plasma proteome was compared with the concentration based rank in human LV. Through this comparison several categories of proteins could be classified. We observed that proteins found in the top 100 of the human plasma proteome were also retrieved from human LV, indicative of potential contamination of the LV proteome with plasma proteins (Figure 4, grey data points). Among these 100 abundant human plasma proteins, ~20 proteins were found in human LV with a 0.3-3 µg/mg concentration, such as serotransferrin (3 µg/mg of LV protein, 3rd most abundant protein in human plasma), human serum albumin (3.4 µg/mg of LV protein, 5th most abundant protein in human plasma) and hemoglobin (2.7 µg/mg of LV protein, 16th most abundant protein in human plasma). On the other hand, approximately 23 proteins with a 1-4 µg/mg concentration in LV, but with a low abundance in plasma (rank >1000, Figure 4, black data points), can be classified as potential tissue leakage dependent proteins in plasma, such as creatine kinase M-type (3.25 µg/mg, 2135th position in human

plasma) and fatty acid-binding protein (2.45 µg/mg, 2589th position in human plasma), but also the earlier mentioned troponins (Troponin I (1.24 µg/mg) and Troponin T (1.08 µg/mg)). In this cluster, more cardiac specific proteins reside which form putative novel tissue leakage markers.

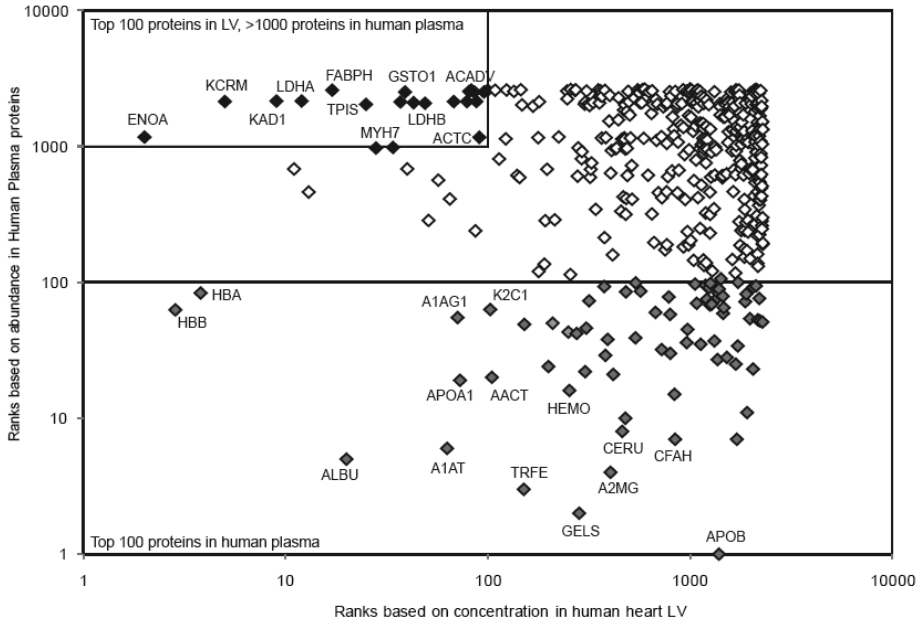

Figure 4. Correlation of abundance of 447 overlapping LV and plasma proteins. Proteins found abundantly in plasma (top 100) are depicted in grey. Proteins which are relatively low abundant in plasma but high abundant in LV are depicted in black. Classical plasma proteins such as hemoglobin (HBA, HBB) and albumin (ALBU) and tissue leakage proteins including myosin (MYH7) and Creatine kinase M-type (KCRM) are highlighted. Protein gene names refer to Swissprot/Uniprot Gene names. The list of proteins that overlapped between the plasma and LV were tabulated in Supplemental Table 5.

4.2.6. Annotating the cardiac signaling proteome

We next focused on signaling proteins, as they are important players in the transition from normal to diseased cardiovascular function (6,7,18,19) and therefore potentially early-stage biomarkers. The absolute abundance of numerous members of three important signaling protein families: kinases, phosphatases and GTPases, were assessed. A detailed of these signaling proteins is listed in Supplemental Table 6.

4.2.7. Kinases and Phosphatases of the Left Ventricle

We identified 69 unique protein kinases of which 45 were classified as "high confidence proteins" with a minimum of two unique peptides, also 6 kinase regulatory subunits were detected, and these were classified according to their kinase subfamily as presented in the Swissprot database and the Cell Signaling kinase tree (20) (Figure 5A). In terms of protein concentration, the observed kinases varied between 2-225 ng/mg (Figure 5B). The most abundant kinases in the human heart are MAPK1 (Erk2, 225 ng/mg) and MAPK3 (Erk1, 103 ng/mg), closely followed by calcium/calmodulin-dependent protein kinase type delta (CAMK2D, 71 ng/mg), cAMP dependent protein kinase (PKA, 52 ng/mg), and integrin linked protein kinase (ILK, 52 ng/mg).

Erk1 and Erk2 are both important downstream regulators of peptide growth factor signaling during cardiac development, but their dysfunction is also critically involved in for instance hypertrophy, myopathy and ischemic reperfusion injury. They seem to have a critical concentration balance, since uncontrolled over-activity of ERKs induces hypertrophy, whereas inhibition induces vulnerability towards stress-induced myocyte death (21).

Calcium/calmodulin-dependent protein kinase type II (CaMKII) is observed with 3 isoforms (α, β and δ) of which the δ-isoform is found to be most abundant, as expected. CaMKII is activated upon a rise in Ca^{2+} concentration and has a plethora of downstream targets that are also involved in Ca^{2+}-homeostasis. Not surprising, an excess of CaMKII activity was found to result in myocardial dysfunction, electrical instability and arrhythmia (7,22).

PKA is also involved in a large set of functional heart pathways, which include excitation contraction coupling and Ca^{2+}-homeostasis. Modulations in PKA activity are also known to be involved in pathological remodeling of the heart. PKA activity is strongly modulated through interaction of its regulatory subunits (PKA-R) with the diverse family of A-kinase anchoring proteins (AKAPs), which tether PKAs action to specific intracellular locations. We observed 4 AKAPs in this dataset, including AKAP12 (24.4 ng/mg) and AKAP2 (21.9 ng/mg), SPHKAP (2.8 ng/mg), and myospryn (2.07 ng/mg). Noteably, in a targeted approach we identified previously around 12 different AKAPs in murine and rat ventricular tissue (16). Several examples of dysfunctional anchoring of PKA have been implicated in detrimental cardiac events, such as hypertrophy and long QT-syndrome (23). Surprisingly, both dominant PKA-R isoforms in cardiac tissue (PKA-RIα, 538 ng/mg and PKA-RIIα, 404 ng/mg) were approximately 10-fold more abundant than the catalytic subunit (PKA-C 52 ng/mg), indicative of the tight regulation PKA is under, as interaction of PKA-C with PKA-R renders it inactive. Upon a rise in cAMP, PKA-C is released from PKA-R and becomes active. Integrin-linked protein kinase (ILK) is observed with a concentration of about 52 ng/mg. ILK is essential in the regulation of cardiac growth, contractility and repair (24). It is considered upstream of hypertrophy through mediating glycogen synthase kinase 3,

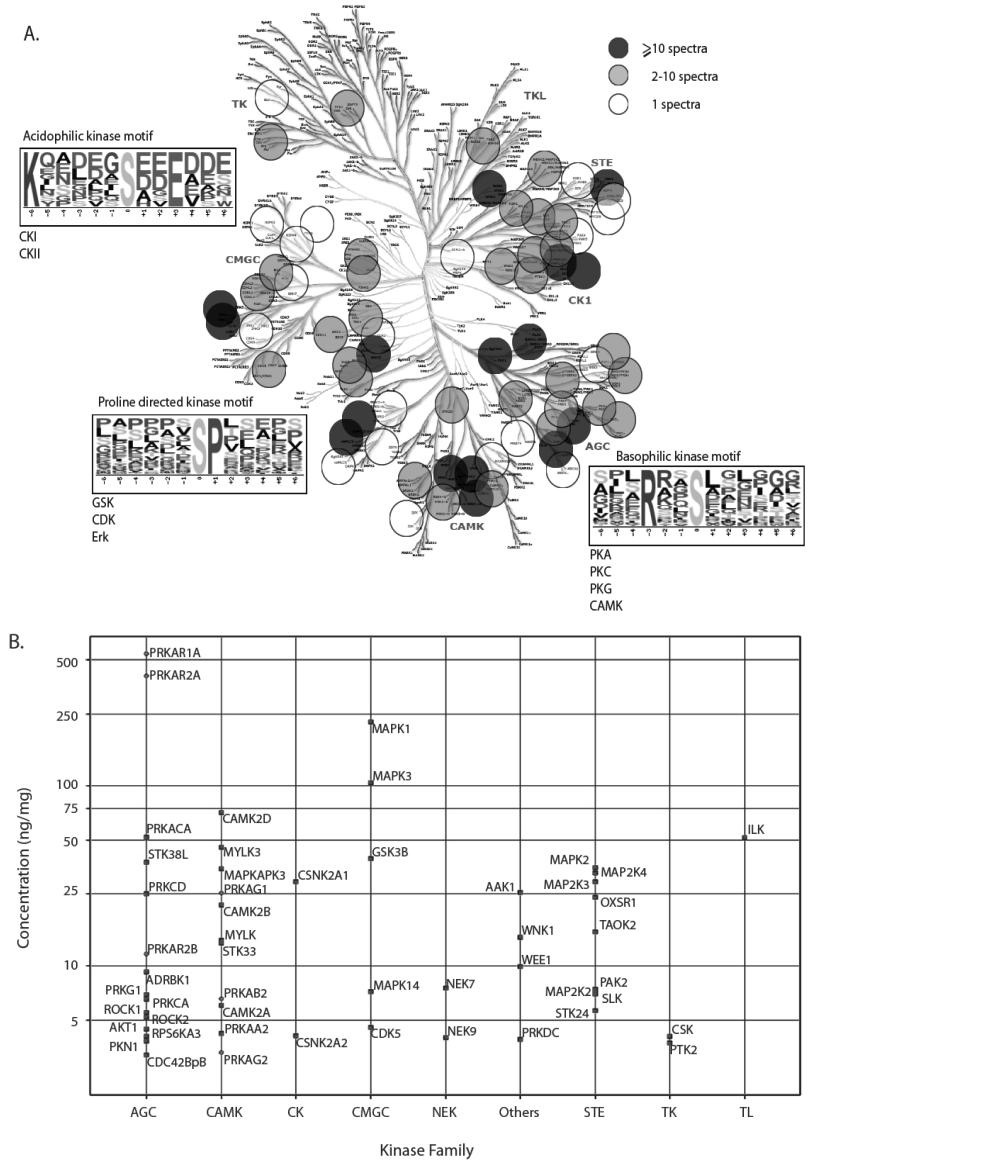

Figure 5. (A) Representation of all identified kinases over the protein kinase tree (adapted from Cell Signaling Inc. (http://www.cellsignal.com/). From the phosphopeptide dataset, multiple enriched kinase consensus motifs could be retrieved. Peptides phosphorylated by MAPK, GSK3, CDK, PKA, PKG, PKC and casein kinase II could be identified and their motifs are represented close to the branch of their corresponding kinase(s). (B) Absolute concentration of 45 kinases observed in the human left ventricle sorted by kinase family; full kinases and catalytic sub-units are shown in squares, whereas regulatory kinase subunits are depicted in circles. For the meaning of the acronyms see Supplemental Table 6.

abundant than MYLK (14 ng/mg), which is considered the dominant form in cardiac tissue (26). Recently, alterations in MYLK3 gene expression were shown to correlate with cardiovascular disease (27). Another interesting observation is the high abundance of Serine/Threonine Kinase 38-like (STKL38, also called NDR2), belongs to the NDR-kinase subfamily of the AGC-kinases (28). another abundant kinase in heart (39.6 ng/mg in totalprotein concentration) (25). Other abundant kinases include Protein Kinase C, two myosin light chain kinases (MYLK3 and MYLK). Interestingly, our data suggest that MYLK3 (45 ng/mg) is about 3-fold more which STKL38 has not been studied extensively, and has no direct functional annotation in heart. It is known to function in neuronal growth and differentiation and its expression in heart was suggested based on mRNA data. Also, it interacts, and is activated through auto-phosphorylation by, the Ca^{2+} binding protein S100B. S100B itself has been implicated as a marker of myocardial infarction (29). Our observation, in conjunction with these data could prone the investigation of STKL38s function in heart. OXSR1 (24 ng/mg) is a STE20 kinase family member which regulates key ion transport mechanisms through interaction with, and phosphorylation of cation-chloride co-transporters (30). High expression levels have been reported in heart (31). It's functional involvement in specific cardiac pathways has not been documented, but would be of interest, given the high abundance of this kinase in human LV tissue.

A total of 32 protein phosphophatases (PPs) were identified of which 19 were observed with a minimum of two unique peptides (Supplemental Table 6). An additional 4 regulatory subunits were also detected with a minimum of two unique peptides. The phosphatase concentrations were observed within a range of 1-600 ng/mg (Supplemental Figure 4). DUSP3 (612 ng/mg), is by far the most abundant phosphatase in the heart LV according to our data, which is in line with its substrate preference for MAPK targets such as ERK2 (32), one of the most abundant kinases in LV. A clear specific role of DUSP3 in heart function has not been reported yet. Other, abundant phosphatases in hert LV include members of the PPP family, like PP1ß (50 ng/mg) and PP2Aα (8 ng/mg). ACP1 (68 ng/mg) is the most abundant tyrosine directed phosphatese, but lack also a clear annotation in heart (dys)function.

4.2.8. Motif analysis of the precisely localized phosphorylation sites

In order to further expose predominant kinase/phosphatase signaling pathways present in the human heart LV, we investigated our dataset for the presence of phosphorylation sites, although we did not perform dedicated phosphopeptide enrichment strategies (33). Still, for 153 proteins detected (6%) we detected also phosphorylated peptides. In total, 222 phosphopeptides were detected, carrying 227 phosphorylation sites localized on 178 serines, 42 threonines, and 7 tyrosines. To classify phosphorylation sites by kinase specificities, we used Motif-X (34), focusing only on serine specific motifs as their numbers were more significant. As shown in Figure 5A, the most significant motif in our dataset was for proline-

directed protein kinases, which appeared in 57 unique sequences, covering 16% of the phosphopeptide data set. Kinases recognizing that motif include MAPKs, GSK3 and CDK. Indeed, those kinases are high abundant in the human heart LV, and their important role in heart function has been described to some extent. The basophilic motifs (26 unique sequences) are likely recognized by AGC kinases such as PKA, PKG and PKC, which are among the most abundant kinases in the LV. Proteins bearing the acidophilic motif (24 unique sequences) are potential substrates of casein kinase II which has been described to have various roles in cardiac signal transduction (35). Summarizing, most phosphopeptides identified in our experiments are likely substrates of the high abundant protein kinases present in the human LV proteome. More detailed analysis of the phosphoproteomics data using the NetworKIN algorithm (36) revealed 18 putative PKA substrates in our data set (for instance, Ser282 and Ser273 of myosin-binding protein C (MYPC3, 2.43µg/mg)). These sites are involved in the regulation of myocardial function and cardioprotection (37,38). We identified 4 putative PKA induced phosphorylation sites on AHNAK (39.8 ng/mg), which is a key player in the β-adrenergic mediated regulation of L-type Ca^{2+} channels (39). NetworKIN further annotated 20 putative PKC kinase substrates, 22 for GSKs, 3 for PKG and several ERK targets such as 2 phosphorylation sites on Heat shock protein beta-8 (8 ng/mg) and also two on Ribosomal protein S6 kinase alpha-1 (RSK1) (5 ng/mg) (40). All phosphopeptides and phosphorylation sites are presented in Supplemental Table 6.

4.2.9. Other proteins of interest

It is impossible, and possibly not very relevant, to describe every protein detected in the human heart LV. Out of own interest, and because of their role in cardiac function we primarily focused on kinases. Two groups of proteins we still like to mention. First, our dataset is also very rich in the number of GTPase signaling nodes. The detailed descriptions of 69 GTPase signaling proteins detected are presented in the supplemental data (Supplemental Figure 5 and Supplemental Table 7).

Curiously, 25 proteins identified in our high quality data are listed as uncharacterized proteins, with very different orders of protein concentrations. Notably, the highest ranked uncharacterized protein is Uniprot Q5JTJ3 with a concentration in LV of 92ng/mg. For these proteins, it may be interesting to study their function in LV. We performed BLAST analysis on all these proteins (Supplemental Table 8). For instance, Q5JTJ3was found to be similar to Sec61, a protein involved in protein import into the ER.

4.3 Materials and methods

Material: All chemicals were purchased from commercial sources and were of analysis grade, unless stated otherwise. High purity water was obtained from a Milli-Q system (Millipore, Bedford, MA USA) and used for all experiments.

4.3.1. Sample preparation and LC/MS/MS analysis

Human transmural, free wall LV tissue was obtained from a 38 year old male without any diagnosed cardiovascular disease. All investigations conform to the principles outlined in the Declaration of Helsinki (41) and experimental protocols were approved by the Ethical Review Boards of the Albert Szent-Györgyi Medical University (Hungary) and University Medical Center Utrecht (The Netherlands). Lysate preparation protocols were as described previously for mouse and rat ventricular tissue (14,42). Briefly, a piece of human left ventricular free wall tissue (~1cm^3) was frozen in liquid nitrogen and pulverized in a pre-cooled steel mortar. The pulverized tissue was taken up in a mild lysis buffer (phosphate buffer, pH 7.4, 0.1% Tween20) including protease inhibitor cocktail (Roche complete mini, 1 tablet per 15 mL buffer) and 0.1% phosphatase inhibitor cocktail (Sigma-aldrich). 600 µg of protein was collected. In order to achieve high quality annotation of the LV proteome, we performed a 3-tier approach in which 3 important parts of the analysis strategy were varied generating a total of seven different datasets which originate from five digestions with four different protease mixtures, of which some were analyzed with two different peptide fragmentation techniques. The experiments can be categorized as follows:

Method A (Trypsin in-gel digestion): The LV protein extract (50 µg) was loaded onto two different SDS-PAGE gradient gels (4-15% and 10-20%, BioRad). Both gel lanes were cut into 70 pieces using Mickle gel slicer prior to in-gel digestion. Gel pieces were subsequently treated with DTT (6.5 mM in 50 mM ammonium bicarbonate, pH 8.5) and iodoacetamide (54 mM in 50 mM ammonium bicarbonate, pH 8.5) for respective reduction and alkylation of cysteine residues. The alkylated proteins were digested with trypsin (Roche Diagnostics, Almere, The Netherlands) overnight at 37^{o}C. After digestion, the supernatants were collected and the remaining gel pieces were extracted with acetonitrile. The LC/MS/MS analysis was performed using a nano LC−LTQ-FTICR (Thermo Electron, San Jose, CA) as described in the supplemental methods section and Aye *et. al.* (42).

Method B (Lys-C/Trypsin In-solution digestion): 200 µg protein lysate was diluted in 200 -µL ammonium bicarbonate (50 mM, pH 7.4) with 96 mg of urea to attain a final urea concentration of 8 M. Subsequently, digestion with 4 µg Lys-C (Roche Diagnostics, Almere, The Netherlands) for 4hr at 37°C, was followed by reduction with 2µM dithiothreitol for 15 min at 65 °C and alkylation with 4 µM iodoacetamide in the dark for 30 min at room temperature. Further digestion was performed in 2 M urea with 4 µg trypsin (Roche Diagnostics, Almere, The Netherlands) for 16hr at 37°C. The resulting peptide mixture was separated using strong cation exchange (SCX). The detailed SCX set up and elution gradient was performed as described in the supplemental methods and Gouw *et. al.* (43). In total 50 SCX fractions were collected and dried in *vacuo* and re-suspended in 20 µl of 10% formic acid. 10 µl of these were subjected to nano-LC−LTQ-Orbitrap (Thermo, Electron). The nano-

LC set up and MS operating parameters are described in the supplemental methods and by Gauci *et. al.* (44).

Method C (Lys-C/chymotrypsin In-solution digestion): 100 µg of protein material was taken up in 8 M urea and reduced and alkylated as described above in method B. Primary digestion was performed using 2 µg Lys-C similarly as above, followed by digestion with 2 µg chymotrypsin (Roche Diagnostics, Almere, The Netherlands) in 2 M urea for 16hr at 37 °C prior to SCX fractionation. The peptide mixture was loaded onto two C18 Opti-Lynx cartridges, using an 1100 HPLC system (Agilent Technologies), at a flow rate of 100 µL/min with 0.05% FA. The detailed refined SCX setup is described by Gauci *et al* (44). A total of 50 SCX fractions were collected and dried *in vacuo*. The LC-MS/MS analysis was performed using the nano LC−Orbitrap-ETD (Thermo Electron). The LC set up as well as the elution gradient is the same as described in method B. The MS operating parameters are described in the supplemental methods.

Method D (Lys-N In-solution digestion): 200 µg of lysate was reduced and alkylated as described above in method B and C, followed by Lys-N digestion (from *Grifola Frondosa*, Seikagaku Corp. (Tokyo, Japan). Lys-N was added at a ratio of 1:85 (w/w) and the sample was incubated overnight at 37 °C (45). The digest was dried *in vacuo* and re-suspended in 0.05% formic acid (FA), followed by the refined SCX fractionation as mentioned in method C. The LC/MS/MS analysis was performed using a nano-LC−LTQ-ETD setup (Thermo Electron) described in supplemental method section (for details, see (45)).

4.3.2. Data analysis

MS/MS spectra collected from the total of 260 LC-MS/MS runs were processed with Bioworks 3.3 (Thermo Electron). Orbitrap-ETD data was analyzed using Proteome Discoverer (v1.1, Thermo Electron). Subsequent MASCOT (v2.2 Matrix Science) searching was performed against an in-house build concatenated forward/reverse (46) Swissprot database (v56.2, released september 23, 2008, 20328 human sequences). Search criteria included: carbamidomethylation on cysteine residues as a fixed modification, methionine oxidation, serine-, threonine and tyrosine-phosphorylation and N-terminal protein acetylation as variable modifications. Two missed cleavages were allowed. A peptide mass tolerance of 25 ppm and an MS/MS mass tolerance of 0.9 Da were set in LTQ-FTICR (method A), Orbitrap CID (method B, C) and Orbitrap-ETD (method C) datasets, whereas 0.9 Da peptide mass tolerance and 0.9 Da MS/MS tolerance was set for data from the LTQ-CID/ETD (method D). All data generated by the FTICR (method A) and the OrbiTrap (method B and C) were recalibrated at individual gel-band or SCX fraction level for mass accuracy using MSQuant (47). For LTQ data (method D) this step was omitted.

The (recalibrated) data of the individual fractions were combined experiment-wise into seven large mascot generic files using MGF-combiner (v1.05 MSQuant), and re-searched using MASCOT with above mentioned parameters except that the precursor mass tolerance was set to 10 ppm. To determine false discovery rates (FDR) in each dataset, the MASCOT peptide score cutoff was adjusted to yield a number of false-positive spectra identifications of <1%. All cutoffs were around a mascot score of 30, except for the LTQ data in method D, where cutoffs for <1% FDR were 45 and 43 for CAD and ETcaD, respectively. Since the FDR calculations are mainly suited for data acquired with high mass accuracy, an arbitrary Mascot score cutoff of 30 was used for the LTQ data in method D resulting in a higher FDR for these data (4.25 % and 3.5% for CAD and ETcaD, respectively). However, a FDR <1% was still observed for proteins with at least 2 unique peptides for this dataset.

Protein organization and redundancy reduction within single datasets was performed using the Scaffold software (v2.1.1; www.Proteomesoftware.com). FDR thresholds were used as filtering criteria. Subsequently, the final protein outputs of seven datasets generated by Scaffold were combined manually. Remaining protein identification redundancy was reduced manually. Protein classification in terms of biological function was performed with the online available Panther software (www.pantherdb.org) (48). Spotfire software (http://spotfire.tibco.com/) was used for cluster analysis. To further investigate the predominant presence of specific phosphopeptide sequences, motifs of all phosphopeptides data were analyzed using Motif-X (34). The significance threshold was set to $P<10^{-6}$ whereas the minimum number of motif occurrences was set to 20 for pSer and 5 for pThr and pTyr.

4.3.3. Protein abundance calculations

The F_{abb} index was used to calculate relative abundances in each dataset following the same procedures as reported by us previously (14). Briefly, F_{abb} is the number of identified spectra of a particular protein divided by its molecular weight, multiplied by $10e^6$ for clarity of plots. Subsequently, proteins can be ranked based on their abundance by descending F_{abb}. For absolute protein concentration determination based on spectral counts, the APEX Quantitative Proteomics Tool (48) was applied. APEX uses the *observed* spectral count for individual proteins normalized by their theoretically *expected* peptides. A relative APEX score is obtained by dividing the sum of the values for all proteins being quantified. The high quality trypsin datasets (method A and B) were imported in the APEX software from the protXML file generated by Scaffold. A MASCOT score threshold yielding <0.1% false positive rate (FPR) was chosen. For absolute quantitation, the calculated APEX value is multiplied by a normalization factor of 25 µg of protein, which was the total amount of protein injected into the mass spectrometer after initial separation on gel or SCX. The APEX values for method A-I, AII and B were averaged and the final absolute concentration ($APEX_{trypsin}$) for the trypsin data was reported.

4.4. Conclusion

Ideal protein biomarkers for cardiac diseases are evidently proteins of cardiac origin. Therefore, it is useful to have as a resource a depository of the identity and abundance of all cardiac proteins. Here we show that a multiplexed proteomics approach using two separation methods, three different proteases and two different peptide activation methods can produce a high quality quantitative (using spectral counts) protein catalogue of an important part of the human heart, the healthy LV. Most currently used biomarkers for myocardial infarction, were as expected found at the higher abundance end of the LV concentration spectrum, with concentrations ranging from 1-4 μg/mg. Several more of these tissue leakage proteins could be annotated by comparing the LV proteome to the human plasma proteome. Many interesting proteins involved in signaling were also detected, albeit at two to three orders of magnitude below (i.e. 2-200 ng/mg) most of the currently used biomarkers. Proteome wide determination of protein concentrations may aid in establishing a set of (signaling) protein based biomarkers with concentrations likely to be detectable in plasma. Alterations in such markers are more likely to present at an earlier stage of CVDs. The specific function of the abundant kinases STK38L and OXSR1, and the phosphatase DUSP3 form interesting new targets for further research, especially in the cardiac context.

4.5. Data availability

The proteomics raw and processed data associated with this manuscript may be downloaded from ProteomeCommons.org. Tranche hashes are given in the supplemental data.

4.6. Acknowledgements

We like to acknowledge the Heck-group members and in particular Henk van der Toorn for bioinformatic support and Shabaz Mohammed, Low Teck Yew and Javier Munoz on data analysis issues. Reinout Raijmakers of the group is acknowledged for critical reading of the manuscript. Utrecht University (Focus & Massa, AS, TAV) Fondation Leducq: the Alliance for CamKII signaling in heart disease (AS, TAV, AJRH, MAV) and the Netherlands Proteomics Centre, embedded in the Netherlands Genomics Initiative, (TTA, NT, AJRH) are kindly acknowledged for financial support.

References:

1. Arab, S., Gramolini, A. O., Ping, P., Kislinger, T., Stanley, B., van Eyk, J., Ouzounian, M., MacLennan, D. H., Emili, A., and Liu, P. P. (2006) *J Am Coll Cardiol* **48**, 1733-1741
2. McGregor, E., and Dunn, M. J. (2006) *Circ Res* **98**, 309-321
3. Jaffe, A. S., Ravkilde, J., Roberts, R., Naslund, U., Apple, F. S., Galvani, M., and Katus, H. (2000) *Circulation* **102**, 1216-1220
4. Westbrook, J. A., Wheeler, J. X., Wait, R., Welson, S. Y., and Dunn, M. J. (2006) *Electrophoresis* **27**, 1547-1555
5. Kline, K. G., Frewen, B., Bristow, M. R., Maccoss, M. J., and Wu, C. C. (2008) *J Proteome Res* **7**, 5055-5061
6. Shenolikar, S. (1994) *Annu Rev Cell Biol* **10**, 55-86
7. Maier, L. S., Zhang, T., Chen, L., DeSantiago, J., Brown, J. H., and Bers, D. M. (2003) *Circ Res* **92**, 904-911
8. Delmotte, N., Kobold, U., Meier, T., Gallusser, A., Strancar, A., and Huber, C. G. (2007) *Anal Bioanal Chem* **389**, 1065-1074
9. Zakhary, D. R., Moravec, C. S., Stewart, R. W., and Bond, M. (1999) *Circulation* **99**, 505-510
10. Zhang, B., VerBerkmoes, N. C., Langston, M. A., Uberbacher, E., Hettich, R. L., and Samatova, N. F. (2006) *J Proteome Res* **5**, 2909-2918
11. Old, W. M., Meyer-Arendt, K., Aveline-Wolf, L., Pierce, K. G., Mendoza, A., Sevinsky, J. R., Resing, K. A., and Ahn, N. G. (2005) *Mol Cell Proteomics* **4**, 1487-1502
12. Lu, P., Vogel, C., Wang, R., Yao, X., and Marcotte, E. M. (2007) *Nat Biotechnol* **25**, 117-124
13. Malmstrom, J., Beck, M., Schmidt, A., Lange, V., Deutsch, E. W., and Aebersold, R. (2009) *Nature* **460**, 762-765
14. Scholten, A., Poh, M. K., van Veen, T. A., van Breukelen, B., Vos, M. A., and Heck, A. J. (2006) *J Proteome Res* **5**, 1435-1447
15. Mueller, L. N., Brusniak, M. Y., Mani, D. R., and Aebersold, R. (2008) *J Proteome Res* **7**, 51-61
16. Scholten, A., Aye, T. T., and Heck, A. J. (2008) *Mass Spectrom Rev* **27**, 331-353
17. Omenn, G. S., States, D. J., Adamski, M., Blackwell, T. W., Menon, R., Hermjakob, H., Apweiler, R., Haab, B. B., Simpson, R. J., Eddes, J. S., Kapp, E. A., Moritz, R. L., Chan, D. W., Rai, A. J., Admon, A., Aebersold, R., Eng, J., Hancock, W. S., Hefta, S. A., Meyer, H., Paik, Y. K., Yoo, J. S., Ping, P., Pounds, J., Adkins, J., Qian, X., Wang, R., Wasinger, V., Wu, C. Y., Zhao, X., Zeng, R., Archakov, A., Tsugita, A., Beer, I., Pandey, A., Pisano, M., Andrews, P., Tammen, H., Speicher, D. W., and Hanash, S. M. (2005) *Proteomics* **5**, 3226-3245

18. Maier, L. S. (2009) *Front Biosci* **14**, 486-496
19. Vlahos, C. J., McDowell, S. A., and Clerk, A. (2003) *Nat Rev Drug Discov* **2**, 99-113
20. Manning, G., Whyte, D. B., Martinez, R., Hunter, T., and Sudarsanam, S. (2002) *Science* **298**, 1912-1934
21. Wang, Y. (2007) *Circulation* **116**, 1413-1423
22. Couchonnal, L. F., and Anderson, M. E. (2008) *Physiology (Bethesda)* **23**, 151-159
23. Mauban, J. R., O'Donnell, M., Warrier, S., Manni, S., and Bond, M. (2009) *Physiology (Bethesda)* **24**, 78-87
24. Hannigan, G. E., Leung-Hagesteijn, C., Fitz-Gibbon, L., Coppolino, M. G., Radeva, G., Filmus, J., Bell, J. C., and Dedhar, S. (1996) *Nature* **379**, 91-96
25. Antos, C. L., McKinsey, T. A., Frey, N., Kutschke, W., McAnally, J., Shelton, J. M., Richardson, J. A., Hill, J. A., and Olson, E. N. (2002) *Proc Natl Acad Sci U S A* **99**, 907-912
26. Watterson, D. M., Schavocky, J. P., Guo, L., Weiss, C., Chlenski, A., Shirinsky, V. P., Van Eldik, L. J., and Haiech, J. (1999) *J Cell Biochem* **75**, 481-491
27. Min, K. D., Asakura, M., Liao, Y., Nakamaru, K., Okazaki, H., Takahashi, T., Fujimoto, K., Ito, S., Takahashi, A., Asanuma, H., Yamazaki, S., Minamino, T., Sanada, S., Seguchi, O., Nakano, A., Ando, Y., Otsuka, T., Furukawa, H., Isomura, T., Takashima, S., Mochizuki, N., and Kitakaze, M. *Biochem Biophys Res Commun* **393**, 55-60
28. Hergovich, A., Stegert, M. R., Schmitz, D., and Hemmings, B. A. (2006) *Nat Rev Mol Cell Biol* **7**, 253-264
29. Pfeifer, R., Ferrari, M., Borner, A., Deufel, T., and Figulla, H. R. (2008) *Resuscitation* **79**, 46-53
30. Delpire, E., and Gagnon, K. B. (2008) *Biochem J* **409**, 321-331
31. Tamari, M., Daigo, Y., and Nakamura, Y. (1999) *J Hum Genet* **44**, 116-120
32. Patterson, K. I., Brummer, T., O'Brien, P. M., and Daly, R. J. (2009) *Biochem J* **418**, 475-489
33. Lemeer, S., and Heck, A. J. (2009) *Curr Opin Chem Biol* **18**, 18
34. Schwartz, D., and Gygi, S. P. (2005) *Nat Biotechnol* **23**, 1391-1398
35. Cieslik, K., Lee, C. M., Tang, J. L., and Wu, K. K. (1999) *J Biol Chem* **274**, 34669-34675
36. Linding, R., Jensen, L. J., Ostheimer, G. J., van Vugt, M. A., Jorgensen, C., Miron, I. M., Diella, F., Colwill, K., Taylor, L., Elder, K., Metalnikov, P., Nguyen, V., Pasculescu, A., Jin, J., Park, J. G., Samson, L. D., Woodgett, J. R., Russell, R. B., Bork, P., Yaffe, M. B., and Pawson, T. (2007) *Cell* **129**, 1415-1426
37. Sadayappan, S., Gulick, J., Osinska, H., Martin, L. A., Hahn, H. S., Dorn, G. W., 2nd, Klevitsky, R., Seidman, C. E., Seidman, J. G., Robbins, J., Lorenz, J. N., Sargent, M., and Molkentin, J. D. (2005) *Circ Res* **97**, 1156-1163

38. Sadayappan, S., Osinska, H., Klevitsky, R., Lorenz, J. N., Sargent, M., Molkentin, J. D., Seidman, C. E., Seidman, J. G., Robbins, J., Gulick, J., Martin, L. A., Hahn, H. S., and Dorn, G. W., 2nd. (2006) *Proc Natl Acad Sci U S A* **103**, 16918-16923
39. Haase, H. (2007) *Cardiovasc Res* **73**, 19-25
40. Dalby, K. N., Morrice, N., Caudwell, F. B., Avruch, J., and Cohen, P. (1998) *J Biol Chem* **273**, 1496-1505
41. (1997) *Cardiovasc Res* **35**, 2-3
42. Aye, T. T., Mohammed, S., van den Toorn, H. W., van Veen, T. A., van der Heyden, M. A., Scholten, A., and Heck, A. J. (2009) *Mol Cell Proteomics* **8**, 1016-1028
43. Gouw, J. W., Tops, B. B., Mortensen, P., Heck, A. J., and Krijgsveld, J. (2008) *Anal Chem* **80**, 7796-7803
44. Gauci, S., Helbig, A. O., Slijper, M., Krijgsveld, J., Heck, A. J., and Mohammed, S. (2009) *Anal Chem* **81**, 4493-4501
45. Taouatas, N., Drugan, M. M., Heck, A. J., and Mohammed, S. (2008) *Nat Methods* **5**, 405-407
46. Elias, J. E., and Gygi, S. P. (2007) *Nat Methods* **4**, 207-214
47. Mortensen, P., Gouw, J. W., Olsen, J. V., Ong, S. E., Rigbolt, K. T., Bunkenborg, J., Cox, J., Foster, L. J., Heck, A. J., Blagoev, B., Andersen, J. S., and Mann, M. (2009) *J Proteome Res* **18**, 18
48. Braisted, J. C., Kuntumalla, S., Vogel, C., Marcotte, E. M., Rodrigues, A. R., Wang, R., Huang, S. T., Ferlanti, E. S., Saeed, A. I., Fleischmann, R. D., Peterson, S. N., and Pieper, R. (2008) *BMC Bioinformatics* **9**, 529

Chapter 5

Reorganized PKA-AKAP Associations in the Failing Human Heart

Thin-Thin Aye[1,2]
Toon A.B. van Veen[3]
Marcel A.G. van der Heyden[3]
Andras Varro[4]
Roel A. de Weger[5]
Nicolaas de Jonge[6]
Marc A. Vos[3]
Albert J.R. Heck[1,2]
Arjen Scholten[1,2]

[1]Biomolecular Mass Spectrometry and Proteomics Group, Bijvoet Center for Biomolecular Research and Utrecht Institute for Pharmaceutical Sciences, Utrecht University, Sorbonnelaan 16, 3584 CA Utrecht, the Netherlands
[2]Netherlands Proteomics Centre
[3]Department of Medical Physiology, Division of Heart & Lungs, University Medical Centre Utrecht, Yalelaan 50, 3584 CM Utrecht, The Netherlands
[4]Department of Pharmacology & Pharmacotherapy, Faculty of Medicine, University of Szeged, Hungary
[5]Department of Pathology, University Medical Centre Utrecht, Utrecht, The Netherlands
[6]Department of Cardiology, University Medical Centre Utrecht, Utrecht, The Netherlands

Manuscript in preparation

Abstract

Hyperactivity of adrenergic signaling in the heart is a mechanism that ultimately leads to heart failure. The cAMP pathway, with the cAMP-dependent protein kinase (PKA) in a key role, acts directly downstream of adrenergic receptors to mediate cardiac function at different levels through phosphorylation of multiple proteins (e.g. modulation of contractility, heart rate, repolarization times). To improve local organization, the regulatory subunit of PKA (PKA-R) is associated with diverse A-kinase anchoring proteins (AKAPs) that tightly localize PKA's function to distinct loci within the cell. In failing hearts, maximal activity of PKA and cAMP-levels were reported unaltered, while a decrease of 30-40% in PKA-R expression and in autophosphorylation was observed. This suggests that PKA-AKAP complex formation is hampered. To detail which PKA-AKAP complexes are affected, we utilized mass spectrometry based chemical proteomics with cAMP immobilized on beads for specific enrichment. For the first time, eight distinct PKA-AKAP interactions could be quantitatively compared between healthy and failing human left ventricular tissue. Association of PKA-R with six AKAPs was unaltered, however PKA-Yotiao (AKAP9) was 9-fold reduced, while the association PKA-MAP2 at the microtubule was increased 12-fold in failing heart. Association of PKA close to key myofilament target proteins was found to be reduced as well (TroponinC 9-fold, cMyBP-C 10-fold). Altogether our data suggest that PKA activity is redistributed to distinct different loci in the failing human heart, which will mediate altered cAMP signal transduction and can consequently form the basis of blunted contractility, and impaired repolarization seen in human heart failure.

5.1. Introduction

Cardiovascular disorders are a leading cause of mortality in western society. Deterioration into heart failure generally results from a plethora of alterations in gene and protein expression.[1] Pathophysiological conditions including dilated cardiomyopathy (DCM), are associated with a reduced density of β1-adrenergic receptors.[2] Proteins controlling cAMP signals downstream of β-adrenergic stimulation are of crucial importance to modify cardiac contraction and rhythm.[3] In failing conditions impairment of β-adrenergic coupling to adenylate cyclase (the protein that generates the second messenger cAMP from ATP) was observed.[4] Main target of cAMP is the cAMP-dependent protein kinase (PKA), of which the holoenzyme consists of two regulatory (PKA-R) and two catalytic (PKA-C) subunits. Under DCM conditions, the overall concentration of cAMP in the myocardium appeared unchanged, as is the activity of PKA-C.[5] The overall levels of PKA-R type I and II were found to be reduced by 30% and 40% respectively.[5] As a consequence, phosphorylation of several crucial PKA-targets involved in contractility and calcium handling, such as troponin I,[5] and phospholamban[6], were altered in end-stage heart failure. Despite the overall consensus that cAMP signaling pathways are altered during cardiomyopathy[7], the precise mechanisms underlying the observed effects still remain to be elucidated.

PKA is a widely distributed, multifunctional kinase. To prevent simultaneous cross activation of parallel PKA pathways and to guide activity, its function is tightly regulated through interaction of PKA-R with the highly diverse family of A-kinase anchoring proteins (AKAPs).[8] AKAPs tether PKA to distinct sites within the cell. The general importance of AKAPs in the heart was demonstrated by Fink *et al.,* who showed that disruption of PKA/AKAP interactions imbalanced cardiomyocyte function.[9] Autophosphorylation of PKA-R, which aids in the high affinity targeting to AKAPs, was also reduced in end-stage heart failure.[10] Several AKAPs are involved in cardiac EC-coupling downstream of the β-adrenergic response. AKAP18δ (AKAP7) organizes a complex of PKA, phospholamban and the Ca^{2+}-ATPase SERCA2.[11] AKAP18α mediates L-type Ca^{2+} channel phoshporylation to increase inflow of extracellular Ca^{2+}.[12] mAKAP is associated with the Ryanodine receptor to modulate its open probability through PKA phosphorylation thereby mediating Ca^{2+} release from intracellular stores.[13] Gravin[14], and AKAP79[15], associate with the β-adrenergic receptor itself to regulate its phosphorylation state.

Besides their role in normal heart physiology, cAMP/PKA/AKAPs are also involved in pathophysiological conditions. mAKAP is associated with the centrosome and is implicated in the onset of hypertrophy through NFATc mediated gene transcription.[16] AKAP-Lbc is upregulated in hypertrophic cardiomyocytes where it coordinates the activation of PKD to initiate MEF2-mediated transcriptional reprogramming events.[17] Kass *et al.* demonstrated a dysfunction of PKA/Yotiao anchoring to the repolarizing potassium channel KCNQ1/KCNE1 as the underlying cause of inherited Long-QT syndrome.[18] An Ile646-Val polymorphism in D-AKAP2 was found to diminish PKA-RIα binding affinity by 3-fold, without an effect on PKA-RIIα affinity, resulting in a shorter P-R interval, suggestively caused by altered localization of RIα.[19]

Altogether, the unaltered cAMP concentration and activity of PKA-C in conjuction with reduced PKA-R expression and autophosphorylation suggest an imbalanced regulation of localized PKA activity and the strong involvement of AKAPs in the deteriorating events occurring during end-stage heart failure. Consequently, to elucidate which specific PKA-AKAP complexes are involved in these detrimental processes, it is important to understand these processes which may raise novel therapeutic opportunities.

In the present study we used immobilized cAMP agarose beads, to specifically enrich a large set of PKA-AKAP complexes from human left ventricular samples. Using quantitative proteomics, differences in cAMP binding proteins were quantitated between end-stage failing (dilated cardiomyopathy tissue) and control tissue. We observed that PKA, but also cGMP-dependent protein kinase (PKG) expression, were altered in DCM tissue. More importantly, this method also allowed us to quantitate, which PKA-AKAP interactions are altered in end-stage heart failure and which remain unaffected. Many observed changes fit well with the loss-of-function and reduced contractility observed in DCM. Interestingly, these changes are

not necessarily influenced by altered expression levels alone, but also due to changes in the association of PKA to different AKAPs.

5.2. Material and methods

5.2.1. Patients selection and ECG recordings

Patients with end-stage chronic heart failure who underwent heart transplantation at the UMC Utrecht were selected from the database using the following criteria: age > 30 years, DCM as underlying cause, available 12-lead surface ECG in sinus-rhythm of acceptable quality. Using Adobe Photoshop, RR, QRS, QT intervals were measured from the digitized ECGs. QT was corrected for heart rate according to Bazett's formula. Patients were age and sex matched to 15 controls without any documented cardiac disease.

5.2.2. Tissue lysate preparation and global proteome survey

Control donor left ventricular free wall tissue was obtained from 38 (C1) and 40 (C2) and 28 (C3), year old males without any diagnosed cardiovascular disorders. Before cardiac explantation, these organ donor patients did not receive medication except for dobutamine, furosemide, and/or plasma expanders. DCM affected donor heart tissue originated from explanted hearts from two male patients aged 37 (P1) and 64 (P2). Prior to transplantation those patients were classified as NYHA IV. All investigations conform to the principles outlined in the Declaration of Helsinki (Cardiovascular Research 1997, 35:2 to 35:4) and experimental protocols were approved by the Ethical Review Boards of the Albert Szent-Györgyi Medical University (Hungary) and University Medical Center Utrecht (The Netherlands). Lysate preparation protocols were as described previously for mouse and rat ventricular tissue.[20] The global left ventricle proteome survey was performed using the protein lysate from C1.

5.2.3. cAMP-pull downs

The pulldowns with 2-AHA-cAMP agarose (100 µL dry volume, BIOLOG, Bremen, Germany, ligand concentration: 6µmol/mL) were performed as described previously.[21] 20 mg total protein was used as input for all four experiments. After pull-down, bound proteins were eluted with 90 µl of 8 M Urea under denaturing conditions. Subsequently, digestion with Lys-C (Roche Diagnostics, Almere, The Netherlands) for 4 hr at 37 ^{o}C, was followed by reduction with 2 µM Dithiothreitol for 15 min at 65 ^{o}C and alkylation with 4 µM iodoacetamide in the dark for 30 minutes at room temperature. Further digestion was performed in 2 M urea with trypsin (Roche Diagnostics, Almere, The Netherlands) for 16 hr at 37 ^{o}C.

5.2.4 MS analysis, protein identification and quantitation

Nano-HPLC-MS/MS-analysis was performed as described previously[21], and is further detailed in the Supplemental Methods. Generated spectra were processed with Bioworks 3.3

(Thermo, Bremen, Germany) and data analysis was carried out using the Mascot (version 2.2.0) software platform (Matrix Science, London, UK). Protein redundancy was reduced using Scaffold version 2.1.1 (www.Proteomesoftware.com). Quantitation using normalized spectral counts[22] is described in detail in the Supplemental Methods.

5.2.5 Immunoblotting

Left ventricle lysate samples were resolved prior and after cAMP affinity purification by SDS-PAGE, electro-transferred to nitrocellulose membranes (Amersham Bioscience) and immersed in the TBST-buffer (20 mM Tris-HCL, pH 7.5, 0.5 M NaCl, 0.1% Tween 20) with 5% (w/v) BSA. Antibodies used are outlined in the Supplemental methods.

5.3. Results

5.3.1 ECG analysis

ECG analysis (Table 1) revealed significant prolongation of the QRS and QTc time between controls and DCM patients meaning that both ventricular activation and relaxation were affected. Despite administration of β-blockade, the RR interval in patients was significantly shorter (increased heart rate). Obviously, contractility was dramatically impaired in patients who displayed an EF < 20%.

Table 1. Age- and sex-matched DCM control comparison. Average values per group are given with the corresponding standard deviation (SD). RR represents rhythm, QRS the depolarization time. QT time was corrected for rhythm (QTc). P-values were determined by a t-test.

	Controls	**DCM patients**	
	Average (SD)	**Average (SD)**	**p-value**
Number	**15**	**18**	**-**
Age (SD)	**52 (10)**	**46 (8)**	**0.068 (ns)**
RR (ms)	**911 (153)**	**773 (178)**	**0.025**
QRS (ms)	**99 (11)**	**145 (43)**	**0.001**
QT (ms)	**381 (30)**	**412 (67)**	**0.108 (ns)**
QTc (ms)	**401 (13)**	**471 (50)**	**0.001**

5.3.2. Global proteomic analysis of human heart tissue

To test the feasibility of using a global proteomics approach to study cyclic nucleotide signaling proteins, a large analysis of the healthy human left ventricular proteome (C1) was evaluated. Using the LC-MS/MS strategy depicted in Figure 1A on the 2nd gel lane of Figure 1B yielded the identification of 1430 proteins. A high dynamic range of identifications was achieved based on spectral counts for the individual proteins that varied from 7226 for myosin heavy-chain type 7 (MYH7_HUMAN) to two unique peptides (our cut-off, Supplemental Methods and Supplemental Table 1). Only two PKA isoforms, and two AKAPs could be

retrieved, and with low spectral counts, indicative of their relatively low abundance compared to cytoskeletal and house-keeping proteins.

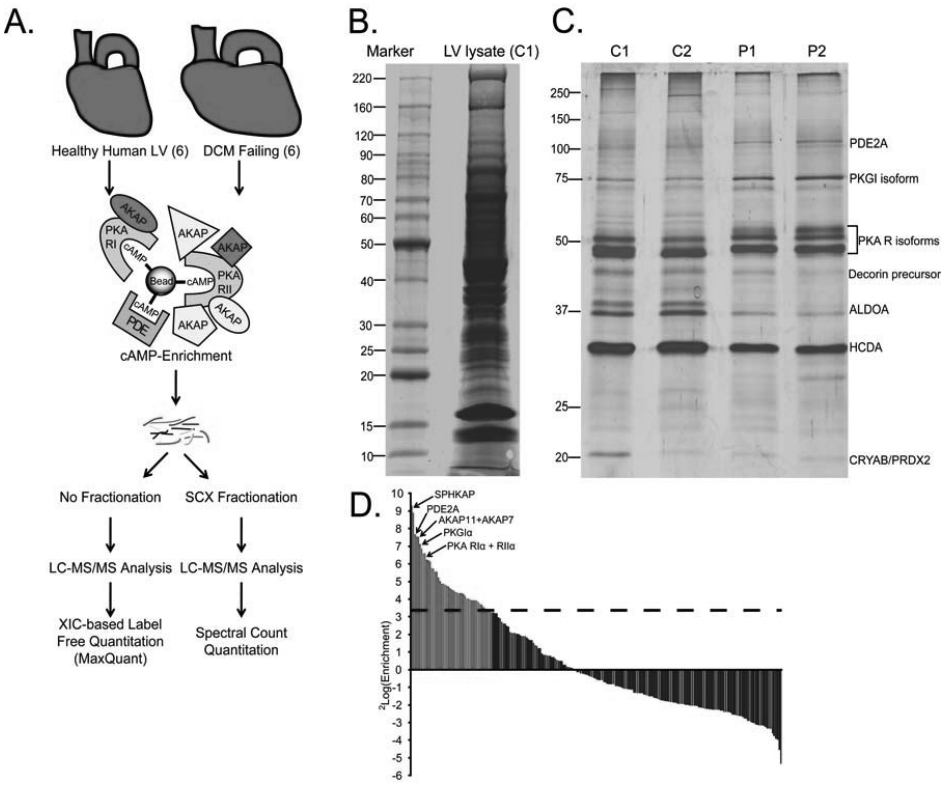

Figure 1. (A) Experimental strategies to investigate potential alterations in PKA-AKAP interactions during heart failure as outlined in the (Supplemental) Methods section. On the left, a global approach in which the total protein extracts was investigated using in-gel digestion prior to LC-MS/MS analysis. On the right, the targeted cAMP-affinity enrichment approach combined with 1D-SDS PAGE prior to MS-analysis. (B) SDS-PAGE gel of left ventricular free wall tissue protein lysate from a healthy control donor (C1). (C) SDS-PAGE gel of cAMP pull-downs in human left ventricular tissue. The left ventricle tissue lysates from Controls (C1 and C2) and Patients (P1 and P2) with DCM were treated with 2-AHA-cAMP-agarose beads to purify cyclic nucleotide signaling modules. (D) Proteins identified in the cAMP pull-down experiments (at least two unique peptides) plotted with their enrichment factor ($NSC_{cAMP,\ max}/NSC_{total,\ LV}$) as compared to the whole left ventricular lysate of control 1. Proteins with an enrichment factor ≥2 are presented above the dotted line.

5.3.3 Affinity enrichment of cAMP/PKA/AKAP signaling proteins

To study these low-abundant signaling proteins by mass spectrometry based proteomics, in the background of much higher abundant proteins requires specific enrichment. Therefore, we used an immobilized cAMP-resin to capture and characterize PKA-AKAP complexes and other cyclic nucleotide signaling proteins.[20]

Equal amounts of soluble protein lysates from left ventricle free wall tissue of two controls and two DCM patients were incubated with cAMP-affinity beads (Figure 1A). For an initial qualitative comparison, a fraction of the four obtained protein precipitates was separated by SDS-PAGE (Figure 1C). Strikingly, controls and patients displayed a very similar pattern of bands, although consistent differences between them were also present, especially in the molecular weight regions around 37 kDa, 55 kDa and 75 kDa. To meticulously evaluate which proteins associated with cAMP and whether they showed differential expression between patients and controls, the cAMP-pull-down fractions from each donor were digested directly off-bead. The resulting peptide mixtures were separated by strong cation exchange chromatography before analysis by LC-MS/MS. Using stringent criteria (Supplemental Methods), this resulted in the identification of 140, 160, 153 and 136 proteins in sample C1, C2, P1 and P2 respectively (Supplemental Table 2) with very similar amounts of overall spectra. The inter-donor overlap among reliably identified proteins appeared high, indicative for the reproducibility of the approach (Supplemental Figure 1). To discriminate high abundant but less specific proteins from specific low abundant "real" cAMP binding proteins and their interactors, the global proteome survey from C1 was used (Supplemental Table 1). For each protein, the maximum spectral count in one of the four cAMP-bead experiments was compared to the spectral count in the whole heart lysate. The quotient of these two counts was used to identify the low abundant specific interactors of the beads. Only proteins with a quotient ≥ 2 were further evaluated (Figure 1D, blue bars). This led to the isolation of 60 proteins from the total dataset (Supplemental Tables 2A+2C). For spectral count quantitation only proteins with a significant amount of spectra may be considered, therefore only proteins with more than 10 spectra summed over either patients or controls were selected, further reducing our protein set of interest to 24 (Supplemental Table 2A). Among these proteins were ample examples of cAMP signaling proteins, such as all four isoforms of PKA-R, PDE2A and eight AKAPs, all with high spectral counts.

5.3.4. Semi-quantitative Profiling of protein abundance

These 24 proteins were quantitated in each of the four samples. Therefore, the spectral counts were normalized[20, 22], and subsequently compared between the four donor samples. The outcome is depicted in Figures 2A and 2C, where the normalized spectral count (NSC) ratio (Patients/Controls) is plotted against the significance of the identification as measured by the maximum amount of spectra observed for a particular protein in any of the four samples. The G-test was applied to isolate significant changes (Supplemental Tables 2A and 2B).

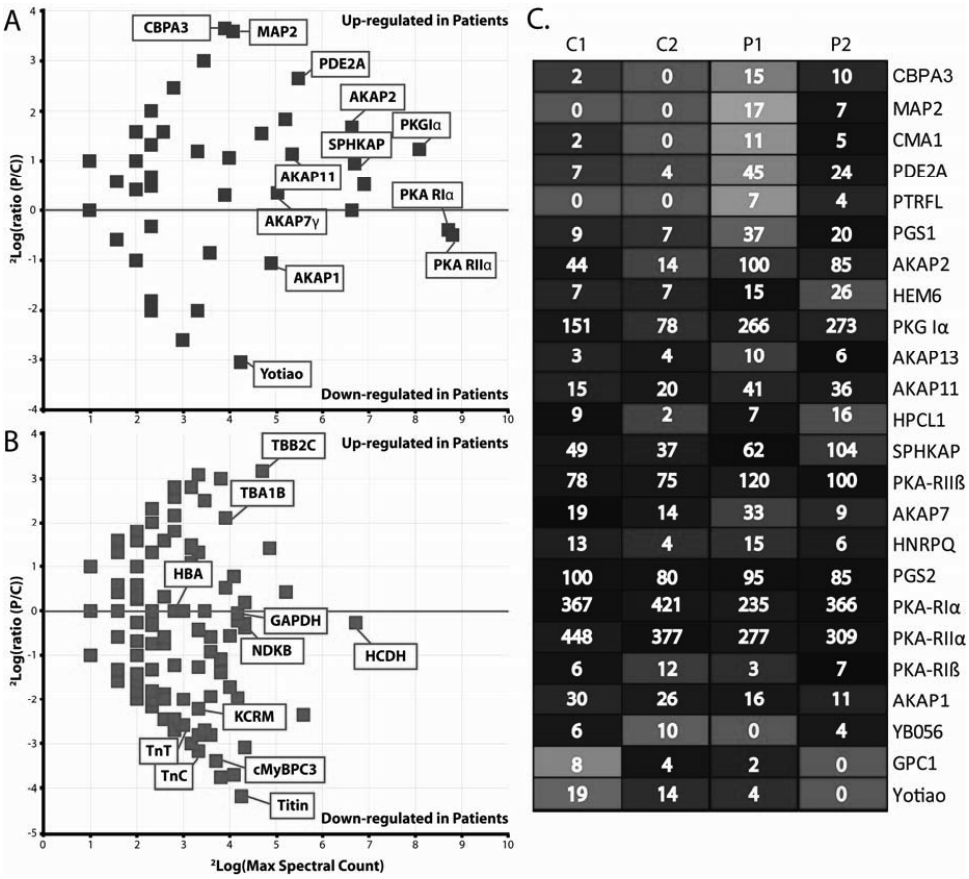

Figure 2. (A) Scatter plot for the proteins that were specifically enriched and quantitated. NSC-ratio (Patient/Control (P/C), ^{2}log scaled y-axis) representing abundance of proteins in patients and controls versus the maximum spectral count observed for C1, C2, P1 or P2 (^{2}log scaled x-axis) representing the abundance in the pull down. Swissprot abbreviations are listed in Supplemental Table 2A (B) As A., but for the proteins without specific enrichment on the beads (Supplemental Table 2B). (C) Heatmap of the proteins presented in Figure 2A with the normalized spectral counts retrieved from each sample.

5.3.5. Direct interactors of cAMP

First, the direct interactors of cAMP were evaluated. The amounts of PKA-RIα (ratio 0.8) and PKA-RIIα (ratio 0.7) isoforms were not dramatically altered in DCM. In contrast, cGMP-dependent protein kinase (PKG Iα), which also equips the ability to interact with cAMP, albeit at much higher, non-physiological cAMP concentrations, seems about 2-fold upregulated (ratio 2.4). Moreover, the phosphodiesterase PDE2A is strongly upregulated in the patients (ratio 6.3).

Typical proteins such as NDKB and HCDH which are known to have some affinity for cAMP due to binding domains that are related to the cyclic nucleotide binding pocket[20] were also found in our pull-down. These were not enriched since the spectral counts in the global approach were significantly higher. These co-purifying proteins had typical ratios of close to one (Figure 2B, Supplemental Table 2B), indicating that they were not altered in DCM and thereby signifying the observed changes for PKG and PDE2A. Also sticky high abundant background proteins without known affinity for cAMP such as hemoglobin (HBA) have a ratio of close to 1, indicating that the background behaves similarly in both patients and controls and reiterating our reproducibility and specificity.

To confirm observed mass spectrometric changes in protein abundance, we selected several direct cAMP interacting proteins from our 24-membered prime candidate list for which specific antibodies were available, and probed their expression level using Western blotting (Figure 3). Clearly, the relative amounts observed at total lysate level (left column) correlate well with the observed changes in spectral counts observed in the cAMP pull down (middle column).

5.3.6. Secondary Interactors

The cAMP-pulldown assay not only allowed us to quantify specific changes in proteins directly binding to cAMP, such as PKA, but it also has a unique feature, as it allows the quantitation of proteins associating to PKA under the two studied conditions. Since cAMP is the bait and PKA its primary target, the AKAPs, and other secondary interactors, are evaluated based on their association with PKA rather than on their absolute expression profile. Therefore the semi-quantitative method supplies information on the relative population of distinct AKAPs with PKA. Interestingly, two of the most altered proteins in Figure 2A are AKAPs; microtubule associated protein 2 (MAP2, ratio 12.0) and Yotiao (AKAP9, ratio 0.12, 8.3-fold down).

To investigate whether the alteration of MAP2 in our pull-down originated from an overall change in expression level or from increased association to PKA at this scaffold, we performed western blotting in the whole lysate and compared this with our proteomics data (Figure 4A). MAP2 expression did not change significantly at lysate level but showed a large increase in the patient pull-downs only. Western blots on the pull down fraction of C3 and P2 showed a similar ratio as the proteomics data (~7.2-fold). This seems to be a reflection of the difference in overall Tubulin-α expression as the ratio is very similar in the whole lysate. Western blots for Yotiao in the whole lysate (even at 200 µg input) did not succeed, likely due to the very low abundance. In the pull-down fraction, where Yotiao is significantly enriched, Western blotting confirmed the observed changes in the proteomics data (Figure 4B).

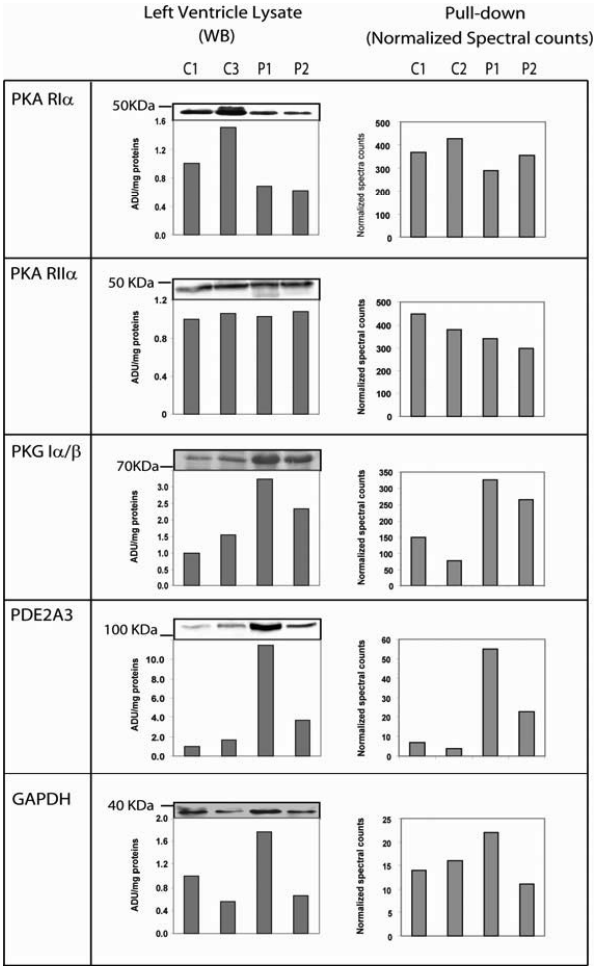

Figure 3. Differential protein expression of direct cAMP interactors. Left column: selection of direct interactors of cAMP immunoblotted for expression in 50 µg total protein from human left ventricular lysate. The histograms represent the levels of selected proteins as arbitrary densitometric unit (ADU). Middle column: Normalized spectral counts of those particular proteins in the pull-down experiments. Right column: Immunoblots on the cAMP pull-down fraction.

5.3.7. Altered enrichment of myofilament PKA targets

In Figure 2B and Supplemental Table 2B many of the non-enriched proteins have a ratio of close to 1.0 in our pull-down. Others show significant up and down regulation. The ratios of these proteins may indicate two things; (i) these high abundant proteins were expressed at different levels in patients and controls, and therefore aspecifically co-purified with the pull-down with a ratio reflecting their expression levels, or (ii) a sub-fraction of the

total amount of the protein is a PKA interactor or an interactor of one of the AKAPs and thereby explaining its ratio. Several examples of the first set of proteins, which are typically among the top-ranking identifications in the global proteome survey (Supplemental Table 1), were observed.

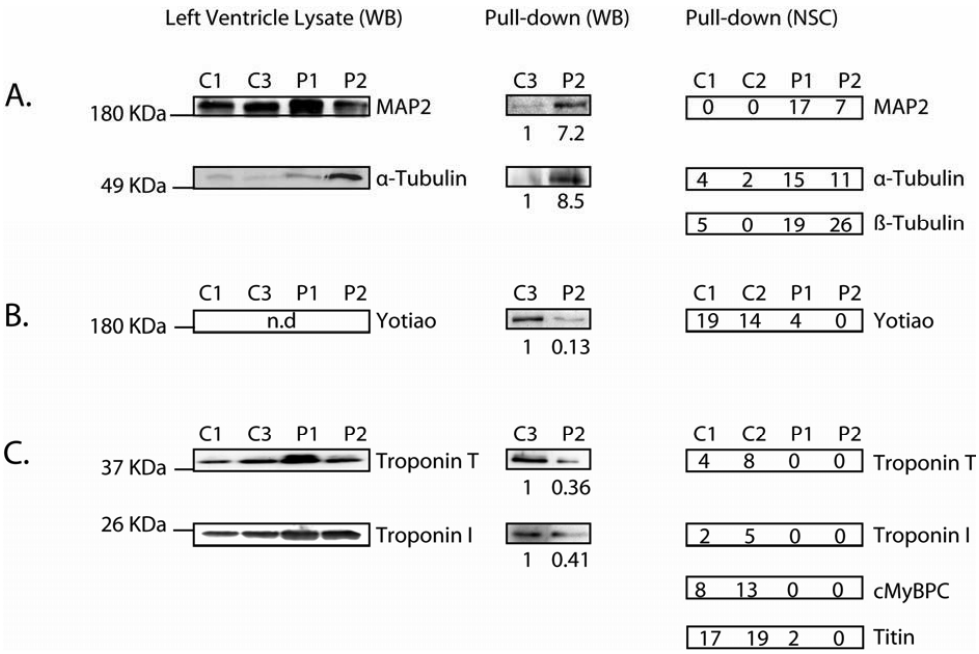

Figure 4. Secondary interactors of cAMP show redistribution of PKA. ***(A)*** *Immunoblots representing expression levels of MAP2 and tubulin-α in 50µg whole left ventricular lysate (left), compared with the amount associating with PKA as assessed by immunoblotting (middle) and MS analysis (right, depicted are NSCs) of cAMP pull down fractions.* ***(B)*** *Differental amount of Yotiao associating with PKA assayed by Western blot (middle) and NSC (right).* ***(C)*** *As A and B, but for myofilament proteins.*

Not surprisingly, changes in these proteins are currently used as markers for DCM. For example creatine kinase type S was down regulated in DCM patients, as expected.[23] Also the down regulation of aconitate hydratase (ratio 0.15) in DCM tissue was observed previously.[24] Interestingly, Figure 2B also contains several proteins that could serve as candidates for the second category. PKA is known to phosphorylate several myofilament proteins, namely titin [25], the troponin I/C/T complex at troponin I (TnI) [26] and cardiac myosin binding protein C (cMyBPC).[27] The proteomics data clearly indicate a decrease in enrichment of these myofilament proteins from the patient material, (Figure 4C), while Western blots of TnT and TnI at lysate level showed a slight increase of these proteins in the patients. The decreased

enrichment of TnT and TnI by cAMP was confirmed by Western blotting on the pull-down fractions as well.

5.4. Discussions

5.4.1. Alteration of cAMP signaling in the failing heart

At tissue level, the implication and alteration of cAMP signaling proteins in failing hearts has been established over the past decade. However at the molecular level, it is still debated whether increased cAMP signaling has a detrimental, pathogenic or a beneficial, compensatory effect on cardiac function. The contrasting results obtained in knock-out mouse models seem difficult to capture in a single hypothesis as reviewed previously.[7] It is not unlikely that the origin of these disparate results lies in the complex localization profile of PKA in the heart. We hypothesize that PKA-R can redistribute itself to different AKAPs to accommodate, or even compensate for, the altered signaling pathways induced in the failing heart. As evidence for this hypothesis, general disruption of PKA-AKAP complex formation was found to inhibit proper myocyte contractility.[9] In addition, several PKA phosphorylation targets were found altered in the failing human myopathic hearts, such as CREB[28] and Phospholamban[29], which are both hyper-phosphorylated, while phosphorylation of troponin I was found downregulated[5] in human DCM tissue. Also PKA-R itself was observed autophosphorylated at lower levels, thereby reducing its affinity for AKAPs. Furthermore, the earlier mentioned involvement of PKA-AKAP complex malformation in several pathological outcomes[16-19] shows that proper PKA association is crucial. With the chemical proteomics approach described in this manuscript we were able to map global changes in expression levels of PKA-R, but also of other cyclic nucleotide binding proteins. More importantly, at the same time the association of PKA-R to eight distinct AKAPs could be quantitatively compared between the healthy and failing heart.

5.4.2. Direct Interactors of cAMP

Previously, PKA-RI (~40%) and PKA-RII (~30%) expression was found to be down-regulated in the human DCM heart.[5] These numbers fit well with our observed ratios for PKA-RIα (ratio 0.8) and PKA-RIIα (ratio 0.7). At the same time, we found PKG Iα 2.4-fold upregulated. This is an important observation, as in recent literature, more and more evidence is reported for cross-talk between the cAMP and cGMP pathways with PKA and PKG as crucial pillars therein.[30] These two cyclic nucleotide signaling pathways often counteract each other in cardiac function. PKG functions downstream of the NO/natriuretic peptide signals and in heart it has a negative inotropic effect through phosphorylation of L-type Ca^{2+}-channels, thereby reducing open probability and therefore also intracellular Ca^{2+} levels.[31] It is not unlikely that the increase in PKG contributes to the reduced contractility of the failing heart. Directly related to this pathway, we found that PDE2A was 6-fold up-regulated. PDE2A has dual specificity for cAMP and cGMP, while the hydrolytic activity is increased

by cGMP binding to the N-terminal GAF-domain.[32] Mongillo *et al*. demonstrated that PDE2A has a strong limiting effect on the intracellular cAMP concentration induced by β-adrenergic stimulation of rat neonatal cardiomyocytes.[33] This mechanism of increased cAMP hydrolysis was shown to be dependent on cGMP/PKG acting downstream of the β_3-adrenergic receptor (β3-AR). In light of these data, it is tempting to speculate that the upregulation of several components of this pathway, as observed in our data, are a (harmful) compensatory mechanism to control the increased β1-AR and β2-AR stimulus in failing hearts via the β3-AR/NO/cGMP/PKG/PDE2 pathway.

5.4.3. Alteration of localization and increased PKA association at microtubules

Recently, we and others identified the presence of at least 18 different AKAP family members in the heart.[34, 35] Our data show directly that PKA-AKAP associations are changing in failing hearts, however this seems to be restricted to a small subset of AKAPs of which potential implications are discussed below. The presence of microtubules in cardiac myocytes is well established. Also an increased microtubule polymerization, as well as increased expression of α and β-tubulin is observed in heart failure tissue.[36] The concomitant reduction in contractility is attributed to increased stiffness and viscosity of the cardiomyocytes with higher microtubule content. In addition, it was shown that the microtubules become more heavily decorated by microtubule associated protein 4 (MAP4), which has a dampening effect on the active transport required in the diffusion limited cardiomyocyte.[37]

In the past decade, additional roles of the microtubules in heart, beyond the described cytoskeletal one, have emerged. Gomez *et al*. showed that microtubules are functionally coupled to the two main Ca^{2+} regulatory mechanisms; Ca^{2+} current and sarcoplasmic reticulum Ca^{2+} release. Decreased microtubule function through inhibition by colchicine increased Ca^{2+} levels and hence contractility via a cAMP dependent mechanism.[38] Recently, in dendrites and neurons, cAMP and PKA have been shown to mediate microtubule bundling and crossbridging via interactions with MAP2.[39] In these cells, increased PKA phosphorylation at microtubule sites increased microtubule polymerization.

Our data confirm the previously described increase in tubulin expression and show an increased anchoring of PKA to MAP2, while the overall MAP2 levels are not changed in the failing heart (Figure 4A). In conjunction with this observation, both α- and β-tubulin seem to be more enriched in our pull-down as well, however this seems to originate from the differential expression. Our observations fit well into the described microtubule behaviour in heart failure tissue. The observed increased polymerization of microtubule in cardiomyocytes of heart failure patients could be formed through a cAMP dependent mechanism, not by increased concentrations of cAMP, but through PKA relocation to MAP2 which thereby increases phosphorylation of microtubule targets and hence causes further polymerization of microtubule. Along these lines, Nath *et al*. discovered that cAMP induced arrests of rhythmic

and synchronous contractions of fetal rat myocytes could be reversed by colchicine, in other words, destabilization of microtubules restored proper contraction.[40]

5.4.4. Yotiao

In heart, Yotiao (AKAP9) functions at the I_{Ks}-channel, which is slowly activated in response to changes in membrane potential, thereby contributing to the crucial repolarizing current of the cardiac action potential. I_{Ks} current amplitude is increased upon induced β-adrenergic stimulation, thereby shortening the action potential. Coupling of the β-adrenergic stimulus to the shortened I_{Ks} response is mediated by PKA phosphorylation through formation of a multiprotein complex of Yotiao, PKA-RII, PKA-C, PP1 and PDE4D3 at the I_{Ks}-channel.[41, 42] Two mutations, KCNQ1-G589D[41] and Yotiao-S1570L[43], both disrupt proper coupling of Yotiao to the I_{Ks} channel, thereby causing long QT syndrome. The involvement of disrupted I_{Ks} function in DCM conditions was not earlier established. Our data indicate that in DCM affected tissue the coupling of PKA to Yotiao is downregulated, thereby impairing proper channel phosphorylation and contributing to the increased QT-time observed in Table 1. We propose that the uncoupling of PKA to Yotiao would have a similar effect on QT-time as observed with the earlier mentioned mutations.

5.4.6. Myofilament and Inflammatory Proteins

PKA anchoring close to the myofilaments, the core of the β-adrenergic contractile response, has been proposed, however a specific AKAP was never elucidated.[9] Our data now indicate that anchoring of PKA in this compartment of the cell is hampered in DCM tissue. Obviously a reduction in the presence of PKA near its myofilament targets can have a dramatic effect on the contractile machinery. In Supplemental Table 2A and 2B many inflammatory proteins show up-regulation in our analyses. Besides many IgG proteins, two mast cell proteins, CBPA3 (mast cell carboxypeptidase A) and CMA1 (Chymase, Mast cell protease I) are of particular interest. The upregulation of these two proteins fits well with the current understanding that mast cell density and excretion is increased in human failing heart tissue.[44] In addition, chymase inhibition was recently shown to improve outcome in a rat autoimmune heart failure model system.[45] These proteins seem connected to PKA due to the high enrichment in our pull down, however to date no direct interaction has been described.

5.5. Conclusion

Altogether, the data presented here connects alterations in several cyclic nucleotide signaling pathways with the impaired contractility and signaling observed in the failing human heart. Figure 5 recapitulates our prime findings. With our chemical proteomics approach we were able to show that several proteins binding directly to cyclic nucleotides changed in their expression profile, such as PKG and PDE2. More importantly, the approach

allowed us to quantify the amount of PKA-association to several different AKAPs. Particularly interesting examples of this are MAP2 and Yotiao, as well as several myofilament proteins that showed dramatically altered association behavior. All these changes imply that reduced contractility and signaling in the failing heart is accommodated by complex changes in signaling proteins at multiple levels, which are not necessarily restricted to the β-adrenergic receptor or PKA-R alone.

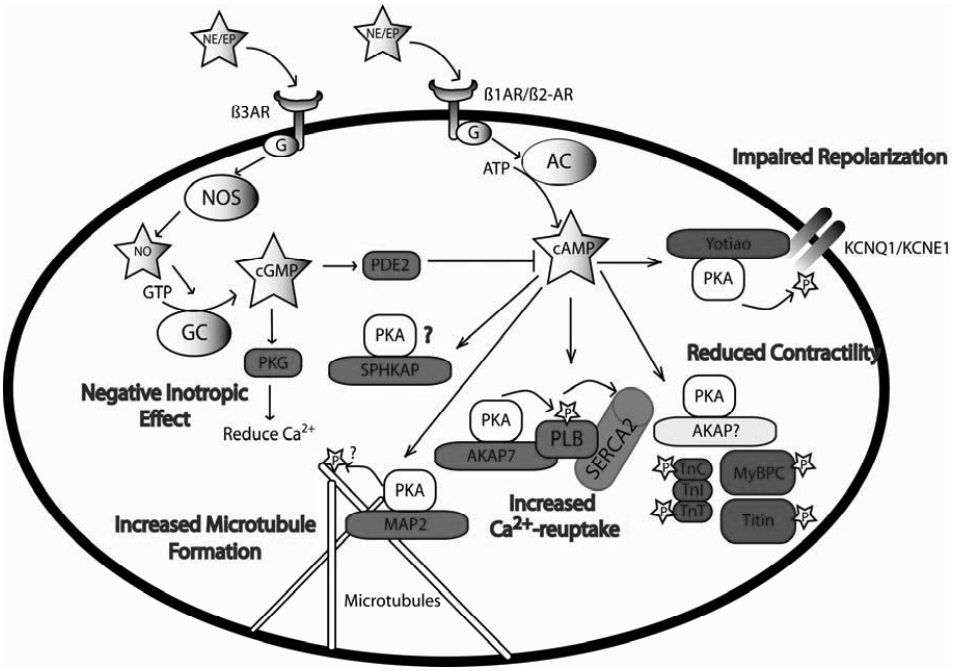

Figure 5. Altered PKA-AKAP association under DCM conditions affects signaling at multiple levels. Changes in expression of cyclic nucleotide binding proteins (PKG, PDE2A), as well as, differential association of AKAPs to PKA-R form the basis of the blunted adrenergic response of failing hearts. Green indicates an increase in expression or association, while red represents a decrease.

5.6. Acknowledgements

The Netherlands Proteomics Centre is acknowledged for funding (T.T.A.; A.S.; A.J.R.H.). The Fondation Leducq is also kindly acknowledged for funding (T.A.B.V.; A.S.; M.A.V.; A.J.R.H.). Bart Kok is kindly acknowledged for technical assistance.

References:

1. Margulies KB, Bednarik DP, Dries DL. Genomics, transcriptional profiling, and heart failure. *J Am Coll Cardiol.* 2009;53(19):1752-1759.

2. Bristow MR, Ginsburg R, Umans V, Fowler M, Minobe W, Rasmussen R, Zera P, Menlove R, Shah P, Jamieson S, et al. Beta 1- and beta 2-adrenergic-receptor subpopulations in nonfailing and failing human ventricular myocardium: coupling of both receptor subtypes to muscle contraction and selective beta 1-receptor down-regulation in heart failure. *Circ Res.* 1986;59(3):297-309.

3. Kass DA. Message delivered: how myocytes control cAMP signaling. *Circ Res.* 2008;102(9):1002-1004.

4. Bristow MR, Hershberger RE, Port JD, Minobe W, Rasmussen R. Beta 1- and beta 2-adrenergic receptor-mediated adenylate cyclase stimulation in nonfailing and failing human ventricular myocardium. *Mol Pharmacol.* 1989;35(3):295-303.

5. Zakhary DR, Moravec CS, Stewart RW, Bond M. Protein kinase A (PKA)-dependent troponin-I phosphorylation and PKA regulatory subunits are decreased in human dilated cardiomyopathy. *Circulation.* 1999;99(4):505-510.

6. Schwinger RH, Munch G, Bolck B, Karczewski P, Krause EG, Erdmann E. Reduced Ca(2+)-sensitivity of SERCA 2a in failing human myocardium due to reduced serin-16 phospholamban phosphorylation. *J Mol Cell Cardiol.* 1999;31(3):479-491.

7. Movsesian MA. Altered cAMP-mediated signaling and its role in the pathogenesis of dilated cardiomyopathy. *Cardiovasc Res.* 2004;62(3):450-459.

8. Beene DL, Scott JD. A-kinase anchoring proteins take shape. *Curr Opin Cell Biol.* 2007;19(2):192-198.

9. Fink MA, Zakhary DR, Mackey JA, Desnoyer RW, Apperson-Hansen C, Damron DS, Bond M. AKAP-mediated targeting of protein kinase a regulates contractility in cardiac myocytes. *Circ Res.* 2001;88(3):291-297.

10. Zakhary DR, Moravec CS, Bond M. Regulation of PKA binding to AKAPs in the heart: alterations in human heart failure. *Circulation.* 2000;101(12):1459-1464.

11. Lygren B, Carlson CR, Santamaria K, Lissandron V, McSorley T, Litzenberg J, Lorenz D, Wiesner B, Rosenthal W, Zaccolo M, Tasken K, Klussmann E. AKAP complex regulates Ca2+ re-uptake into heart sarcoplasmic reticulum. *EMBO Rep.* 2007;8(11):1061-1067.

12. Gray PC, Johnson BD, Westenbroek RE, Hays LG, Yates JR, 3rd, Scheuer T, Catterall WA, Murphy BJ. Primary structure and function of an A kinase anchoring protein associated with calcium channels. *Neuron.* 1998;20(5):1017-1026.

13. Kapiloff MS, Jackson N, Airhart N. mAKAP and the ryanodine receptor are part of a multi-component signaling complex on the cardiomyocyte nuclear envelope. *J Cell Sci.* 2001;114(Pt 17):3167-3176.

14. Lin F, Wang H, Malbon CC. Gravin-mediated formation of signaling complexes in beta 2-adrenergic receptor desensitization and resensitization. *J Biol Chem.* 2000;275(25):19025-19034.

15. Fraser ID, Cong M, Kim J, Rollins EN, Daaka Y, Lefkowitz RJ, Scott JD. Assembly of an A kinase-anchoring protein-beta(2)-adrenergic receptor complex facilitates receptor phosphorylation and signaling. *Curr Biol.* 2000;10(7):409-412.

16. Dodge-Kafka KL, Soughayer J, Pare GC, Carlisle Michel JJ, Langeberg LK, Kapiloff MS, Scott JD. The protein kinase A anchoring protein mAKAP coordinates two integrated cAMP effector pathways. *Nature.* 2005;437(7058):574-578.

17. Carnegie GK, Soughayer J, Smith FD, Pedroja BS, Zhang F, Diviani D, Bristow MR, Kunkel MT, Newton AC, Langeberg LK, Scott JD. AKAP-Lbc mobilizes a cardiac hypertrophy signaling pathway. *Mol Cell.* 2008;32(2):169-179.

18. Saucerman JJ, Healy SN, Belik ME, Puglisi JL, McCulloch AD. Proarrhythmic consequences of a KCNQ1 AKAP-binding domain mutation: computational models of whole cells and heterogeneous tissue. *Circ Res.* 2004;95(12):1216-1224.

19. Kammerer S, Burns-Hamuro LL, Ma Y, Hamon SC, Canaves JM, Shi MM, Nelson MR, Sing CF, Cantor CR, Taylor SS, Braun A. Amino acid variant in the kinase binding domain of dual-specific A kinase-anchoring protein 2: a disease susceptibility polymorphism. *Proc Natl Acad Sci U S A.* 2003;100(7):4066-4071.

20. Scholten A, Poh MK, van Veen TA, van Breukelen B, Vos MA, Heck AJ. Analysis of the cGMP/cAMP interactome using a chemical proteomics approach in mammalian heart tissue validates sphingosine kinase type 1-interacting protein as a genuine and highly abundant AKAP. *J Proteome Res.* 2006;5(6):1435-1447.

21. Aye TT, Mohammed S, van den Toorn HW, van Veen TA, van der Heyden MA, Scholten A, Heck AJ. Selectivity in enrichment of cAMP-dependent protein kinase regulatory subunits type I and type II and their interactors using modified cAMP affinity resins. *Mol Cell Proteomics.* 2009;8(5):1016-1028.

22. Paoletti AC, Parmely TJ, Tomomori-Sato C, Sato S, Zhu D, Conaway RC, Conaway JW, Florens L, Washburn MP. Quantitative proteomic analysis of distinct mammalian Mediator complexes using normalized spectral abundance factors. *Proc Natl Acad Sci U S A.* 2006;103(50):18928-18933.

23. McGregor E, Dunn MJ. Proteomics of the heart: unraveling disease. *Circ Res.* 2006;98(3):309-321.

24. Corbett JM, Why HJ, Wheeler CH, Richardson PJ, Archard LC, Yacoub MH, Dunn MJ. Cardiac protein abnormalities in dilated cardiomyopathy detected by two-dimensional polyacrylamide gel electrophoresis. *Electrophoresis.* 1998;19(11):2031-2042.

25. Fukuda N, Wu Y, Nair P, Granzier HL. Phosphorylation of titin modulates passive stiffness of cardiac muscle in a titin isoform-dependent manner. *J Gen Physiol.* 2005;125(3):257-271.

26. Solaro RJ, Moir AJ, Perry SV. Phosphorylation of troponin I and the inotropic effect of adrenaline in the perfused rabbit heart. *Nature.* 1976;262(5569):615-617.

27. Jeacocke SA, England PJ. Phosphorylation of a myofibrillar protein of Mr 150 000 in perfused rat heart, and the tentative indentification of this as C-protein. *FEBS Lett.* 1980;122(1):129-132.

28. Fentzke RC, Korcarz CE, Lang RM, Lin H, Leiden JM. Dilated cardiomyopathy in transgenic mice expressing a dominant-negative CREB transcription factor in the heart. *J Clin Invest.* 1998;101(11):2415-2426.

29. Minamisawa S, Hoshijima M, Chu G, Ward CA, Frank K, Gu Y, Martone ME, Wang Y, Ross J, Jr., Kranias EG, Giles WR, Chien KR. Chronic phospholamban-sarcoplasmic reticulum calcium ATPase interaction is the critical calcium cycling defect in dilated cardiomyopathy. *Cell.* 1999;99(3):313-322.

30. Zaccolo M, Movsesian MA. cAMP and cGMP signaling cross-talk: role of phosphodiesterases and implications for cardiac pathophysiology. *Circ Res.* 2007;100(11):1569-1578.

31. Schroder F, Klein G, Fiedler B, Bastein M, Schnasse N, Hillmer A, Ames S, Gambaryan S, Drexler H, Walter U, Lohmann SM, Wollert KC. Single L-type Ca(2+) channel regulation by cGMP-dependent protein kinase type I in adult cardiomyocytes from PKG I transgenic mice. *Cardiovasc Res.* 2003;60(2):268-277.

32. Martinez SE, Wu AY, Glavas NA, Tang XB, Turley S, Hol WG, Beavo JA. The two GAF domains in phosphodiesterase 2A have distinct roles in dimerization and in cGMP binding. *Proc Natl Acad Sci U S A.* 2002;99(20):13260-13265.

33. Mongillo M, Tocchetti CG, Terrin A, Lissandron V, Cheung YF, Dostmann WR, Pozzan T, Kass DA, Paolocci N, Houslay MD, Zaccolo M. Compartmentalized phosphodiesterase-2 activity blunts beta-adrenergic cardiac inotropy via an NO/cGMP-dependent pathway. *Circ Res.* 2006;98(2):226-234.

34. Mauban JR, O'Donnell M, Warrier S, Manni S, Bond M. AKAP-scaffolding proteins and regulation of cardiac physiology. *Physiology (Bethesda).* 2009;24:78-87.

35. Scholten A, Aye TT, Heck AJ. A multi-angular mass spectrometric view at cyclic nucleotide dependent protein kinases: in vivo characterization and structure/function relationships. *Mass Spectrom Rev.* 2008;27(4):331-353.

36. Tagawa H, Koide M, Sato H, Zile MR, Carabello BA, Cooper Gt. Cytoskeletal role in the transition from compensated to decompensated hypertrophy during adult canine left ventricular pressure overloading. *Circ Res.* 1998;82(7):751-761.

37. Takahashi M, Shiraishi H, Ishibashi Y, Blade KL, McDermott PJ, Menick DR, Kuppuswamy D, Cooper Gt. Phenotypic consequences of beta1-tubulin expression

and MAP4 decoration of microtubules in adult cardiocytes. *Am J Physiol Heart Circ Physiol.* 2003;285(5):H2072-2083.

38. Gomez AM, Kerfant BG, Vassort G. Microtubule disruption modulates Ca(2+) signaling in rat cardiac myocytes. *Circ Res.* 2000;86(1):30-36.

39. Leterrier JF, Kurachi M, Tashiro T, Janmey PA. MAP2-mediated in vitro interactions of brain microtubules and their modulation by cAMP. *Eur Biophys J.* 2009;38(4):381-393.

40. Nath K, Shay JW, Bollon AP. Relationship between dibutyryl cyclic AMP and microtubule organization in contracting heart muscle cells. *Proc Natl Acad Sci U S A.* 1978;75(1):319-323.

41. Marx SO, Kurokawa J, Reiken S, Motoike H, D'Armiento J, Marks AR, Kass RS. Requirement of a macromolecular signaling complex for beta adrenergic receptor modulation of the KCNQ1-KCNE1 potassium channel. *Science.* 2002;295(5554):496-499.

42. Terrenoire C, Houslay MD, Baillie GS, Kass RS. The Cardiac IKs Potassium Channel Macromolecular Complex Includes the Phosphodiesterase PDE4D3. *J Biol Chem.* 2009;284(14):9140-9146.

43. Chen L, Marquardt ML, Tester DJ, Sampson KJ, Ackerman MJ, Kass RS. Mutation of an A-kinase-anchoring protein causes long-QT syndrome. *Proc Natl Acad Sci U S A.* 2007;104(52):20990-20995.

44. Patella V, Marino I, Arbustini E, Lamparter-Schummert B, Verga L, Adt M, Marone G. Stem cell factor in mast cells and increased mast cell density in idiopathic and ischemic cardiomyopathy. *Circulation.* 1998;97(10):971-978.

45. Palaniyandi SS, Nagai Y, Watanabe K, Ma M, Veeraveedu PT, Prakash P, Kamal FA, Abe Y, Yamaguchi K, Tachikawa H, Kodama M, Aizawa Y. Chymase inhibition reduces the progression to heart failure after autoimmune myocarditis in rats. *Exp Biol Med (Maywood).* 2007;232(9):1213-1221.

Chapter 6

Summary and Outlook

6.1. Summary

Cardiovascular diseases are among the most common causes of death in the developed world. Therefore, to be able to predict and evaluate risks for such diseases, identifying suitable biomarkers has become an important part of cardiovascular research. Evidently, understanding cardiovascular biology is also important in this respect. Among bio-molecules, proteins are considered ideal candidates for such biomarkers as they are the primary effectors of dynamic cellular functions. In the search for protein biomarkers, proteomics emerges as a useful tool as it allows examination of global protein expression in response to pathologically and/or pharmacologically induced states in a comprehensive and unbiased way. Nevertheless, proteomics in biomarker discovery and drug development is still in its infancy, particularly with respect to the proper statistic relevant large sample sizes, i.e. number of patients and controls. This calls for refinement of complex sample separations and for increasing sensitivity and dynamic range of mass-spectrometers to allow a more comprehensive picture of induced changes, also of more low-abundant proteins. This thesis focuses on (i) exploring chemical probes to increase sensitivity and specificity for the investigation of low abundant cardiac proteins applicable to both biology and biomarker discovery, and (ii) exploiting different aspects of mass spectrometry-based proteomics for building a concentration-based cardiac proteome inventory.

Chapter 1 is an overview of the applications of proteomics in cardiac diseases, including detailed descriptions of proteomics platforms used to analyze protein expression, function and quantity. The advantages of affinity- and activity-based proteomics for monitoring the spatial and temporal changes of the targeted cardiac proteome are also discussed. Furthermore, it is illustrated how these methods can be coupled to label-based and label-free mass spectrometry methods to monitor changes in the proteome in a quantitative manner. Finally, the traditional biomarker discovery approach is described, which is a combination of information originating from animal models, and clinical studies and how such approaches have contributed to the identification of currently available diagnostic/prognostic biomarkers for cardiovascular disease.

The cardiac system is a highly complex system in which signal transduction plays a critical physiological, but also a patho-physiological, role. Understanding how signaling mechanisms are perturbed under pathological conditions can give valuable insights into the potential origin of the disease. Chapter 2 reviews the specific contribution of mass spectrometry to the understanding of two particular cardiac signaling pathways that evolve around the second messenger cyclic nucleotides cAMP and cGMP. Two major downstream effectors of these cyclic nucleotides are Protein Kinase A (PKA) and Protein Kinase G (PKG) respectively. Their relations to A-kinase anchoring proteins (AKAPs) and G-kinase anchoring proteins (GKAPs), both scaffold proteins that compartmentalize these kinases are discussed. Finally, in this chapter an overview of mass spectrometry-based techniques applied to study

the structure/function relationships of these kinases, such as native mass spectrometry, H/D exchange and ion mobility mass spectrometry, are presented.

Sub-cellular compartmentalization of PKA through interaction with AKAPs provides a mechanism to restrict signal transduction events at specific subcellular localizations, so-called compartmentalization. In chapter 3, a chemical proteomics approach is combined with stable isotope labeling and mass spectrometry to study the specificity of different PKA isoforms for different AKAPs. Three different immobilized cAMP-analogues, with different specificities for PKA-isoforms were used to enrich for PKA from several cell types and rat tissues. Stable isotope labeling was used to quantify the differential enrichment of the PKA-isoforms and thus their interacting AKAPs. Of the twelve AKAPs detected, seven preferentially bound to RII, whereas the remaining five displayed at least dual-specificity with a potential preference for RI. For the first time, the specificity of AKAP14, AKAP2 and AKAP12 could be established.

The cAMP pathway is documented to act downstream of the adrenergic receptors that mediate cardiac contractility at multiple levels. Under myopathic conditions of the heart, contractility is heavily affected. Related to this, changes in concentration of several cAMP affected proteins, such as PKA, have been reported under these pathological conditions, however no relation of these changes towards AKAPs has been described. Therefore, in chapter 4 cAMP-based chemical proteomics is employed to identify potential changes in concentration and association of PKA in the dilated cardiomyopathy (DCM) affected human heart. Specific enrichment of PKA, PKG, several phosphodiesterases and many AKAPs from both healthy and DCM hearts were quantitatively compared in a label-free manner. We confirmed that PKA-R concentrations were lower in DCM affected tissue. Interestingly, our pull-down experiments also showed that the specific interactions of PKA with AKAPs was altered in the diseased heart; several showed increased association with PKA, whereas others showed decreased interaction under DCM conditions. Hence, it can be implicated that aberrant signaling through AKAP complexes contributes to certain heart diseases. These experiments, for the first time, demonstrate the powerful combination of chemical proteomics with isotopic labeling as a potential application for cardiac biomarker discovery.

Chapter 5 continues with the application of a multiplexed proteomics approach to generate a concentration-based human left ventricle proteome library. We used two separation methods (gel-based and off-gel electrophoresis), four different proteases (LysC, Trypsin, chymotrypsin and LysN) and two different gas phase fragmentation methods (CAD and ETcaD) in order to identify, but also quantify, as many proteins as possible. We identified 3,584 distinct proteins with high confidence, of which 65% (2,306 proteins) were observed with at least two unique peptide sequences. These highly confident proteins were quantitated using a sophisticated label-free spectral counting method to yield a comprehensive ranking of human left ventricular proteins by concentration. In this library, therapeutically/diagnostically interesting protein classes can be studied in relation to their concentration. Most currently

used CVD-biomarkers, as well as many muscle machinery proteins are present in the 1ug-4 ug/mg region of high abundant proteins in LV. The pathophysiological dysfunction of signaling pathways underlies the molecular basis of several manifestations of cardiovascular diseases, such as hypertrophy and other types of left ventricular remodeling, ischemia/reperfusion injury, angiogenesis, and atherogenesis. Given their roles in such a wide variety of disease states, several signaling proteins, in particular, protein kinases and phosphatases are rapidly becoming extremely attractive targets for drug discovery. In this chapter the signaling proteins, protein kinases (~2-200 ng/mg), phosphatases (~1-600 ng/mg) and small GTPase (~2-1000 ng/mg) were studied in the context of their concentrations and the endogenous phosphorylation sites observed in heart. These data form an interesting starting point to prioritize future targets for drug and biomarker discovery efforts in the cardiac context.

6.2. Outlook

cAMP/PKA/AKAP signaling complexes

The original AKAP hypothesis postulates that spatial resolution of PKA-mediated phosphorylation events provides specificity to cAMP signaling. In addition, AKAPs scaffold multiple other signaling proteins such as other kinases, phosphodiesterases and phosphatases to comprise an adequate, specific signaling node. Such a regulatory mechanism can also increase the intensity of a cAMP-mediated hormonal response. Carr *et al.* reported that 5-10 AKAPs are found to be expressed in most cell types by using two predominant techniques, RII overlay and screening of bacterial expression libraries with RII as a probe (1). Most characterized AKAPs preferentially bind to PKA-RII while some have been reported to be dual specific for both PKA-RI and PKA-RII. Recently, Kovanich *et al.* reported that SPHKAP which was first discovered as a putative novel AKAP by our group (2) can be considered as the first mammalian AKAP that preferentially binds to PKA-RIα (3). However, till now, very few AKAPs specific to PKA-RI have been assigned as PKA-RI is predominantly cytoplasmic whereas PKA-RII is more often associated with cellular structures and organelles. As mentioned in chapter 3, we have shown that quantitative chemical proteomics, based on dimethyl labeling, is able to distinguish the cAMP binding affinity between PKA-RI and PKA-RII. Consequently, AKAPs specific to different PKA-isoforms can now be screened for in tissues/cells of any origin in a single pull-down experiment. Furthermore, this combined approach could be used for identifying potential PKA-RI specific AKAPs in different tissues. In fact, the above-mentioned characterization of SPHKAPs specificity was performed in part by applying this method directly to heart tissue (3). Advantage of this technique is that it can be applied directly to the endogenous protein in its endogenous source tissue.

Several AKAPs have been found to be expressed in cardiac tissue (4). Recently, Rohman *et al*. discovered that the gene expression level of mAKAP, RyR and the SR Ca^{2+}-ATPase (SERCA2A) is decreased in the heart of an *mdx* mouse, a mouse model of DMD (Duchenne muscular dystrophy which is a common genetic disease resulting from mutations in the dystrophin gene) (5). Cardiac hypertrophy is usually observed in *mdx* mice because of the alterations in contractile properties that are likely due to defective Ca^{2+} handling. Zakhary *et al*. recently demonstrated that three cardiac AKAPs, mAKAP, AKAP-Lbc, and AKAP15/18, have different binding affinities for PKA-RII and these binding affinities are altered upon the phosphorylation of RII in cardiac myocytes (6). Hence, we hypothesize that the expression levels of AKAPs or AKAP tethering of PKA R-subunits may be altered in the failing heart, to compromise the ability of the myocyte to respond to stimuli. To investigate this hypothesis, we have again used chemical proteomics in chapter 4 to probe the differential protein expression as well as interaction between PKA and AKAPs during the development of DCM. We have found that some AKAPs (for instance, AKAP2, AKAP11 and SPHKAP) have a greater affinity for PKA than other AKAPs (AKAP9, AKAP1) in the failing heart when compared to the healthy heart. Hence, further study is necessary to elucidate how re-arrangements of PKA-AKAP complexes can occur in cardiac myocytes that progress into a myopathic state. In addition, Zakhary *et al.* reported that the level of PKA-RII phosphorylation at Ser95 is decreased in failing heart tissues (7). Thus, future study is necessary to determine (i) the role of RII phosphorylation in preferentially targeting PKA to specific AKAPs, (ii) other possible means to regulate the PKA–AKAP interaction, and (iii) how the selective targeting of PKA to a specific AKAP alters substrate phosphorylation in the cardiac myocyte. Furthermore, it would be interesting to study whether these dynamics also occur within much shorter timeframes as a potential regulatory mechanism. Temporal changes in PKA/AKAP interactions could be monitored using quantitative chemical proteomics, for instance, through PGE2 stimulation or forskolin treatment of various cell types where cyclic nucleotide signaling is prominent. In addition to protein dynamics, phosphorylation dynamics of PKA, PKG AKAPs and PDEs can be monitored more specifically and in more detail using this approach. Hence, other than the spatial aspect, chemical proteomics in combination with dimethyl labeling can also be used to study the temporal dynamics of PKA and AKAPs at the level of protein expression and post translational modification. This could reveal crucial temporal events occurring during the onset of specific cyclic nucleotide signaling pathways.

Finally, we foresee the importance of extending these approaches to more controlled in *vivo* systems by generating animal models in order to elucidate the functional implications of AKAPs in for instance cardiac myocytes. It would be very interesting to apply our methods tocommon animal models of various CVDs, such as transverse aortic constriction models of myopathy.

Cardiac biomarker discovery

In recent years, body fluids, such as plasma have been thoroughly investigated for possible protein markers of cardiac disease. Obviously, sampling is in this case less invasive and readily available from any patient, however, the enormous drawback of the plasma proteome is the dynamic range that easily spans 10-12 orders of magnitude, whereas current mass spectrometry is limited to a dynamic range of 3-4 orders of magnitude. In addition, the plasma proteome is dominated by 22 proteins with a much larger abundance of which depletion is cumbersome. Therefore, to increase sensitivity, attention is shifted from body fluids to the diseased tissues of interest. In chapter 5, a robust method is developed to generate a human left ventricle proteome library in terms of relative and/or absolute protein concentration. Several known and classic biomarker proteins were observed with high abundance in left ventricle. However, as mentioned earlier, signaling proteins become attractive therapeutic targets because of their central role in organ function. However, most signaling proteins have a much lower abundance than the classical biomarkers and have therefore not been considered as biomarkers. In this study we have emphasized the exact abundances of kinases, phosphatases and GTPases in the LV to prioritize targeted biomarker suitability tests. Hopefully signaling proteome based biomarkers have more potential to diagnose at a much earlier stage, which is the main drawback of the classical 'tissue leakage' markers used today for myocardial infarction. As multiple signaling pathways can be activated simultaneously and, with the potential for cross-talk, the identification of specific kinases as targets for drug therapy is a highly complex process and still at an early stage. Anderson *et al*. highlighted that selective inhibition of protein kinases results in greater refinement of biological responses (*8*). Although only two kinase inhibitors are currently registered for cardiovascular indications, it can be concluded that there is still a lot of room for expansion in this area. For this it is important to establish which kinases are dysregulated in the complex disease states of the cardiovascular system through kinase activity profiling (*9*).

SRM as novel approach in the clinical validation process

While proteomics plays a major role in the discovery phase of potential biomarkers, validation is as important and probably also the most time-consuming phase, particularly when performed in the required large prospective clinical studies required to prove clinical value. In most studies, antibody-based methods such as ELISA are used to measure the concentrations of candidate biomarkers in larger cohorts. However, suitable antibodies for those validation experiments are not always available, and it is excessively expensive when sample numbers rise. In addition, it is time consuming to develop proper antibodies for all potential protein markers or when specific panel of protein markers are to be analyzed. Recently, selected reaction monitoring (SRM) has been introduced as a mass spectrometry

based method that can be exploited to specifically select and quantify promising protein biomarkers in body fluids or tissues (*10*). In the future, this technique may complement or possibly replace immunological methods for biomarker verification and for selection of potential biomarker candidates. SRM assays can be highly multiplexed such that a moderate number of candidate proteins (in the range of 10–50) can be simultaneously targeted and measured in a statistically viable number of patient samples (up to hundreds of samples). However, sensitivity for unambiguous detection and quantification of proteins by mass spectrometry based assays is often constrained by sample complexity, particularly when the measurements are being made in complex fluids such as plasma. Initial SRM studies have been reported for cardiac biomarkers in plasma (*11*). However, no SRM studies have been described for cardiac tissues yet.

As discussed in this thesis, proteomics is a critical tool to address cardiac diseases at the level of signal transduction, cellular mechanisms, but also at the level of biomarker development. The future challenges for such studies will include reduction of discovery to follow-up time for biomarker strategies and translation of these approaches to the clinic. Strong ties between basic and clinical sciences will be essential to facilitate this transition. Likewise, as the field continues to develop strategies for high through-put quantitation, the ability of proteomics to serve as a clinical tool will similarly increase. Thus, proteomics tools described in this thesis will continue to be an indispensable approach to decipher cellular mechanisms and to link these mechanisms to cardiac diseases and health.

References:

1. Carr, D. W., and Scott, J. D. (1992) Blotting and band-shifting: techniques for studying protein-protein interactions, *Trends Biochem Sci 17*, 246-249.
2. Scholten, A., Poh, M. K., van Veen, T. A., van Breukelen, B., Vos, M. A., and Heck, A. J. (2006) Analysis of the cGMP/cAMP interactome using a chemical proteomics approach in mammalian heart tissue validates sphingosine kinase type 1-interacting protein as a genuine and highly abundant AKAP, *J Proteome Res 5*, 1435-1447.
3. Kovanich, D., Heyden, A. G., Aye, T. T., Veen, T. A. B., Scholten, A., and Heck, A. J. (2010) Sphingosine kinase interacting protein (SPHKAP) is an A-kinase anchoring protein (AKAP) specific for type I cAMP-dependent protein kinase (PKA-RI), *Chembiochem*.
4. Ruehr, M. L., Russell, M. A., and Bond, M. (2004) A-kinase anchoring protein targeting of protein kinase A in the heart, *J Mol Cell Cardiol 37*, 653-665.
5. Rohman, M. S., Emoto, N., Takeshima, Y., Yokoyama, M., and Matsuo, M. (2003) Decreased mAKAP, ryanodine receptor, and SERCA2a gene expression in mdx hearts, *Biochem Biophys Res Commun 310*, 228-235.
6. Zakhary, D. R., Fink, M. A., Ruehr, M. L., and Bond, M. (2000) Selectivity and regulation of A-kinase anchoring proteins in the heart. The role of autophosphorylation of the type II regulatory subunit of cAMP-dependent protein kinase, *J Biol Chem 275*, 41389-41395.
7. Zakhary, D. R., Moravec, C. S., and Bond, M. (2000) Regulation of PKA binding to AKAPs in the heart: alterations in human heart failure, *Circulation 101*, 1459-1464.
8. Anderson, M. E., Higgins, L. S., and Schulman, H. (2006) Disease mechanisms and emerging therapies: protein kinases and their inhibitors in myocardial disease, *Nat Clin Pract Cardiovasc Med 3*, 437-445.
9. Vlahos, C. J., McDowell, S. A., and Clerk, A. (2003) Kinases as therapeutic targets for heart failure, *Nat Rev Drug Discov 2*, 99-113.
10. Lange, V., Picotti, P., Domon, B., and Aebersold, R. (2008) Selected reaction monitoring for quantitative proteomics: a tutorial, *Mol Syst Biol 4*, 222.
11. Schiess, R., Wollscheid, B., and Aebersold, R. (2009) Targeted proteomic strategy for clinical biomarker discovery, *Mol Oncol 3*, 33-44.

6.3. Samenvatting

Cardiovasculaire ziekten zijn de nummer één doodsoorzaak in de westerse wereld. Om het risico en de ernst van de ziekte in te kunnen schatten zijn geschikte indicatoren, biomarkers, nodig. Om het ontstaan van deze ziekten te begrijpen is er ook intensief onderzoek nodig naar de gedetailleerde verschillen in de functie van eiwitten in het gezonde en zieke hart. Het vinden van biomarkers is de afgelopen jaren een sterk ontwikkelend veld binnen het cardiovasculaire onderzoek geworden. Bij niet genetisch veroorzaakte cardiovasculaire ziekten zijn eiwitten ideale biomoleculen om als biomarker te fungeren omdat ze de primaire werkpaarden van het werkende hart zijn die zich bij ziekte direct aanpassen aan de nieuwe condities. In de zoektocht naar nieuwe biomarkers is proteomics een zeer geschikte techniek omdat hiermee op grote schaal naar verandering van eiwitconcentratie als functie van ziekte of medicijngebruik kan worden gekeken. Ook kan met deze op massaspectrometrie gebaseerde techniek gekeken worden naar veranderingen in chemische modificaties op eiwitten. Ondanks veelbelovende eerste resultaten is er voor het toepassen van proteomics binnen het biomarkerveld nog veel werk te verrichten omdat in een ideaal geval van zoveel mogelijk patiënten gegevens moeten worden verzameld. Dit kost echter teveel tijd en dus geld met huidige proteomics technieken. Daarom moet er op korte termijn veel geïnvesteerd worden in het verder ontwikkelen van proteomics in de biomarker richting. Er kan dan gedacht worden aan het verbeteren van massaspectrometers, het nog beter scheiden van de eiwitfragmenten waarvan de concentraties worden vergeleken zodat nog meer eiwitten tegelijkertijd gemeten kunnen worden, maar ook aan slimme technieken om een bepaalde klasse eiwitten beter te kunnen bestuderen omdat daarvan al bekend is dat ze van invloed zijn op het ontstaan of verslechteren van het ziekteproces. Dit proefschrift beschrijft twee verschillende invalshoeken voor het vinden van biomarkers voor cardiovasculaire ziekten. In het eerste deel word ‘chemical proteomics’ toegepast om heel specifiek naar een kleine set eiwitten te kijken en hoe die veranderen tijdens ontwikkeling van hartziekte. Ook word er ingegaan op hoe deze nieuwe techniek op een unieke manier bijdraagt aan het begrijpen van de achterliggende biologie van deze eiwitten. In het tweede deel wordt een grootschalige proteomics aanpak gepresenteerd om zoveel mogelijk harteiwitten tegelijkertijd in kaart te brengen en om tegelijkertijd de concentratie van elk te bepalen. Voor het samenstellen van deze eiwitbibliotheek zijn de grenzen opgezocht van de huidige proteomics technieken en hiermee kunnen potentieel ziekteverwekkende eiwitten worden geselecteerd voor nader onderzoek.

Hoofdstuk 1 is een inleiding tot cardiovasculaire proteomics. Naast de gedetailleerde beschrijving van de meest gebruikte proteomics technieken is er aandacht voor hoe die zijn toegepast binnen het cardiovasculaire onderzoeksveld. Ook worden verschillende ‘chemical proteomics’ technieken beschreven. Deze techniek maakt gebruik van de specifieke

eigenschappen van een bepaald eiwit en een klasse van eiwitten om te binden aan kleine moleculen zoals bijvoorbeeld medicijnen of andere kleine natuurlijke moleculen. Als laatste worden een aantal verschillende proteomics methoden voor het vinden van nieuwe biomarkers beschreven.

De werking van het hart is te herleiden tot een samenspel van verschillende eiwitten die gecoördineerd met elkaar samenwerken. Zo kan een signaal uit de hersenen via het bloed bij het hart worden omgezet in actie, zoals bijvoorbeeld het sneller laten kloppen. Deze chemische signalen vanuit de hersenen moeten in de cellen van de hartspier worden doorgegeven. Dit gaat onder ander via kleine signaalmoleculen cAMP en cGMP die weer binden aan de signaaleiwitten PKA en PKG. Signaalmoleculen en signaaleiwitten vertalen het signaal van buiten naar binnen en zijn dus uitermate belangrijk voor de functie van het hart. In **hoofdstuk 2** worden PKA en PKG uitvoerig besproken. Beide eiwitten zijn kinases die andere eiwitten aan of uit kunnen zetten door een fosfaatgroep op deze eiwitten aan te brengen. Deze fosforilatie is als het ware de aan of uitknop voor deze eiwitten. Zo kan middels een signaalnetwerk van fosforileringen het signaal uit de hersenen op celniveau worden verwerkt tot bijvoorbeeld een snellere spiercontractie. Hoofdstuk 2 focust vooral op hoe massaspectrometrie in de afgelopen jaren heeft bijgedragen aan het onderzoek naar de functie van PKA en PKG. Er is aandacht voor zowel de structuren van de eiwitten als de context waarin ze opereren, dat wil zeggen de andere eiwitten waarmee ze samenwerken.

Een grove schatting zegt dat PKA in een enkele cel wel 50 verschillende taken heeft, met andere woorden meer dan 50 verschillende fosforilaties moet uitvoeren. Om ervoor te zorgen dat deze functies elkaar niet storen en alleen het juiste doel word gefosforileerd, bind PKA aan een grote groep verschillende eiwitten die we AKAPs noemen. Deze AKAPs zorgen ervoor dat PKA op de juiste plek op het juiste moment is. Inmiddels zijn er 28 verschillende AKAPs bekend (Tabel 1 in hoofdstuk 2). Van PKA bestaan twee verschillende vormen, type I en type II. Deze hebben verschillende functies die waarschijnlijk door binding aan verschillende AKAPs kunnen worden gereguleerd. Er is echter voor veel AKAPs niet bekend aan welke vorm van PKA ze binden. In **hoofdstuk 3** is een chemical proteomics methode beschreven die hierbij kan helpen. Verschillende geïmmobiliseerde analogen van cAMP bleken verschillende affiniteiten voor PKA type I en type II te hebben. 8-AHA-cAMP en 2-AHA-cAMP bleken min of meer gelijke affiniteit voor PKA te hebben, terwijl 2'OMe-8AHA-cAMP een ongeveer 4-5 voudig hogere affiniteit voor type I had. Deze geïmmobiliseerde analogen werden gebruikt om de verschillende PKA vormen samen met de daaraan bindende AKAPs te vangen. Door middel van kwantitatieve massaspectrometrie de 8-AHA-cAMP fractie te vergelijken met de 2'OMe-8AHA-cAMP konden de specificiteiten van twaalf verschillende AKAPs worden bepaald. Hierbij konden 3 nieuwe specifcteiten voor AKAP2, AKAP12 en AKAP14 worden bepaald.

Het vinden van biomarkers voor cardiovasculaire ziekten door het vergelijken van ziek met gezond weefsel heeft reeds een aantal biomarkers voor bijvoorbeeld gedilateerde cardiomyopathie opgeleverd. Haast al deze eiwitten behoren tot de meest geconcentreerden in het hartweefsel. De veranderingen in deze eiwitten lijken echter eerder een gevolg van de ziekte, dan een oorzaak. Om meer oorzakelijke biomarkers te vinden zouden de signaaleiwitten een veelbelovende klasse eiwitten kunnen zijn, echter hebben deze over het algemeen een veel lagere concentratie en zijn dus moeilijker te meten met massaspectrometrie. Van enkele spelers in de PKA en PKG singaalpaden is bekend dat ze veranderen onder myopathische condities. Daarom is de chemical proteomics techniek beschreven in hoofdstuk 2 en 3 gebruikt in **hoofdstuk 4** om juist verschillen in die eiwitten te bepalen met massaspectrometrie. Uit de bepalingen in dit hoofdstuk bleek dat chemical proteomics een veelbelovende techniek is om heel specifiek veranderingen in PKA/PKG signaalpaden aan te tonen. Zo werden bestaande veranderingen teruggevonden, zoals de lichte daling in aanwezigheid van PKA, maar werden ook een heel aantal nieuwe verbanden gevonden, zoals het sterk toenemen van de concentratie van PKG en phosphodiesterase 2 (PDE2). Door bestudering van de AKAPs kon worden aangetoond dat PKA zich anders verankerd aan AKAPs in het gezonde en in het zieke hart, iets wat met andere technieken zeer moeilijk te bestuderen is in het humane hartweefsel.

In **hoofdstuk 5** is op een andere manier naar signaaleiwitten van het humane hart gekeken.
Door alle moderne massaspectrometrietechnieken in parallel toe te passen op de analyse van een stukje humaan hart is getracht een zo groot mogelijke bibliotheek van aanwezige eiwitten te genereren. Na een intensieve analyse (260 runs) konden ruim 3500 humane eiwitten in kaart worden gebracht. Omdat bij deze techniek de eiwitten in kleine stukjes worden geknipt die vervolgens gesequenced worden met de massaspectrometer zou je kunnen zeggen dat het aantal stukjes wat je van een eiwit terugvind correleert met de hoeveelheid van dat eiwit in het weefsel. Op deze manier hebben we met behulp van de zogenoemde ‘spectral counting’-techniek tot in detail van ruim 2200 eiwitten de concentratie kunnen bepalen. Binnen deze groep van 2200 eiwitten zijn vervolgens alle relevante signaaleiwitten in kaart gebracht, met een speciale focus op kinases, fosfatases en GTPases. Door het in kaart brengen hiervan konden nieuwe spelers in de signaaltransductie van het hart worden gevonden. Deze zijn uitermate interessant voor nadere bestudering in de context van hun functie in het hart.

Curriculum Vitae

The author of this thesis was born on 2nd June 1978 in Yangon, Myanmar (formally known as Burma). She graduated B.Eng (Chemical Engineering) from Yangon Technical University, Yangon, Myanmar. After graduation, she was offered a research scholarship from National University of Singapore, Singapore. Since then she left Myanmar to pursue her future dream as an engineer. She graduated M.Eng (Chemical Engineering) in 2004. Her Master project was emphasized on building a bioreactor for waste-water treatment. However, working as a research assistant in Genome Institute of Singapore changed her dream by introducing her in proteomics field, especially mass spectrometry. At early 2006, she started her PhD training at the Biomolecular Mass Spectrometry and Proteomics group of the Utrecht University. She worked on the biomarker discovery in cardiac research using chemical proteomics under supervising of Prof. Albert J.R Heck and Dr. Arjen Scholten. In 2010, she started as a Senior Engineer at the Proteomic Unit, PROBE in Bergen, Norway.

Publication List

1. **Thin Thin Aye**, van Veen TA, van der Heyden MA, Varro A, de Weger RA, Jonge N, Vos MA, Heck AJ, Scholten A, Reorganized PKA-AKAP Associations in the Failing Human Heart, **2010**, *in preparation*

2. **Thin Thin Aye**, Scholten A, Taouatas N, Varro A, Toon A.B. van Veen, Vos MA, Heck AJ, Protein-wide protein concentrations in the human heart. Mol Biosyst. **2010** Jul 1. [Epub ahead of print]

3. Kovanich D, van der Heyden MA, **Thin Thin Aye**, van Veen TA, Heck AJ, Scholten A, Sphingosine kinase interacting protein is an A-kinase anchoring protein specific for type I cAMP-dependent protein kinase. Chembiochem. **2010** May 3;11(7):963-71

4. **Thin Thin Aye**, Mohammed S, Toorn HW, Veen TA, Heyden MA, Scholten A, Heck AJ, Selectivity in enrichment of PKA RI and RII isoforms and their interactors using modified cAMP affinity resins. Mol Cell Proteomics **2009** May; 8(5):1016-28.

5. Boersema PJ, **Thin Thin Aye**, van Venn TA, Heck AJ, Mohammed S, Triplex protein quantification based on stable isotope labelling by peptide dimethylation applied to cell and tissue lysates.Proteomics. **2008** Nov;8(22):4624-32

6. Scholten A, **Thin Thin Aye**, Heck AJ, A multi-angular mass spectrometric view at cyclic nucleotide dependent protein kinases: in vivo characterization and structure/function relationships. Mass Spectrom Rev. **2008** Jul-Aug: 27(4):331-53. Review

7. **Thin Thin Aye**, Low TY, Sze NSK, A Nanosecond Laser-Induced Photochemical Oxidation Method for Protein Surface Mapping with Mass Spectrometry. Anal. Chem, **2005**, **77**(18), 5814-22

Dankwoord

This thesis would not have been possible without the support and encouragement, during my stay in the Netherlands for the past 4 years, from many people, all of whom I acknowledge greatly. Hopefully, I did not leave out any names here.

First of all, my utmost gratitude goes to my supervisor, Albert for providing me with the opportunity to pursue my PhD in the field of chemical proteomics, something that I had never experienced. I thank you for your expertise, guidance, faith and endless support. Working here has helped me discover myself and to improve my knowledge. I thank you for all these.

It is difficult to overstate my gratitude to my co-promoter, Arjen who is more than just a co-promoter of my thesis. You were here from my first workday. With your enthusiasm, inspiration, and great efforts to explain things clearly, you helped to make chemical proteomics fun for me. Throughout my PhD studies, especially during the thesis-writing period, you have provided me with ongoing encouragement and sound advice which I sincerely value.

I would like to thank many people who had taught me various ways in proteomics. First, Reinout, I am really grateful for your helps throughout my journey. Shabaz, you gave me very tough and useful training for operating MS in which I am more confident than 4 years ago. I really appreciate your encouragement while I was feeling down. Jeron (J) for teaching me how to assemble the mini-gel cascade and helping me how to run the gel and Silvia (queen of the lab) for gave me western blot protocol and taught me all tips. Thank you, Silvia. Sail through the North Sea and visit me, will you? Joost, I miss your SCX setup. It was very easy to use. I also thank Teck who stood beside me and encouraged me constantly. I learnt a lot from you since we were in Singapore. Henk, thanks a lot for generating the html files which were used in chapter 5. It was really helpful for re-calibrating the file and finally gave us highly confident data. I just hope that you set the office hours (14:00-16:00) is not because of me ☺.

Rui, it was great working with you for 9 months. You chose part of my project as your Masters research. Although we haven't obtained publishable data, I am glad that your preliminary data is very useful for the future. And here is Erwin, the computer geek, it is much pleasure to work with you for 9 months. Thank for helping me for some computer programming. Wish you all the best for your PhD!

Many thanks and appreciation goes to my collaborator, Toon. Without you, all chapters in my thesis would not be possible. Whenever I asked for samples, you are the one who gave me

without questions. I really appreciate your trust. And Marcel, the western blot expert, thank for helping and teaching me to do proper western blot. Sid, it was a good time to work with you but too bad that you joined the lab late. I wish you good luck for your 4 years journey. Other collaborators whom I would like to thank for providing samples as well as much fruitful biological thought; Niki (from Olso for providing me with T-cells), Venessa (from Singapore for providing me with human stem cells) and Benschof (from UMC for providing me with tons of yeast lysates). Although these data have not reached publishable stages, I hope it will be very useful for the future.

I am also greatly indebted to Corine who has been helping me once I landed in the Netherlands till I left the country. Corine, I will never forget your coffee packages with no sugar (not knowing that I couldn't drink coffee without sugar), packages of cookies that you brought me the day I just arrived in the Netherlands. It made me think like…WOW! Dutch are very helpful and friendly. You sent me to city hall and help me for everything. I really appreciated for what you had done for me. Nasrin, thanks for inviting me for Christmas dinner every years. I wish I would get one more chance to visit you and your family again on next Christmas. Ursula, I will miss the time we spent together in Amsterdam for fund-raising and all activities about Burma.

I am indebted to my many colleagues for providing a stimulating and fun environment in which to learn and grow. I am especially grateful to Nadia who is with me since the day she joined the group. Nadia! Before you joined the group, I was very quiet and aloof. Arjan can prove it as he didn't even notice of my presence till you joined to our lab ☹. Thank for bringing me along for adapting to the European, especially Scandinavian culture. You always made my day full of laughter and smiles. I will miss you! Then Sharon, I have been too much influenced by you. I swear☺. Donna, I will miss all the time we spent together at office sharing Asian food, Asian celebrities' juicy news and more! I wish you good luck with your journey and publish more papers. Pepijn, welcome to our PKA team and wish you good luck! Sarah and Glen, the friendliest Canadians I ever met. I am sorry that I will not have a chance to take care of your lovely and over-active kitten for the next Christmas. Rebecca and Tom, thank for inviting me for the birthday party at your lovely home. It was my first time drinking flaming Sambuca. What a great experience! Javier, you always give me good suggestion whenever I am stuck in data analysis. It was great pleasure to know you and I hope I will see you and Anna again. Sarena, the most energetic and fun girl in the lab, I will miss you. Keep on going like this for 4 years! Chhiti, you brought back my old memories of Singapore. There are so many things that you can learn here, success! Luigi and Ales, the two different Italians I worked with. It was great pleasure to work with you guys. Kristina, thanks for your delicious dinner and wish I could have it one more time☺. Paul, my great office mate in Went building, thank for all the helps, especially translating of Dutch to English ☺. And Poupak

who encouraged me unconditionally, I will miss you. Charlotte, thank for pancake that you made at your birthday party. Danny, Pieter, Bas, Wim, Shahram (you made me happy by giving me the best computer☺), Robert and Bobby, the computer guys- I am greatful of all the helps. And Ajda (very supportive girl I had ever met), Andreas (thank for all the tips), Ayse (for helping me using Q-TOF at my last days of work), Benjamin, Christian Sr, Christian Jr, Erik, Esther, Gideon, Harm, Ioana, Jeff (too bad that you are not here to read my thesis as you promised), Jeffery (I will always remember the time we made delicious Danish dinner at your home for Xmas), Lars (Thank for spending time for providing me cell, it was a very laborious work), Marco, Maarten, Martje, Martina, Mirjam (I am very greatful for ordering reagents which are needed for my every experiments), Monique, Natasja, Nikolai, Onno (thank for your encouragements), Renske, Sara, Thomas (you are right! I have been trying not to get depressed☺) and Vincent G for their help and company. Hongtao and Zhou, thank for lovely Chinese dinners that I had with you guys. I will really miss your cooking, especially the spicy fish curry. Vincent and Ivy, thank for being my friends. Love you guys and Jonathan! And I thank to my best friend, Mya for her continuous encouragement and support and Anka who helped me since the day I arrived in Norway.

Last but not least, I would like to thank my mother whose love is boundless and my father who is my role model. They bore me, raised me, supported me, taught me, and loved me. To them I dedicate this thesis.

XOXO, Thin Thin